

Impact of mesenchymal stromal cell-derived vesicular cargo on B-cell acute lymphoblastic leukemia progression

Dissertation

Zur Erlangung des Doktorgrades
der Naturwissenschaften

vorgelegt am Fachbereich 14
der Johann Wolfgang Goethe-Universität
in Frankfurt am Main

von

Christina Karantanou
aus Athen, Griechenland

Frankfurt (2021)
(D30)

vom Fachbereich Biochem, Chemie und Pharmazie (FB14) der
Johann Wolfgang Goethe-Universität als Dissertation angenommen.

Dekan: Prof. Dr. Clemens Glaubitz

Gutachter:

Prof. Dr. Rolf Marschalek

Prof. Dr. Daniela S. Krause

Datum der Disputation: 16/12/2021

Die Veröffentlichung in gedruckter und elektronischer Form aller in dieser
Dissertation verwendeten Abbildungen erfolgt mit Genehmigung der jeweiligen
Rechteinhaber.

DECLARATION

I herewith declare that I have not previously participated in any doctoral examination procedure in mathematics or natural science discipline.

Frankfurt am Main,
(Signature)

(Date)

Authors' declaration

I hereby declare that I produced my doctoral dissertation on the topic of

“Impact of mesenchymal stromal cell-derived vesicular cargo on B-cell acute lymphoblastic leukemia progression”

independently and using only the tools indicated. In particular, all references borrowed from

external sources are clearly acknowledged and identified.

I confirm that I have respected the principles of good scientific practice and have not made

use of the services of any commercial agency in respect of my doctorate.

Frankfurt am Main,
(Signature)

(Date)

Table of Contents

<i>Zusammenfassung</i>	8
<i>Summary</i>	14
<i>Introduction</i>	17
1. Hematopoiesis	17
1.1 Regulation of hematopoiesis	19
2. Bone marrow microenvironment (BMM).....	22
2.1 Endothelial cells.....	22
2.2 Osteoblasts and osteoclasts.....	23
2.3 Mesenchymal stromal cells (MSC)	25
2.4 Extracellular matrix (ECM).....	26
3. Leukemia	28
3.1 Chronic myeloid leukemia (CML).....	29
3.2 B-cell acute lymphoblastic leukemia (B-ALL).....	30
3.3 Chronic lymphocytic leukemia (CLL).....	32
3.4 Acute myeloid leukemia (AML)	34
4. The bone marrow microenvironment in leukemia	34
4.1 The altered niche as predisposing factor.....	35
4.2 Niche remodeling by leukemia cells	36
5. Bone marrow microenvironment in B-ALL.....	41
6. Autophagy	43
6.1 The process of autophagy	43
6.2 The role of autophagy in health and disease	45
7. The endocytic pathway.....	47
7.1 Multivesicular bodies.....	47
8. Extracellular vesicles	47
8.1 Pathways of exosome biogenesis	50
8.2 Extracellular vesicles and cancer	53
9. PLEKHM1: a hub between autophagy and the endolysosomal system.....	54
<i>Hypothesis</i>	55
<i>Materials and Methods</i>	56
1. Mice and Genotyping.....	56
2. Virus production and titration.....	56
3. Bone marrow (BM) transduction/transplantation	57
3.1 CML.....	57
3.2 AML	58

3.3	BALL - Primary transplant.....	58
3.4	BALL - Secondary transplant.....	58
3.5	Preincubation of BCR-ABL1-transduced BM cells with sEV	59
4.	Homing.....	59
5.	Analysis of diseased mice and tumor burden	59
6.	Flow cytometry.....	59
7.	Quantitative real-time PCR	61
8.	Osteoclast isolation and differentiation	61
9.	Osteoclast resorption assay	62
10.	Proliferation of BCR-ABL1 ⁺ BA/F3 cells on osteoclasts	62
11.	Preparation of mesenchymal stromal cells	62
12.	Mesenchymal stromal cell culture.....	64
13.	Colony forming unit fibroblast assay (CFU-F).....	64
14.	Differentiation of MSC	64
15.	Immunofluorescence	65
16.	Preparation of extracellular vesicles (EV)	66
17.	Immunoblotting	66
18.	Mass Spectrometry	67
19.	Imaging flow cytometry.....	70
20.	<i>In vitro</i> treatment of BCR-ABL1 ⁺ BA/F3 cells.....	71
21.	<i>In vitro</i> treatment of MSC with TNF α or coculture with BCR-ABL1 ⁺ BA/F3 cells	71
22.	Statistical Analysis	71
	Results	72
1.	<i>Plekhm1</i> KO and WT mice have comparable hematological profiles	72
2.	PLEKHM1 deficiency in the bone marrow microenvironment differentially influences specific leukemias	74
i.	Chronic myeloid leukemia (CML)-like myeloproliferative neoplasia (MPN)	74
ii.	Acute myeloid leukemia (AML)	76
iii.	BCR-ABL1 ⁺ B-cell acute lymphoblastic leukemia (B-ALL)	77
3.	PLEKHM1 deficiency in the BMM does not alter the homing capacity of BCR-ABL1 ⁺ B-ALL cells	78
4.	Characterization of B-ALL cells in the <i>Plekhm1</i> KO BMM.....	79
i.	Apoptosis and cell cycle	79
ii.	B-cell markers on B-ALL cells from WT or <i>Plekhm1</i> KO mice	81
5.	A <i>Plekhm1</i> KO microenvironment increases the number and/or function of B-ALL-initiating cells (LIC).....	85
6.	Characterization of the <i>Plekhm1</i> KO BMM	89

i.	PLEKHM1 in osteoclasts is dispensable for the proliferation of B-ALL cells	89
ii.	Differentiation to osteoblasts and adipocytes and vesicular trafficking are altered in <i>Plekhm1</i> KO mesenchymal stromal cells	91
7.	<i>Plekhm1</i> KO MSC release syntenin- and syndecan-1-enriched small extracellular vesicles (sEV)	98
i.	PLEKHM1 does not affect the number of sEV released by MSC.....	98
	100
ii.	PLEKHM1 regulates MSC-derived sEV cargo	100
	102
8.	<i>Plekhm1</i> KO MSC-derived sEV alter B-ALL cells	104
i.	<i>Plekhm1</i> KO MSC-derived sEV increase syntenin, syndecan-1, pAKT and pFAK in BCR-ABL1 ⁺ BA/F3 cells.....	104
ii.	<i>Plekhm1</i> KO MSC-derived sEV may increase B-ALL aggressiveness.....	110
9.	Leukemia cells or TNF α reduce PLEKHM1 levels in BM MSC.....	112
	<i>Discussion</i>	114
	<i>References</i>	123
	<i>Acknowledgments</i>	138
	<i>Curriculum Vitae</i>	140

Zusammenfassung

Leukämien sind eine heterogene Gruppe von Neoplasien, bei denen eine unkontrollierte Vermehrung bösartiger Zellen, so genannter Leukämiezellen, zu einer abnormen Blutbildung im Knochenmark (KM), in der Milz und in den Lymphknoten führt. Die Leukämiezellen wachsen auf Kosten des normalen blutbildenden Systems, was zu lebensbedrohlichen Symptomen wie Anämie, Thrombozytopenie und Immunschwäche führt. Je nach der Abstammung der neoplastischen Zellen und dem zeitlichen Auftreten der Krankheit werden diese bösartigen Erkrankungen in vier Haupttypen eingeteilt, die wiederum in weitere Untertypen unterteilt werden: chronische myeloische Leukämie (CML), akute myeloische Leukämie (AML), chronische lymphatische Leukämie (CLL) oder akute lymphatische Leukämie (ALL). In unserer Studie konzentrierten wir uns auf die B-Zell ALL (B-ALL), die das Resultat einer unkontrollierten Vermehrung bösartiger B-Zellen ist und am häufigsten bei Kindern zwischen zwei und fünf Jahren auftritt. BCR-ABL1, ein Onkogen, das durch die reziproke Translokation zwischen den Chromosomen 9 und 22, t(9;22), gebildet wird, führt zur Produktion einer konstitutiv aktiven Kinase und ist ein Kennzeichen der CML. Es ist auch in 3-5% der pädiatrischen und 25% der erwachsenen B-ALL-Fälle vorhanden. Insgesamt ist die Prognose der B-ALL mit einer 5-Jahres-Überlebensrate von 85% bei Kindern recht gut, während sie bei Erwachsenen aufgrund der hohen Rückfallrate deutlich schlechter ist. Die Häufigkeit von Rückfällen bei BCR-ABL1+, aber auch bei BCR-ABL- B-ALL, ist ein Hindernis für die dauerhaft erfolgreiche Behandlung und macht die Entdeckung neuer Zielstrukturen zu einer Notwendigkeit.

Die Mikroumgebung des Knochenmarks ist eine komplexe Einheit aus mesenchymalen Stromazellen (MSZ), Osteoblasten und Osteoklasten, Immunzellen,

der extrazellulären Matrix und löslichen Faktoren. Sie steuert die Funktion und das Überleben normaler hämatopoetischer Zellen, aber auch die derer malignen Äquivalente. MSZ verfügen über ein trilineares (adipogenes, osteogenes und chondrogenes) Differenzierungspotenzial und sind ein wichtiger Bestandteil der KM-Nische. Obwohl die Rolle der Osteoblasten und ihrer Vorläufer-MSZ intensiv untersucht wurde, ist die Rolle der Osteoklasten im Zusammenhang mit Leukämie nicht ausreichend definiert. Selbst für die gesunde Hämatopoese gibt es bisher nur Hinweise darauf, dass Osteoklasten durch den Abbau des Knochens den Austritt hämatopoetischer Stammzellen aus dem Knochenmark unterstützen. Obwohl Skelettanomalien bei Kindern mit ALL häufig vorkommen, ist nicht geklärt, wie genau die knochenmarkseigene Mikroumgebung (KMM) verändert wird. Darüber hinaus wurden bei ALL eine gestörte B-Lymphopoese, eine verminderte Kollagenproduktion und ein Rückgang der osteoblastischen Zellen beobachtet, aber auch hier ist die Funktion der Osteoklasten in diesem Zusammenhang weniger gut untersucht.

Osteoklasten sind große mehrkernige Zellen, welche die Knochenmatrix resorbieren. Während der Knochenresorption führt die Verschmelzung saurer Vesikel mit der dem Knochen zugewandten Plasmamembran der Zelle zur Bildung der so genannten „gekräuselten Borte“ (engl. ruffled border (RB)). Der Transport sekretorischer Vesikel (so genannter sekretorischer Lysosomen) ist für die Bildung der RB unerlässlich und wird streng reguliert. Zu den Schlüsselmolekülen, die bei der strikten Regulierung dieses Prozesses eine Rolle spielen, gehören kleine Rab-GTPasen und ihre Bindungspartner. In der RB wird der Inhalt der sekretorischen Lysosomen, z.B. knochenresorbierende Enzyme wie Cathepsin K, freigesetzt und baut das Hydroxylapatit-Mineral ab. Mutationen in Genen, die für Proteine kodieren, die in den sekretorischen Lysosomen der Osteoklasten lokalisiert sind, führen zu einer

seltenen genetischen Störung, die Osteopetrose genannt wird und durch Defekte in der Osteoklastenbildung oder -funktion verursacht wird. Eines dieser Gene, PLEKHM1 (pleckstrin homology domain-containing family M member 1), kodiert für ein zytosolisches Protein von 117 kDa, das an die GTPase Rab7 bindet und mit späten Endosomen und Lysosomen assoziiert ist. Der verkürzten Form des PLEKHM1-Proteins bei Menschen mit Osteopetrose fehlt die Rab7-bindende Region, weshalb das Protein nicht an späte Endosomen und Lysosomen rekrutiert wird und stattdessen im Zytosol verbleibt. Der Transport von körpereigenem und körperfremdem Material über Membranen in den Extrazellulärraum oder zu Lysosomen zum dortigen Abbau ist in allen Zellen von wesentlicher Bedeutung. Er erleichtert die Funktionsweise wichtiger Stoffwechselwege, wie die des endozytären und des autophagischen Weges. PLEKHM1 spielt auch bei diesen Stoffwechselwegen eine Rolle. PLEKHM1 ist am späten Endosomen-Transport beteiligt und ist für die letzten Schritte der Autophagie, die Fusion von Autophagosomen mit Lysosomen, wichtig.

Autophagie ist ein von den Lysosomen abhängiger Abbauweg, der mit dem endolysosomalen System verbunden ist, das darauf abgestimmt ist, auf spezifische Reize in adäquater Weise zu reagieren. Mit dem endolysosomalen System und der Autophagie verbunden sind die Biogenese und Freisetzung von Fracht-beladenen extrazellulären Vesikeln (EV), den Exosomen, in den extrazellulären Raum. Exosomen werden als kleinere Vesikel in größeren Vesikeln, den so genannten multivesikulären Körpern (MVK), die als eine spezialisierte Art von späten Exosomen gelten, gebildet und von diesen freigesetzt. Bisher ist nicht bekannt, dass PLEKHM1 eine Rolle bei der Exosomen-Biogenese oder der Freisetzung von Exosomen spielen würde, aber angesichts seiner Funktion im späten Endosomen-Transport besteht die Möglichkeit, dass es auch am Transport der multivesikulären Körper beteiligt ist.

Vor diesem Hintergrund stellten wir die Hypothese auf, dass PLEKHM1 in der KMM das Fortschreiten von B-ALL beeinflussen könnte, indem es den vesikulären Transport in Osteoklasten oder anderen Zellarten reguliert.

Tatsächlich konnten wir beobachten, dass Mäuse, denen PLEKHM1 in der KMM fehlt, im Vergleich zu ihren Wildtyp (WT)-Pendants eine deutlich aggressivere Krankheit entwickelten. Es wurde festgestellt, dass Leukämiezellen, die in einer Plekhh1 Knockout (KO) KMM wachsen, überlebensfähiger sind und Marker exprimieren, die auf einen unreifen Phänotyp hindeuten, verglichen mit Leukämiezellen, die einer WT-KMM ausgesetzt sind. Die Blockade der Differenzierung ist eines der Kennzeichen von Stammzellen und bei vielen Leukämien wird berichtet, dass eine Subpopulation von Zellen mit stammzellähnlichen Eigenschaften das Tumorwachstum aufrechterhält. Leukämienstammzellen sind bei der AML gut untersucht, bei der B-ALL sind sie jedoch nicht ausführlich definiert, und bei der ALL von Kindern deuten Studien auf einen feststehenden lymphoiden Progenitor als Ursprungszelle hin. In unserer Studie konnten wir jedoch nachweisen, dass das Fehlen von PLEKHM1 in der KMM die Anzahl oder die Funktion der B-ALL-auslösenden Zellen erhöhen kann, was sich in einer deutlich erhöhten Aggressivität dieser Zellen in sekundären Transplantationsversuchen zeigt.

Wir bestätigten die bereits bekannte Rolle von PLEKHM1 für die Funktion von KM-Osteoklasten, indem wir in in vitro Experimenten zeigten, dass Osteoklasten in Abwesenheit von PLEKHM1 nicht in der Lage sind knochenresorptive Gruben zu bilden. Allerdings erwiesen sich Plekhh1-KO-Osteoklasten, die morphologisch ihren WT-Pendants ähneln, als ebenso fähig, die Proliferation von B-ALL-Zellen in vitro zu unterstützen wie WT-Osteoklasten. Aufgrund der Schlussfolgerung, dass Osteoklasten nicht direkt an dem beobachteten Phänotyp beteiligt sein können,

stellten wir die Hypothese auf, dass PLEKHM1 auch für andere Zellen in der KMM wichtig sein könnte. Da KM-MSZ eine Schlüsselrolle in der Kommunikation zwischen B-ALL und der KMM spielen, vermuten wir, dass PLEKHM1 in der KMM die Aggressivität von B ALL durch die Kontrolle des vesikulären Transports in KM-MSZ erhöht. In Übereinstimmung mit seiner Rolle beim vesikulären Transport fanden wir heraus, dass PLEKHM1 die Menge an MVK und deren Fracht in KM MSZ kontrolliert. Insbesondere in Abwesenheit von PLEKHM1 sammeln sich MVK in KMM MSZ an, was zu erhöhten Mengen der Proteine Syntenin und Syndecan-1 in den Zellen führt, von denen bekannt ist, dass sie an der Exosomen-Biogenese beteiligt sind. Darüber hinaus akkumulieren Syntenin und Syndecan-1 in Abwesenheit von PLEKHM1 auch in den aus MSZ stammenden kleinen EV. B-ALL-Zellen, die mit kleinen EV, die aus Plekhh1-KO-MSZ stammen, behandelt wurden, lösten eine aggressivere Erkrankung aus als B-ALL-Zellen, die mit kleinen EV aus WT-MSZ behandelt wurden, was darauf hindeutet, dass die veränderte Fracht der kleinen EV, die von Plekhh1-KO-MSZ freigesetzt werden, den beobachteten Phänotyp teilweise erklären könnte. Kleine EV aus Plekhh1 KO-MSZ werden von B-ALL-Zellen aufgenommen und führen zu einer Aktivierung der Phosphorylierung der Proteinkinase B (AKT) und der fokalen Adhäsionskinase (FAK), was die Proliferation der B-ALL Zellen und die Aggressivität der B-ALL fördern könnte. Schließlich identifizierten wir im Einklang mit der wechselseitigen Interaktion zwischen Leukämiezellen und der KMM den Tumornekrosefaktor (TNF) α als eines der Zytokine, das nach Freisetzung durch B-ALL-Zellen die PLEKHM1-Konzentration in MSZ reduziert und gleichzeitig die Konzentration von Syntenin und Syndecan-1 in vitro erhöht, was den in vivo beobachteten leukämieverstärkenden Phänotyp rekapituliert.

Wir glauben, dass wir mit dieser Arbeit einen gegenseitig bedingte Wechselwirkungen identifiziert haben, bei der B-ALL-Zellen ihre Mikroumgebung insofern beeinflussen, dass diese ihr Überleben fördert und ihre Aggressivität steigert. Insbesondere setzen B-ALL Zellen TNF α frei, das sich auf die Konzentration von PLEKHM1 auswirkt, das den vesikulären Transport in den KM-MSZ steuert. PLEKHM1 steuert den MVK-Spiegel in KM MSZ, was wiederum die Beladung der kleinen EV mit spezifischen Proteinen, in unserem Fall Syntenin und Syndecan-1, beeinflusst. Die veränderte Fracht der kleinen EV, die von KM MSZ freigesetzt werden, kann wiederum B-ALL-Zellen erreichen und deren Aggressivität erhöhen.

Summary

B-cell acute lymphoblastic leukemia (B-ALL) is a hematological malignancy affecting both children and adults, however, the highest incidence of the disease is found in children between ages 2 and 5. Among the many B-ALL subtypes BCR-ABL1⁺ B-ALL accounts for 3-5% of pediatric and 25% of adult B-ALL cases and is characterized by the chromosomal translocation t(9;22), which gives rise to the constitutively active tyrosine kinase BCR-ABL1. In adults, BCR-ABL1 is the most common B-ALL-associated genetic abnormality and confers a poor prognosis to both adults and children. The tyrosine kinase inhibitor (TKI) imatinib, which was initially given to treat chronic myeloid leukemia (CML), is also used for the treatment of BCR-ABL1⁺ B-ALL in combination with chemotherapy. However, relapse of patients who do not undergo allogeneic stem cell transplantation (SCT) or of patients with acquired TKI resistance, are still obstacles in B-ALL cure and call for the discovery of novel therapeutic interventions. Furthermore, in BCR-ABL1⁻ B-ALL, where imatinib is not applicable, the discovery of novel interventions is also needed.

The bone marrow (BM) microenvironment (BMM) is a complex entity that consists of different cells types, like endothelial cells, mesenchymal stromal cells (MSC) and neuronal cells, soluble factors, and extracellular matrix proteins. All these elements interact with the hematopoietic stem cells (HSC), the cells that produce all the blood cell types, as well as with their malignant counterparts, the leukemia stem cells (LSC) and the leukemia cells (LC). These interactions can affect leukemia cell function including survival, proliferation, and migration. Among the cells of the BMM, osteoclasts have been found to influence HSC mobilization, but studies on their role in leukemia and specifically in B-ALL have been limited.

Pleckstrin homology domain-containing family M member 1 (PLEKHM1) is an essential protein for the trafficking of secretory lysosomes in osteoclasts. Mutations in *PLEKHM1* have been linked with osteopetrotic phenotypes in both rats and humans which are attributed to defective osteoclasts. Furthermore, consistent with its role in vesicular trafficking, PLEKHM1 promotes the fusion of autophagosomes with lysosomes at the latest steps of autophagy which is an essential cellular homeostatic mechanism. Furthermore, is involved in the endocytic pathway facilitating the fusion of late endosomes, including multivesicular bodies (MVB) with lysosomes. MVB carry small extracellular vesicles (EV) which are released in the extracellular space as exosomes after fusion of MVB with the plasma membrane.

Given the role of PLEKHM1 in vesicular fusion and trafficking we hypothesized that PLEKHM1 in the BMM may influence B-ALL progression via impairment in vesicular formation and/or release from osteoclasts or other cell types.

Indeed, using a murine model of B-ALL we have shown that PLEKHM1 deficiency in the BMM accelerates B-ALL. PLEKHM1 deficient BMM-derived MSC show increased accumulation of MVB which in turn leads to impaired cargo of their released small EV. Specifically, these small EV carry increased levels of syntenin and syndecan-1 which are known to be involved in exosome biogenesis. Syntenin is an adaptor-like protein that interacts with multiple proteins on the plasma membrane, including syndecan-1 and is associated with increased migration of cancer cells. Syndecan-1 is a heparan sulfate proteoglycan and integral membrane protein which is present in both healthy and tumor cells, including leukemia cells. Uptake of these small EV by B-ALL cells increases their aggressiveness possibly via increased phosphorylation of protein kinase B (PKB/AKT) and focal adhesion kinase (FAK). In

turn, B-ALL-derived tumor necrosis factor (TNF) α conditions the BMM, decreasing PLEKHM1, while simultaneously increasing syntenin and syndecan-1 in normal MSC.

Therefore, our study proposes a link between BMM MSC-derived small EV and their cargo and B-ALL progression and might also be applicable to other, non-leukemic cancer types which release TNF α .

Introduction

1. Hematopoiesis

The word hematopoiesis is derived from the Greek words αίμα, "blood" and ποιεῖν "to make" and literally means "to make blood". Hematopoiesis is a constant process that occurs during embryonic development and continuous throughout adulthood when it ensures the replenishment of our blood system¹. During embryonic development, hematopoiesis occurs in the yolk sac and it leads to the production of red blood cells which are important for the oxygenation of the organs of the embryo². This type of hematopoiesis is called primitive. As the embryo develops, the hematopoiesis gradually moves to the spleen, the liver, and the bone marrow (BM) and it is now called definitive or adult hematopoiesis³. Through this process, the blood cellular components are formed and continuously replenished through the lifetime of an organism. It is estimated that an adult human body produces around $4-5 \times 10^{11}$ hematopoietic cells per day⁴.

In mammals, hematopoietic stem cells (HSC) are the cells that are responsible for the production of all the hematopoietic cells and the replenishment of the hematopoietic system and are considered to be at the top of the hematopoietic hierarchy⁵. More specifically, multipotent long-term HSC (LT-HSC) which reside in the BM can either self-renew to generate more HSC, which ensures the non-depletion of the HSC pool or differentiate into short-term HSC (ST-HSC), multipotent progenitors (MPP) or lineage-restricted progenitors which in turn proliferate and differentiate to terminally differentiated hematopoietic cells with different functions⁶. Lineage restricted progenitors involve the common lymphoid (CLP)⁷ and common myeloid (CMP)⁸ progenitors and are identified as such based on the presence of specific

surface markers and *in vitro* and *in vivo* assays that assess their developmental potential⁵. CMP give further rise to megakaryocyte/erythrocyte (MEP) and granulocyte/macrophage (GMP) progenitors and these to megakaryocytes and erythrocytes and monocytes and granulocytes respectively⁹. CPL give rise to T cells, B cells and NK cells⁶. Here, it is important to mention that ST-HSC can only self-renew and replenish the hematopoietic system for a defined (short) interval whereas LT-HSC have the ability to replenish the hematopoietic system throughout the lifespan of the organism⁶ (figure 1).

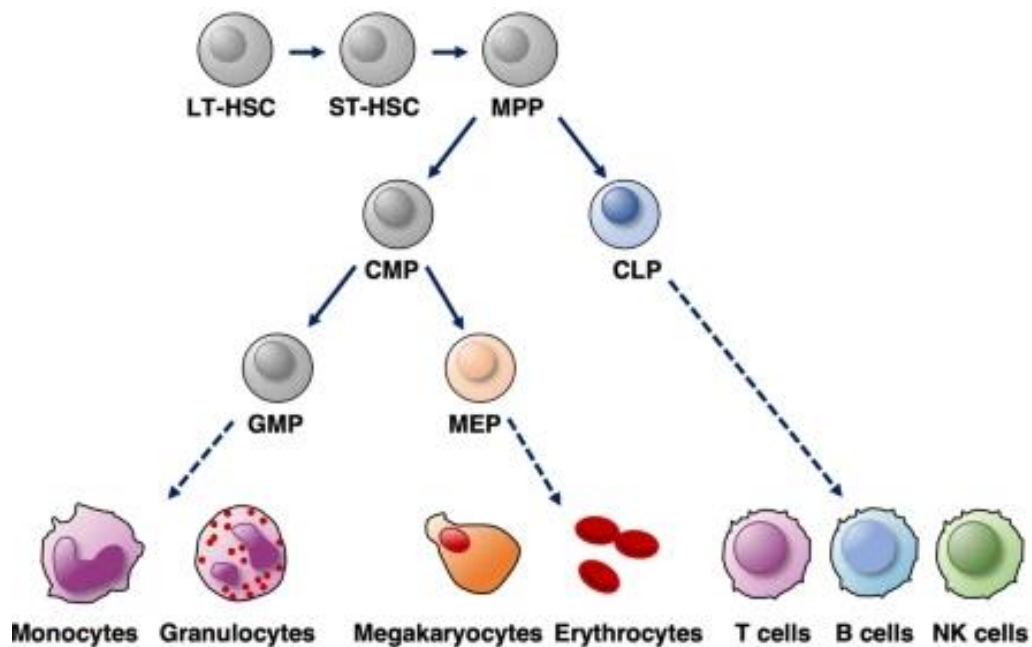


Figure 1: Blood cell development. LT-HSC; long term-HSC, ST-HSC; short term-HSC, MPP; multipotent progenitor, CLP; common lymphoid progenitor, CMP; common myeloid progenitor, GMP; granulocyte-macrophage progenitor, MEP; megakaryocyte-erythroid progenitor⁹.

1.1 Regulation of hematopoiesis

Hematopoiesis is a multistep process that is regulated tightly by a network of signaling molecules including cytokines and growth factors which are released in the BMM and control the proliferation, differentiation, and survival of the various progenitors. This is essential to ensure a balance between self-renewal and differentiation of HSC, as well as production of the right cell type in response to certain stimuli. Deregulation of the process of hematopoiesis can lead in the case of excessive differentiation to depletion of the HSC pool or in the case of restrictive differentiation and uncontrolled self-renewal to hematological malignancies including myeloproliferative diseases and leukemias¹⁰.

Several different transcription factors (TF) control early hematopoietic development by affecting HSC survival and proliferation including stem cell leukemia hematopoietic transcription factor (SCL), GATA-2, lim-finger protein LMPO2, and Runt-related transcription factor 1 (RUNX1)¹¹. Other TF are crucial for the decision of HSC and progenitor cell fate. For example, homeobox (*Hox*) genes, like *Hoxb4*, are important for primitive stem cell fate decisions including myeloid differentiation of HL-60 cells induced by Vitamin D3¹¹. Furthermore, GATA-1 influences progenitor cells towards erythroid rather than megakaryocytic maturation¹², while, HSC depleted for the TF PU.1 failed to maintain the HSC pool and to differentiate into the early myeloid and lymphoid progenitors¹³. Ikaros is a TF that has six zinc finger domains and regulates B cell development on multiple levels¹⁴. Mice homozygous for an Ikaros null mutation show defects in the development of both fetal and adult lymphocytes¹⁵. Finally, Pax5, a member of the paired box (PAX) family of transcription factors, plays a role in normal B-lymphopoiesis¹⁶, while, it has been associated with cancer including lymphoma and lymphocytic leukemias¹⁷.

The regulation of the TF that control hematopoietic cell function and cell fate decisions can be HSC-intrinsic or -extrinsic. All the constituents of the well-defined complex entity that we call BM microenvironment (BMM), and is described in more detail below, belong to the extrinsic factors that influence HSC. In this context, extrinsic regulation of hematopoietic cells' fate involves cytokines and growth factors, as well as, direct interaction with the extracellular matrix and other cells of the BMM. A great example of the latter involves the family of the highly evolutionarily conserved transmembrane receptors Notch. Notch, after it binds to extracellular ligands, for example, ligands provided by endothelial cells (EC) of the BMM¹⁸ it is cleaved and its intracellular domain is translocated to the nucleus and acts as a TF on target genes. Notch is known to serve a dual role in cell differentiation based on its expression levels and it can induce differentiation of adjacent cells towards various pathways. In the hematopoietic system, differential notch expression affects multiple binary cell fate decisions¹⁹(figure 2).

Binary Decisions in Hematopoiesis Directed by Differential Notch Expression

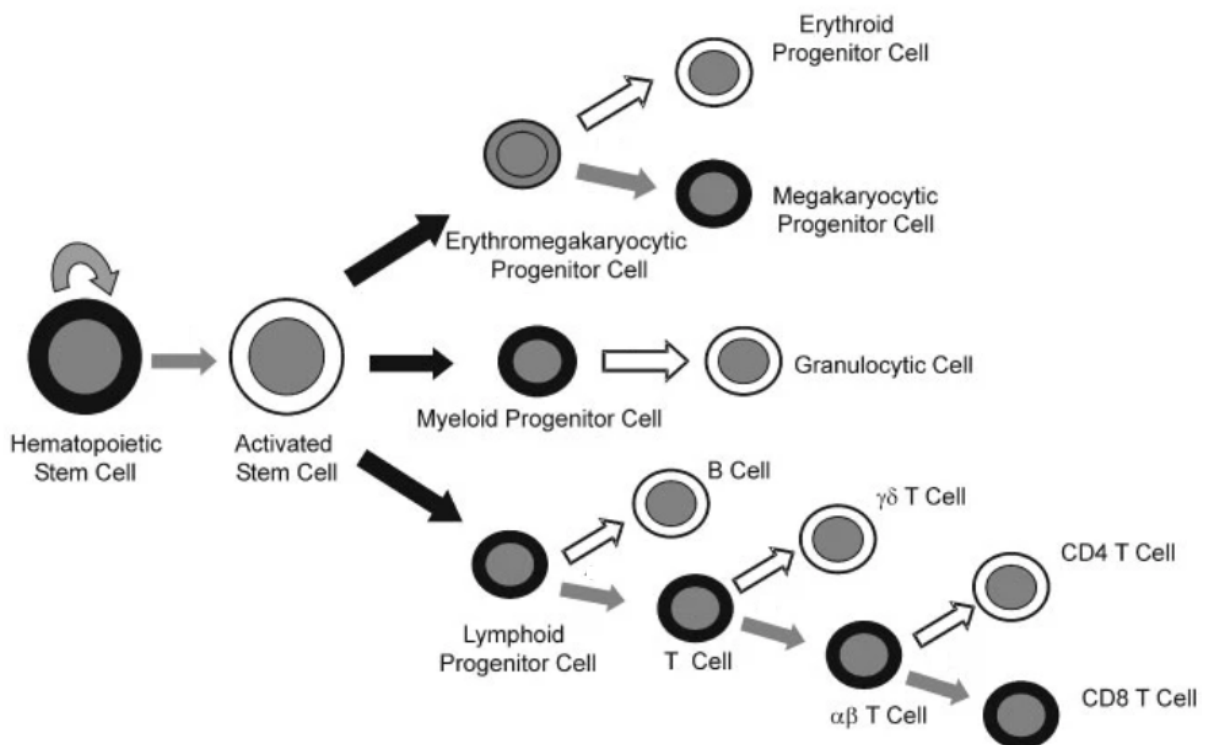


Figure 2: At each differentiation step, cells can differentiate into one of two different fates. Alternatively, the binary decision may be whether or not the stem/progenitor cell should differentiate. The fate that is taken when notch expression is lacking or decreased is shown with a white arrow pointing to a white cell. The alternative pathway, shown with a gray arrow and a black cell, is taken by the daughter cell when notch expression is high¹⁹.

Examples of growth factors that affect HSC and progenitor cell expansion include interleukin (IL)-6 and soluble IL-6 receptor (sIL-6R), stem cell factor (SCF), which is secreted by EC in the BM²⁰, erythropoietin²¹, and transforming growth factor (TGF- β).

In the need for increased leukocyte production, as it happens during infection, SCF binds to its receptor c-Kit on the HSC and controls self-renewal and development of hematopoietic cells²².

TGF- β is a classic example of a soluble growth factor that affects stem cell survival and maintains HSC in a quiescent stem cell state²³. Several other cytokines and colony-stimulating factors regulate hematopoiesis and can lead to alterations in the lineage output of HSC²⁴.

2. Bone marrow microenvironment (BMM)

The concept of the “niche” and the interaction between the microenvironment and the HSC was first described by Schofield in 1978²⁵. Since then, extensive research has revealed the existence of the BMM as a complex entity consisting of different types of secreted factors, cellular components including osteoblasts, osteoclasts, endothelial cells, mesenchymal stromal cells (MSC), and neuronal cells, as well as, extracellular matrix proteins²⁶.

The idea of hematopoietic stem and progenitor cell (HSPC) support and hematopoietic regeneration by vascular structures was suggested from the late 20th century²⁷, while later studies proved the regulatory role of endothelial cells in hematopoiesis²⁸. Even though the division of the BM into vascular and endosteal niches is considered arbitrary, a combination of studies focusing on the sub-compartments and components of either one is beginning to unravel the intricacies of the entire BM in a biologically relevant context. The terms endosteal and vascular are old and not used in the literature anymore, however, are used here only to simplify the content.

2.1 Endothelial cells

Endothelial cells are the cells that line the interior surface of blood vessels and have been found to support HSC by providing several factors²⁹. The central niche, which is found in the inner BM, consists mainly of sinusoids and arterioles and hosts

more than 85% of the HSC³⁰. However, also in the endosteal niche, which is in close proximity to the bone surface, HSC are found close to perivascular niches³¹. Early studies showed that endothelial cells produce angiocrine factors like Notch ligands that promote the regeneration and self-renewal capacity of HSC after BM injury^{18,32}. Furthermore, BM HSC were reduced after conditional deletion of SCF in both endothelial and perivascular cells³³. Interestingly, different endothelial cell types have been identified with fluorescence-activated cell sorting (FACS) methods able to distinguish between arterial endothelial cells and sinusoidal endothelial cells providing further information on the real cells that release some of these factors. For example, it was demonstrated that SCF is exclusively produced by the arterial vasculature of the BM contributing to the maintenance of HSC number²⁰. Finally, permeability and reactive oxygen species of vessels can affect HSC quiescence and differentiation status which is also controlled by HSC proximity to the vessels ^{34,35}.

2.2 Osteoblasts and osteoclasts

Bone remodeling is a continuous process involving the constant formation and degradation of the bone by osteoblasts and osteoclasts, respectively. Osteoprogenitor cells and mature osteoblasts are derived from Nestin⁺ MSC and C-X-C Motif Chemokine Ligand (CXCL) 12-abundant reticular (CAR) cells and line the bone surface of the endosteum. These cells have been found to support hematopoiesis. Specifically, osteoblasts support HSC expansion³⁶, and ablation of osteoblasts in transgenic mouse models proved their importance in HSC and myeloid, lymphoid and erythroid progenitors' maintenance^{37,38}. The influence of osteoblasts in the maintenance of all these populations is linked to a general role of osteoblasts in

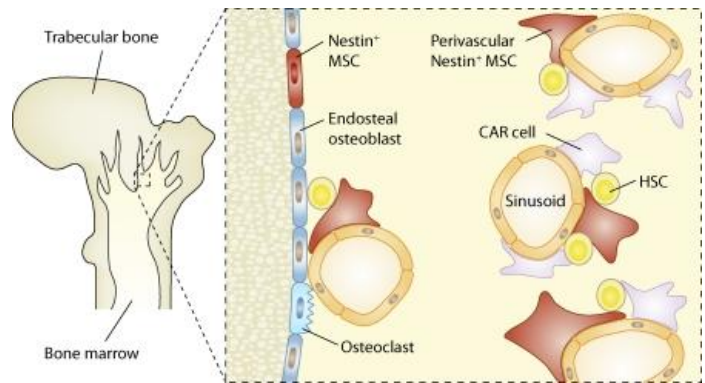
hematopoietic development in the BM and seems to be controlled by the release of specific factors.

The proposed role of osteoblasts in HSC maintenance led to the formulation of the concept of the endosteal niche. The endosteal niche, which is majorly composed of the osteoblastic cells, was the first location proposed as an HSC niche and later was demonstrated that HSC engraft to this niche with the help of their calcium-sensing receptor which recognizes the gradient of Ca^{2+} that is formed during bone remodeling³⁹.

In contrast, osteoclasts derived from the hematopoietic stem cells and their differentiation to bone-resorptive cells depends on the receptor activator of nuclear factor kappa-B ligand (RANKL), a cytokine released by osteoblasts⁴⁰. The data pertaining to osteoclasts role in hematopoiesis are scarce. However, they have been implicated in HSC mobilization by promoting progenitors' egress from the BM. Specifically induced osteoclast activity by RANKL promotes immature progenitors' mobilization to the circulation under both homeostatic and stress conditions. This is achieved by secretion of matrix metalloproteinase 9 (MMP-9) and cathepsin K from osteoclasts which in turn lead to cleavage of components of the endosteal niche known to enhance HSC anchorage and retention to the BM, like osteopontin and (stromal cell-derived factor 1) SDF-1, which are both released by osteoblasts⁴¹.

2.3 Mesenchymal stromal cells (MSC)

MSC are found in many tissues in the body, including the BM. In a 2010 Nature study a strictly perivascular, nestin-expressing MSC population (nestin⁺ MSC) was identified to be



spatially associated with HSC and to express HSC maintenance genes, like *CXCL12*, *KIT ligand (KITLG)*, *IL-7*, maintenance⁴³.

vascular adhesion molecule 1 (VCAM-1), and *secreted phosphoprotein 1 (SPP1)*⁴².

Nestin⁺ MSC are typically found in central areas of the BM, however, they also appear in lower frequencies close to the endosteum (figure 3)⁴³. They are characterized by

increased self-renewal capacity both *in vitro* and *in vivo* and can give rise to all three

tissues namely bone, cartilage, and fat. A similar population of MSC are the

aforementioned CAR cells. CAR cells have similar morphology to vascular pericytes,

are more abundant than nestin⁺ MSC, and either surround sinusoidal endothelial cells

or are located in vessels near the endosteum³¹ (figure 3). CAR-cell depleted mice

show reduced cell size and number of HSC which are also found in a more quiescent

stage⁴⁴. These cells also express proteins that contribute to HSC maintenance like

SDF-1 and SCF, but, there is also evidence of HSC cell cycling and self-renewal

support by these cells⁴³. It is reported that nestin⁺ MSC might be more primitive

compared to the CAR cells⁴³. Furthermore, Nestin-GFP^{high} neural–glial antigen 2

(NG2)⁺ cells are MSC associated with arterioles throughout the BM and with vessels

near the bone surface and contribute to the formation of the HSC niche⁴⁵. Nestin-

GFP^{low}- CAR – leptin receptor (LepR)⁺ MSC are associated with sinusoids in the

central BM and produce SCF which is essential for the maintenance of HSC³³. Finally, paired related homeobox 1 (PRX1)-Cre transgene labels multipotent mesenchymal progenitors that do not express Nestin or LepR and have osteogenic and adipogenic *in vitro* differentiation potential⁴⁶. Deletion of C-X-C Motif Chemokine Ligand 12 (CXCL12) from these cells leads to a rapid loss of HSC⁴⁷. All mesenchymal stromal cells are known to have self-renewal capacity and differentiation potential that forms the important tissues bone, cartilage, and fat and are proved to be a part of the HSC niche.

2.4 Extracellular matrix (ECM)

The ECM is an integral component of the BMM. It consists of proteoglycans, fibrous proteins like collagen, fibronectin, and laminin, glycosaminoglycans like hyaluronic acid, chondroitin sulfate, heparan sulfate, and heparin, and, finally, matricellular proteins such as osteocalcin and periostin⁴⁸. Integrins and syndecans are important proteins that facilitate cell-ECM interactions which control essential cellular properties including migration, survival, and differentiation of cells of hematopoietic origin⁴⁸. In mammals integrins are assembled from eighteen α and eight β subunits. Integrins are non-covalently linked, heterodimeric molecules containing an α and a β subunit. Both subunits are type I transmembrane proteins, containing large extracellular domains and mostly short cytoplasmic domains. Which ligand in the ECM the integrin can bind to is defined by which α and β subunits the integrin is made of. Among the ligands of integrins are fibronectin, vitronectin, collagen, and laminin⁴⁹. Integrin α_4 has been proposed to facilitate the transmigration of pre-B cells and other progenitor cells through the stroma, specifically fibronectin, which is essential for their normal development⁵⁰. Furthermore, mutations in the β_2 integrin gene in humans and mice

lead to leukocyte adhesion deficiency type I which is characterized by significant leukocytosis⁵¹.

BM stromal cells or hematopoietic progenitors themselves secrete soluble factors including fibroblast growth factors (FGF), IL-1, and TGF- β 1, which are stored in the ECM and influence hematopoietic cells' lineage decisions and proliferation⁵². As mentioned above Ca²⁺ ions are trapped in the BM ECM and control the localization function of the cells that are present in the BM including HSC and progenitor cells³⁹. Furthermore, FGF-2 was shown to be essential for HSPC recovery after myeloablation. FGF-2 supported HSPC proliferation partly by facilitating supportive stromal cells' expansion and reduction of levels of reactive oxygen species⁵³.

Collagen type I is the most abundant protein of the BM ECM. However, collagen types II, III, V, and XI also contribute to the maintenance of bone structure⁵⁴. Collagen IXa1-deficient mice showed trabecular bone disorganization and increased levels of fibronectin, while they exhibited a reduction in myeloid cell number and differentiation, and impaired immune response⁵⁵.

Fibronectin is secreted in the BM as a dimer, and cellular components, like HSC, bind to it via integrin molecules. The binding of integrins to fibronectin facilitates the transfer of external signals, like tissue stiffness, matrix composition changes, and growth factor availability to the intracellular space, leading to the control of main cellular functions including survival, proliferation, migration, and adhesion⁴⁸. Consistent with the importance of integrin-mediated interactions of HSC with fibronectin it was demonstrated that fibronectin-integrin β 3 interactions are involved in the aggressive phenotype of therapy-resistant malignant hematopoietic cells⁵⁶.

Integrin signaling is also involved in the interaction of HSC with periostin, another secreted protein of the ECM. Specifically, the interaction of integrin αV with periostin seems essential for primitive HSC maintenance inhibiting the FAK/phosphoinositide 3-kinase (PI3K)/AKT pathway and in turn, increasing cyclin-dependent kinase inhibitor 1B (p27^{Kip1}) expression which leads to the promotion of HSC quiescence⁵⁷. Finally, in a recent study, it was shown that the vitamin K antagonist and anticoagulant warfarin leads to impaired BM macrophage and MSC-derived periostin, its defective binding to integrin $\beta 3$ on HSC, and in turn, reduction of functional HSC and possible predisposition of individuals with such impaired signaling to a higher risk of myelodysplastic syndrome (MDS) development⁵⁸.

3. Leukemia

Leukemias are a heterogeneous group of malignancies characterized by the uncontrolled growth of abnormal blood cells. The word leukemia is derived from the words λευκός “leukos” which means white and αἷμα “haima” which as it was already mentioned means blood. Leukemia means “white blood” due to the accumulation of abnormal leukocytes in the body. It is a disease that – in most types of leukemia - is characterized by high molecular diversity and complexity. Leukemias can be classified by their lineage into lymphoid or myeloid, into acute or chronic depending on the clinical course, and further into subgroups depending on the cell’s differentiation status and genetic features. According to this classification, lymphoid leukemias comprise acute lymphoblastic leukemia (ALL) and chronic lymphocytic leukemia (CLL), while, myeloid leukemias are divided into acute myeloid leukemia (AML) and chronic myeloid leukemia (CML). Depending on the lineage the lymphoid leukemias are further classified to B- and T-cell ALL and B- and T-cell CLL^{59,60}.

3.1 Chronic myeloid leukemia (CML)

CML is a malignancy that originates in the HSC and is characterized by the accumulation of abnormal myeloid cells of different maturation stages in the BM and

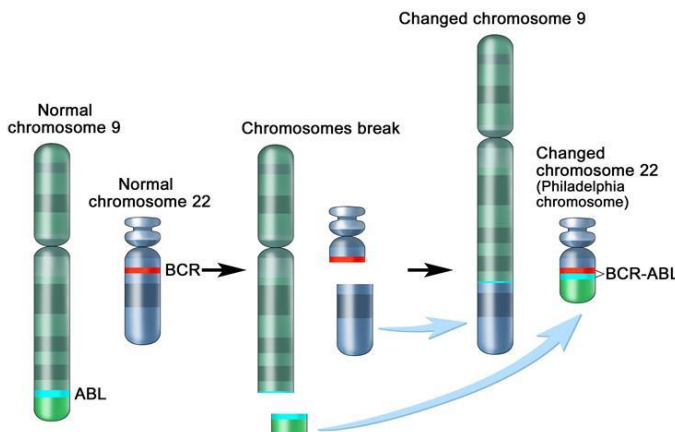


Figure 4: Philadelphia chromosome derived from a reciprocal translocation between chromosome 9 and chromosome 22⁶³.

the peripheral blood (PB). The cause of the disease is a constitutively active tyrosine kinase which is produced after a chromosomal translocation between chromosome 9 and chromosome 22, $t(9;22)^{61}$ and called BCR-ABL1^{62,63}. Specifically, the *ABL1* proto-oncogene on chromosome 9 is translocated to the chromosome 22. This new

chromosome is called Philadelphia chromosome (figure 4).

There are three different BCR-ABL1 proteins which, depending on their molecular weight, are called p210, p190, and p230 and are described in more detail below. Retroviral transduction of murine BM with BCR-ABL1 leads to a CML-like myeloproliferative disorder in mice⁶⁵ and causes cellular transformation of hematopoietic cells^{66,67} proving its central role in CML pathogenesis⁶⁸.

Since about 50% of patients diagnosed with CML are asymptomatic the diagnosis of the disease occurs usually during a routine physical examination or a blood test⁶⁹. CML is classified into three phases: the chronic phase (CP), accelerated phase (AP), and blast phase (BP) and the most common symptoms of CML-CP, which is the most common phase in which patients with CML present to the doctor, involve fatigue,

weight loss, and malaise which are usually the results of anemia and splenomegaly⁶⁹. Until the end of the last century, CML was treated with nonspecific drugs including hydroxyurea and interferon-alpha (INF- α)⁷⁰. Even though INF- α therapy might result in disease regression and improved survival it shows modest efficacy and a degree of toxicity. Furthermore, allogeneic stem cell transplantation (allo-SCT) is curative, however, is linked with high morbidity and mortality, which usually relegates this option to younger patients who have an appropriate donor⁶⁹. The discovery of tyrosine kinase inhibitors (TKI) which target the binding of adenosine triphosphate (ATP) to the kinase domain of BCR-ABL1 was one of the biggest scientific revolutions in recent medicine and improved the 10-year survival of patients from 20% to 80-90%⁶⁹. Imatinib was the first TKI that was designed and still, along with nilotinib, is the gold standard for first-line treatment of CML. However, imatinib resistance and intolerance led to the development of next-generation TKI⁷¹ which include nilotinib, dasatinib, and bosutinib and are approved for treatment of CML patients in CP⁶⁹. All CML cases are by definition positive for BCR-ABL1, however, this oncogene is found also in 25% of adult and 3-5% of pediatric cases of B-ALL⁷².

3.2 B-cell acute lymphoblastic leukemia (B-ALL)

In general, the hallmarks of acute lymphoblastic leukemia (ALL) involve chromosomal translocations and genetic alterations that affect lymphoid precursor cells' differentiation and proliferation. ALL that affects B-lymphocytes (B-ALL) is the most frequent malignancy in the pediatric population (26% of cancers in children 0-14 years old) where it accounts for more than 80% of the ALL cases. However, B-ALL also affects a significant proportion of adults, and 75% of ALL in adults affects cells of the B-lineage⁷³.

ALL subtypes are characterized by a variety of genetic alterations, like point mutations and deletions, as well as, big chromosomal changes like hyperdiploidy or translocations^{74,75}. Often the result is the generation of a fusion gene coding for a protein with altered properties like a constitutively active kinase or a novel transcriptional regulator⁷⁶. Some common and well-studied chromosomal translocations in B-ALL patients are: t(4;11) MLL-AF4, t(12;21) ETV6-RUNX1, t(1;19) E2A-PBX1 and, as already mentioned, t(9;22) BCR-ABL1⁷⁷.

The prognosis of B-ALL ranges from excellent to dismal depending on the cytogenetic abnormality. For example, in the cases of B-ALL with hyperdiploidy or *TEL/AML* rearrangement, the prognosis is significantly better than in the cases of BCR-ABL1 translocation or mixed-lineage leukemia gene (*MLL*) rearrangement. As mentioned above *BCR-ABL1* fusion is present in a significant percentage of B-ALL cases (usually called Philadelphia chromosome-positive (Ph⁺) or BCR-ABL1⁺ B-ALL). Before the introduction of TKI, BCR-ABL1⁺ B-ALL was associated with poor survival. The intensive chemotherapy regimens still remain the main treatment option, however, the introduction of imatinib or related TKI in combination with chemotherapy has improved the survival of these patients^{72,78}. Nevertheless, in general, the prognosis of ALL patients depends on the age, white blood cell count, and response to chemotherapy. The curative rates of the disease are on average quite high, especially in children. However, the resistance of leukemia cells to specific inhibitors, the presence of few resistant and relapse-inducing leukemia stem cells, as well as, the age of patients as a limiting factor for HSCT and/or aggressive chemotherapy, are still factors that can contribute to poor prognosis in a significant number of patients with ALL⁷³.

The normal BCR protein has an intrinsic serine/threonine kinase activity^{79,80}, while ABL1 belongs to the c-ABL kinase family, has DNA-binding activity, and can be found in both the cytoplasm and nucleus with involvement in hematopoiesis and B cell development⁷⁷. As it happens in CML, in BCR-ABL1⁺ B-ALL the chromosomal translocation t(9;22) leads to the constitutively active tyrosine kinase BCR-ABL1⁷².

Three different BCR-ABL1 proteins can be produced depending on the exact site of the chromosomal translocation: A 210 kDa form (p210) accounting for more than 95% of the CML cases, 15% of pediatric and 30-50% of adult B-ALL⁸¹, a 190 kDa BCR-ABL1 protein (p190) found in 85% of BCR-ABL1⁺ pediatric B-ALL cases and 50-70% of adult B-ALL⁸¹ and a rare 230 kDa BCR-ABL1 protein (p230) detected in patients with chronic neutrophilic leukemia (CNL)^{82,83}. Unlike CML, where the transformation occurs in stem cells in most cases of Ph⁺ ALL the genetic defect affects progenitor cells in the more committed lymphoid lineage⁷⁷.

The constitutively active kinase isoforms of BCR-ABL1, p190 and p210, can transform cells causing resistance to apoptosis and increased proliferation by activating multiple pathways including JAK/STAT and PI3K/AKT/mTOR pathways⁸⁴⁻⁸⁶, while the activation of the latter results in upregulation of the antiapoptotic protein B-cell lymphoma 2 (Bcl-2) and the transcription factor c-Myc⁸⁷.

3.3 Chronic lymphocytic leukemia (CLL)

CLL is the most common leukemia in adults and is characterized by the accumulation of monoclonal, mature, CD5⁺ B lymphocytes in the blood, the bone marrow and in secondary lymphoid organs (spleen and lymph nodes)⁸⁸. The clinical course of the disease varies and ranges from asymptomatic that may not require therapy (in 30% of patients) to active disease leading to lymphocytosis (increased

number of lymphocytes in the blood), anemia (reduction of red blood cells in the blood), lymphadenopathy (formation of lymph nodes of abnormal size and/or consistency), weight loss and fatigue among others⁸⁸. The average age at diagnosis is 72 years and the clinical management of the disease depends on its stage. For example, patients with early-stage CLL are normally not treated and have a median life-expectancy of 13 years. On the other hand, patients with advanced-stage CLL had a median life expectancy of only 2 years when only alkylating agents were used as primary treatment. However, the survival of patients with advanced-stage CLL has improved significantly with the use of more recent novel agents. CLL proliferation which occurs mainly in secondary lymphoid organs requires the engagement of the B-cell receptor (BCR) and the activation of its downstream signaling. Specifically, downstream of BCR kinases including spleen tyrosine kinase (SYK), Bruton's tyrosine kinase (BTK) and PI3K are activated and promote downstream pathways including the NF- κ B and ERK pathways. Other molecules on the surface of the CLL cells like CD19 and CD20 are essential, along with BCR, for the transfer of the signal that leads to the survival and proliferation of CLL cells. Blockade of CD20 with specific anti-CD20 antibodies like rituximab and obinutuzumab administered in combination with chemotherapy have significantly improved the survival of CLL patients^{89,90}. Finally, novel agents have been introduced. These involve kinase inhibitors like the BTK inhibitor ibrutinib and venetoclax which binds to the anti-apoptotic protein B-cell lymphoma-2 (Bcl-2) and leads to programmed cell death of CLL cells. The usage of these new agents (venetoclax⁹¹, ibrutinib⁹²) has shown a survival benefit compared to old CLL treatments, including chemoimmunotherapy (chemotherapy + anti-CD20 therapy) especially for advanced stage or chemotherapy resistant CLL⁸⁸.

3.4 Acute myeloid leukemia (AML)

AML is a malignant disorder of HSC or myeloid progenitor cells which is characterized by the accumulation of abnormal myeloid cells in an undifferentiated stage in the BM or other organs. It is the most common acute leukemia in adults⁹³ and despite the improvements in patients' outcome the prognosis remains poor⁹⁴. AML is a heterogeneous disease, both molecularly and cytogenetically, and this heterogeneity is important for disease prognosis, while novel treatment strategies which will take into account this heterogeneity are under intensive research⁹⁴. Genetic abnormalities are commonly present in AML and include mutations in genes such as the tyrosine kinase receptor gene *FLT3*⁹⁴, in genes that code for myeloid transcription factors like *RUNX1*⁹⁴, and in genes that are involved in DNA methylation regulation including *DNMT3A*⁹⁵ and *TET2*⁹⁶. Furthermore, in AML, chromosomal translocations can lead to the occurrence of fusion genes like the mixed-lineage leukemia gene (*MLL1*) which has been associated with aggressive acute leukemia⁹⁷. Specifically, the translocation t(9;11) results in the expression of the *MLL-AF9* fusion gene which is associated with poor prognosis⁹⁸.

4. The bone marrow microenvironment in leukemia

As it happens in many cancers, in non-solid tumors the microenvironment is an important contributor to tumor progression and drug resistance. While the majority of studies so far have focused on intrinsic pathways of leukemia cells that could be targeted for therapeutic purposes, increasing evidence supports the importance of the BMM in the maintenance and survival of malignant cells. Additionally, the BMM has been proven to play a key role in the acquisition of a therapy-resistant phenotype by

leukemia cells, as well as, in their ability to egress from the BM and colonize other organs⁴⁵.

Recently, studies in mice have shown the contribution of the niche at least in hematological malignancies in two different ways: 1) altered niche cells that predispose healthy cells to malignant development^{99,100} and 2) transformed hematopoietic cells that can alter their niche to make it favorable for their survival and consequent disease progression⁴⁵.

4.1 The altered niche as predisposing factor

Several niche alterations have been found to make the normal cells transform into malignant ones. These alterations have been found to occur more frequently in myeloid malignancies. For example, β -catenin constitutively active specifically in osteoblasts led to AML-related chromosomal alterations in hematopoietic cells which resulted in an increased differentiation towards the myeloid lineage¹⁰¹. Studies in mice show that alterations in the niche can initiate oncogenic events in the case of clonal hematopoietic stem cells diseases like myelodysplastic syndrome (MDS) and myeloproliferative neoplasia (MPN) which have high risk of transformation to secondary AML. For example, mice lacking nuclear factor- κ B (NF- κ B) inhibitor α (I κ B α)¹⁰² or retinoic acid receptor- γ (Rar- γ)⁹⁹ in non-hematopoietic cells develop MPN-like disease. Rar- γ deficient microenvironment leads to MPN-like disease partly due to increased levels of tumor necrosis factor (TNF) α (TNF- α) in these mice⁹⁹. Lastly, deletion of *Dicer1* the gene encoding a ribonuclease specifically in MSC, but not in mature osteoblasts, leads to MDS-like disease with sporadic transformation to AML¹⁰³. A common feature in many of these studies is the establishment of a pro-inflammatory environment which which can contribute to excessive myelopoiesis⁴⁵. However, these

studies have been conducted in mice and the relevance of these observations for human disease remain to be elucidated.

4.2 Niche remodeling by leukemia cells

In hematological malignancies the genetic and epigenetic alterations in hematopoietic cells coincide with niche remodeling which favor the survival of malignant cells at the expense of normal HSC.

Cytokines and growth factors

In a BCR-ABL1⁺ CML transgenic model, leukemia cells promoted MSC to overproduce altered osteoblasts which form a remodeled BM niche that favors LSC function while impairing normal hematopoiesis¹⁰⁴. These effects were mediated via direct cell-cell interactions of malignant cells with MSC or by release of factors like thrombopoietin (TPO) and chemokine (C-C motif) ligand 3 (CCL3)¹⁰⁴. CCL3 has also been implicated in niche remodeling by AML cells. CCL3 was found increased in the malignant cells in AML cells and led to inhibition of osteoblastic cells¹⁰⁵. Altered cytokine expression with downregulation of CXCL12, a cytokine involved in homing, and increased production of granulocyte colony-stimulating factor (G-CSF) which is involved in hematopoietic mobilization in the BMM by leukemia cells was also correlated with inhibition of normal long-term hematopoietic stem cells and a growth advantage of malignant cells in both CML¹⁰⁶ and B-ALL¹⁰⁷. Furthermore, IL-1 β produced by mutated HSC triggers neuronal damage in the BM which leads to reduction of MSC number. In turn, *in vivo* depletion of nestin⁺ cells or their CXCL12 production expanded the number of mutated HSC and led to MPN expansion¹⁰⁸. Another way that leukemia cells influence the BMM is by remodeling the ECM. Indeed, it was demonstrated that B-ALL cells induce MMP-9 expression in MSC and possibly

other cells of the BMM via a release of TNF α . Pharmacological inhibition of MMP-9 leads to prolongation of survival in mice with B-ALL.

Neo-angiogenesis is a well-established phenomenon in both acute and chronic leukemias¹⁰⁹ while disruption of vasculature it has also been observed in the presence of leukemia¹¹⁰. These phenomena are partially mediated by specific growth factors released by leukemia cells which affect endothelial cells function. For example, in ALL leukemia cells promote BM endothelial cells proliferation via soluble factors, one candidate being vascular endothelial growth factor (VEGF) and in turn the BM endothelium promotes leukemia cell survival¹¹¹. In AML VEGF-activated endothelial cells enables the proliferation of leukemia cells while decreasing the efficacy of chemotherapeutic drugs to target leukemia cells¹¹². Interestingly, AML cells differentially remodel the vasculature in central and endosteal bone marrow niches. In the presence of AML cells the endosteal endothelium is degraded while the vascular niches in the central marrow expand. In turn, the degraded endosteal endothelium cannot support normal HSC and when the endosteal endothelium is preserved the normal hematopoiesis is rescued¹¹³. Finally, CML cells induce BM stromal cells to upregulate placental growth factor (PIGF) a VEGF homolog which stimulates BM angiogenesis and promotes CML proliferation¹¹⁴.

Exosomes

Exosomes are a type of extracellular vesicles (EV) that carry lipids and proteins and play a key role in cellular communication. The biogenesis and structure of exosomes as well as that of other extracellular vesicles will be discussed in more detail below. Exosomes serve as means by which leukemia cells remodel the BMM. Specifically, AML cells release exosomes enriched for coding and noncoding RNA which are up taken by BM stromal cells and change their secretion profile¹¹⁵. In a more

recent study, it was shown that AML-derived exosomes transform the BM niche to a leukemia-permissive environment. They induced the expression of dickkopf-related protein 1 (DKK1), a suppressor of normal hematopoiesis and osteogenesis, thereby contributing to osteoblast loss. AML-derived exosomes induced a broad downregulation of hematopoietic stem cell-supporting factors, like CXCL12 and insulin-like growth factor 1 (IGF-1), in BM stromal cells and reduced their ability to support normal hematopoiesis¹¹⁶. Furthermore, EV from AML cells can transfer endoplasmic reticulum (ER) stress to MSC leading to upregulation of core unfolded protein response (UPR) components and subsequent induction of their osteogenic differentiation partially through the transfer of the bone morphogenetic protein 2 (BMP2)¹¹⁷. CML cells also release exosomes that can stimulate BM stromal cells to release IL-8 that in turn promotes the adhesion and migration of leukemia cells¹¹⁸. MicroRNA (miRNA) are small non-coding RNA molecules referred to as master regulators of the genome and exosomes are known to carry miRNA which are transferred into neighboring cells and can be translated and functional¹¹⁹. It was demonstrated that CML cells transfer exosomes containing the miRNA mi-126 to endothelial cells and lead to reduction of CXCL12 and VCAM-1 in endothelial cells and to a decrease in the mobility and adhesion of CML cells¹²⁰.

4.3 BMM-mediated survival and therapy resistance of leukemia cells

CXCR4/CXCL12 axis

Resistant LSC may be the reason for resistance to chemotherapy and relapse¹²¹. It is believed that these cells reside in specific niches in the BM where the BMM promotes their maintenance, therapy resistance, and in turn disease relapse¹²². Therefore, targeting of the interactions between leukemia cells and their microenvironment is a potent strategy to increase therapy sensitivity. C-X-C

chemokine receptor type 4 (CXCR4) is a chemokine receptor expressed on the surface of normal hematopoietic cells but also leukemia cells including AML and CML cells. It is demonstrated that CXCR4 and the binding on its ligand CXCL12 (also called stromal cell-derived factor 1 (SDF-1)) regulates the motility and development of AML stem cells¹²³. In this context it was further established that acute promyelocytic leukemia (APL) cells, an aggressive type of AML cells, when are cocultured with stromal cells are protected from chemotherapy-induced apoptosis *in vitro* while injection of these cells to syngeneic recipient mice leads to rapid migration to the BM egress to the spleen and peripheral blood and death. However, administration of AMD3100, a specific inhibitor of CXCR4, in combination with chemotherapy led to decreased tumor burden and improved survival compared to the treatment with chemotherapy alone indicating the importance of the CXCR4-CXCL12 axis in AML chemoresistance¹²⁴. In the same line AMD3100 was used in a clinical trial in combination with chemotherapy for the treatment of relapsed or refractory AML to test whether interference with the interaction between AML blasts and the microenvironment can enhance the cytotoxic effect of chemotherapy with encouraging rates of remission¹²⁵ (NCT00512252). CXCR4 has also been implicated in multiple myeloma, a hematological malignancy caused by the abnormal production of plasma cells, and CML stroma-mediated chemoresistance. In CML the presence of BCR-ABL1 inhibits the CXCR4/CXCL12 axis leading to reduction of adhesion of CML cells to the BM stroma. Consequently, TKI treatment enhances the migration of CML cells to the BMM making them more resistance to the treatment. It was demonstrated that proto-oncogene tyrosine-protein kinase Src-related Lyn kinase was implicated in TKI-induced migration of CML cells which involved the redistribution of CXCR4 into the lipid raft fraction in CML cells¹²⁶. Finally, CXCR4 has also been involved in the

interaction of multiple myeloma cells with their microenvironment where contributes to resistance to therapeutic agents¹²⁷.

Integrins and selectins

As it was already mentioned, integrins represent a large family of adhesion molecules that are widely expressed and mainly interact with extracellular matrix components. From very early on integrins, specifically integrin $\beta 1$ in cooperation with the cell surface glycoprotein CD44, have been involved in the adhesion and migration of CML cells¹²⁸. Incubation of CML cells with the integrin $\beta 1$ activating antibody, 8A2, increases the cooperation between integrin $\beta 1$ and CD44, induces the adhesion of CML to fibronectin and the adhesion-mediated inhibition of proliferation¹²⁸. Minimal residual disease (MRD) is a term used to describe a small number of leukemic cells that remain in the person during treatment, or after treatment when the patient is in remission and it is the major cause of relapse in cancer and leukemia. It has been demonstrated that in AML resistance to drug-induced apoptosis is mediated by the interaction of the very late antigen (VLA-4) expressed on leukemia cells to fibronectin and that in a mouse model of MRD VLA4-specific antibodies in combination with the chemotherapeutic drug cytarabine significantly prolonged mice survival compared to cytarabine treatment alone¹²⁹. Furthermore, $\beta 1$ and $\beta 2$ integrins mediate the interaction of CLL with the endothelial layer, an interaction that decreases the sensitivity of CLL cells to the apoptosis induced by the chemotherapeutic agent fludarabine¹³⁰. Lastly, interaction between VLA-4 on leukemia cells and VCAM-1 in BM MSC mediates the activation of the NK- κ B pathways in both stromal and tumor cells which promote chemoresistance in the transformed cells¹³¹.

Selectins comprise a family of three members (E-, P-, and L-selectin) that are differentially expressed by leukocytes and endothelial cells and are involved in the

early steps of leukocyte extravasation. In a CML-like MPN mouse model was proven that selectins and specifically E- and L-selectin and their ligands are indispensable for the homing and engraftment of BCR-ABL1⁺ leukemia stem cells compared to normal stem cells¹³². In line with these observations, treatment with the E-selectin inhibitor GMI-1271 in combination with imatinib led to increased survival of mice with CML via decrease in the contact of leukemia cells with the BM endothelium¹³³.

5. Bone marrow microenvironment in B-ALL

Several studies have reported the importance of the BM stroma for survival, as well as, the evasion from chemotherapy of B-ALL cells. It was early on demonstrated that the presence of BM stromal cells *in vitro* supports the growth of B-ALL cells and leads to the survival of blast cells¹³⁴. Furthermore, osteoblasts support the survival and migration of B-ALL cells towards them by the release of growth-specific-6 (GAS6) while induce dormancy to the B-ALL cells which in turn prevents chemotherapy-induced apoptosis¹³⁵. The dormancy of B-ALL stem cells was also induced by their anchorage on osteopontin, an extracellular matrix protein released by osteoblasts. In a xenograft mouse model of B-ALL, inhibition of the osteopontin-signaling axis increased B-ALL cell cycle and reduced the tumor burden while osteopontin neutralization in combination with cytarabine reduced BM MRD¹³⁶. In the same lines and as it was mentioned above modulation of the extracellular matrix of the BMM with pharmacological inhibition of BMM MMP-9 can lead to prolonged survival in mice with B-ALL¹³⁷.

B-ALL cells adhere to BM stromal cells¹³⁸ or fibronectin¹³⁹ via integrins, and these interactions lead to reduced apoptosis and increased drug resistance of the leukemia cells. The adhesion of B-ALL cells to the stroma is partially achieved via the CXCR4/CXCL12 axis and targeting of CXCR4 with the drug AMD11070 in

combination with nilotinib led to significant prolongation of survival in mice transplanted with BCR-ABL1 B-ALL¹⁴⁰. Furthermore, in a mouse model of BCR-ABL1 leukemia characterized by alterations in the transcription factors IKAROS, B-ALL cells show increased self-renewal and increased BM stromal adhesion while the usage of retinoids reversed these phenotypes¹⁴¹. Finally, it was shown that BM MSC are stimulated by B-ALL cells and express increased levels of CCL2 and IL-8 and these two cytokines are also found increased in the BM plasma of children with B-ALL at the time of diagnosis. CCL2 and IL-8 enhance the survival and proliferation of MSC and support the adhesion of B-ALL to them¹⁴². In another study it was shown that MSC from B-ALL patients had increased adipogenic capacity while they were expressing increased levels of the bone morphogenetic protein 4 (BMP4)¹⁴³.

The cells of the BMM are reprogrammed in the presence of B-ALL and their metabolism is often altered. In turn the microenvironmental metabolome can influence tumor survival. In addition, drug therapy can affect the metabolism of the BMM cells. In a study where the metabolic profiles of the PB and BM from children with ALL were examined it was demonstrated that the BMM of patients that had not received any treatment had a different metabolic profile enriched in lipids and metabolites of lipid metabolism while the BM upon remission showed a profile enriched in amino acid metabolites and its derivatives¹⁴⁴. Additionally, there is evidence of a crosstalk between ALL and BM MSC metabolic pathways as it was shown that cystine is imported and metabolized by MSC to provide the limiting substrate to ALL to generate and maintain glutathione. This metabolic interaction reduces the oxidative stress in ALL cells and it is essential for their survival¹⁴⁵.

Further studies have identified new strategies by which the BMM can reduce drug efficiency in B-ALL including metabolic reprogramming of B-ALL cells. Drug

resistant ALL cells, the potential cause of MRD, in the presence of BM MSC undergo a redox adaptation process characterized by reduced ROS levels and upregulation of antioxidants productions¹⁴⁶. Furthermore, stromal protein kinase C (PKC)- β controls the expression of adhesion and matrix proteins that are required for the activation of the PI3K pathway and the stabilization of B cells lymphoma-extra large (BCL-XL) mediating drug resistance in tumor cells¹⁴⁷. Finally, the aforementioned integrins and specifically integrin $\alpha 6$ via its role in ALL adhesion it has been implicated in ALL resistance and the usage of the anti-human $\alpha 6$ -blocking antibody Ab P5G10 induces apoptosis in primary ALL cells and sensitizes them to chemotherapy or tyrosine kinase inhibition¹⁴⁸.

6. Autophagy

6.1 The process of autophagy

Autophagy is a degradation process that is essential for cellular homeostasis and response to different forms of cellular stress and it is mediated by evolutionarily conserved autophagy-related (*ATG*) genes¹⁴⁹. During autophagy, the cargo (proteins, glycogenes, lipids, organelles, miRNA etc.) which is delivered to the lysosomes, is derived from the cytoplasm. In contrast, in the endocytic pathway the source of the cargo is either extracellular or plasma membrane-derived. Damaged cytoplasmic organelles and protein aggregates are cleared by a tightly regulated process that involves “eat me” signal tags (prominently ubiquitin chains) on the targeted proteins/organelles, autophagy adaptor, and autophagy receptor proteins¹⁴⁹. In the early years of autophagy research, in the middle to the end of the 20th century, two major discoveries laid the groundwork for the subsequent extensive research in the field. The first one was the discovery of lysosomes by Christian de Duve in 1955¹⁵⁰, along with the regulation of the process of autophagy by nutrient availability¹⁵¹ and

many years later the elucidation of the molecular mechanism of autophagy by the discovery of 15 autophagy related-proteins (ATG) in yeast by Yoshinori Ohsumi in

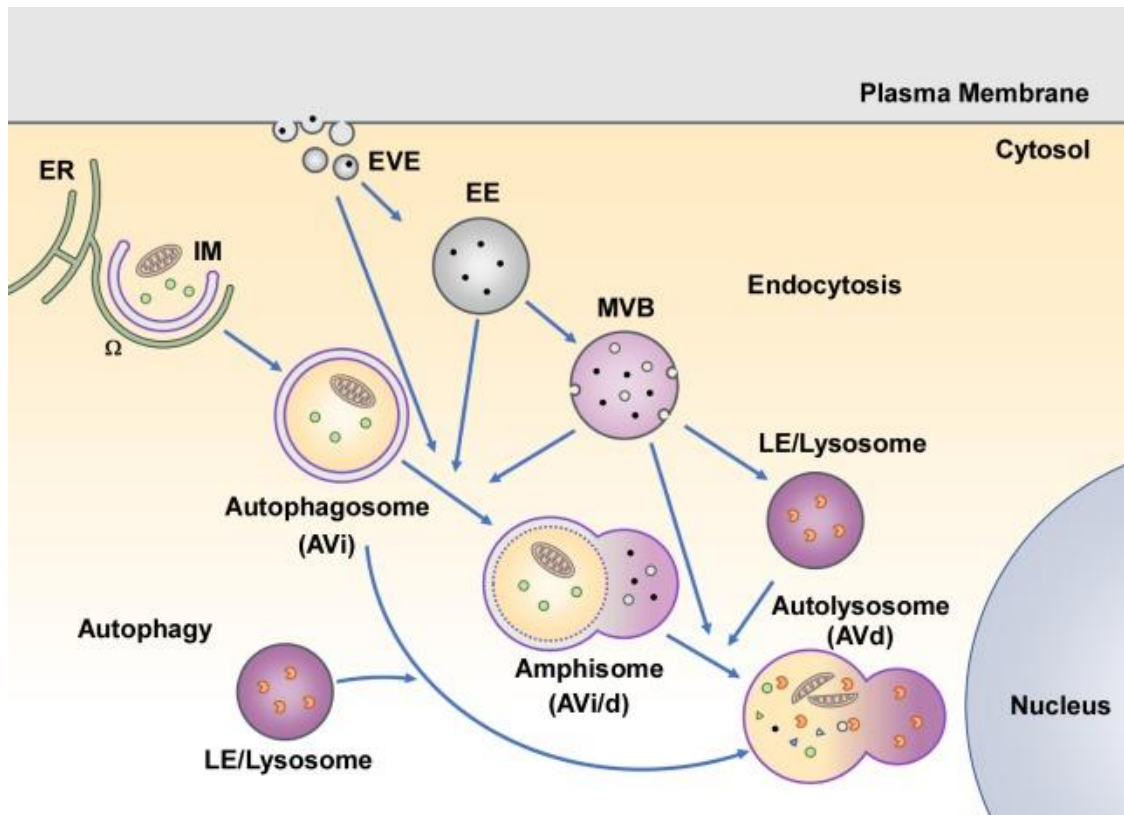


Figure 5: The autophagic pathway. EVE: vesicular endocytic vesicles; EE: early endosomes; MVB: multivesicular bodies¹⁵⁴.

1993¹⁵². The major and most well-studied type of autophagy is called macroautophagy. During the induction of macroautophagy, ATG are recruited to a specific subcellular localization where an isolation membrane called phagophore is formed. This membrane gradually elongates while engulfing cytoplasmic cargo and eventually closes to form a double-membrane structure called an autophagosome. Autophagosomes can fuse with endosomes, mature, and finally fuse with the lysosomes in order for the cargo to be degraded by the lysosomal enzymes^{153,154}(figure 5). The degradation of the cargo on the one hand protects the accumulation of deleterious cargo, like damaged mitochondria, and on the other hand, provides the cells with new building blocks.

Autophagy can be selective or non-selective depending on the cargo. During non-selective autophagy, which is usually induced upon starvation, bulk portions of cytoplasmic cargo are sequestered to the autophagosomes for degradation. By contrast, selective autophagy is recruited in cases of pathogen infection or for the maintenance of the integrity of cellular organelles ensuring cellular homeostasis¹⁵⁵. During this process, several proteins are responsible for autophagosome maturation, elongation, and closure, as well as, fusion with the lysosomes. These proteins belong to the superfamily of ATG8 proteins (microtubule-associated proteins 1A/1B light chain 3B (LC3) / gamma-aminobutyric acid receptor-associated protein (GABARAPs)), are conserved from yeast to human and recruit autophagy adaptors and receptors which contain an LC3-interacting region (LIR). ATG8 proteins promote cargo engulfment by directly binding to autophagy receptors or selective autophagy receptors (SARs) which bind to and serve as a bridge between the cargo and the phagophore^{155,156}. SARs, like sequestosome 1 (SQSTM1/p62¹⁵⁷), nuclear dot protein 52 (NDP52)¹⁵⁸, and neighbor of BRCA1 gene 1 protein (NBR1)¹⁵⁹, are eventually degraded along with the cargo¹⁶⁰. ATG8 proteins interact with another group of essential autophagic proteins that are called autophagy adaptors. Autophagy adaptors are not degraded by autophagy and have diverse roles in the process like in the regulation of the autophagosome formation (e.g. Unc-51 like kinase-1 (ULK1) complex¹⁶¹), the fusion of the autophagosomes with lysosomes (e.g. pleckstrin homology domain-containing family M member 1 (PLEKHM1¹⁶²)), and the transport of the autophagosome (e.g. FYVE And Coiled-Coil Domain Autophagy Adaptor 1 (FYCO1)¹⁶³).

6.2 The role of autophagy in health and disease

The main role of autophagy is to provide the cell with nutrients during fasting and other forms of stress. This is achieved by the recycling of intracellular components into

metabolic pathways, however, the specific substrates that autophagy provides and the metabolic pathways that are supported are not yet known¹⁶⁴.

Mutations in genes which lead to de-regulated autophagy are associated with several pathological conditions, including neurodegenerative diseases, inflammatory disorders, and cancer progression, therefore, modulation of the process of autophagy has great potential as a therapeutic approach¹⁴⁹. In cancer, the role of autophagy is not completely elucidated. Specifically, before the onset of tumorigenesis due to its cytoprotective role autophagy seems to act as a tumor-suppressive mechanism¹⁶⁵ and consequently loss of autophagy can increase cancer risk, while, autophagy blockade in established tumors sensitizes them to therapy^{166,167}. Moving a step further, clinical trials have been initiated which involve the treatment of cancer patients with autophagy inhibitors like hydroxychloroquine in combination with chemotherapy or targeted therapies. One such case is CML in which hydroxychloroquine was used in a randomized phase II clinical trial in combination with imatinib for the eradication of persistent BCR-ABL1+ leukemia stem cells¹⁶⁸. Evident of its dual role, autophagy prevents the onset of lung tumors, while it promotes the progression of lung tumors in the same KRas (G12D)-driven lung cancer mouse model¹⁶⁹. Therefore the exact role of autophagy in cancer seems to be cancer type and context dependent¹⁷⁰.

Even though autophagy has been extensively studied as a tumor-suppressive or tumor-promoting mechanism used by cancer cells its role in the tumor microenvironment has only now become the object of various research efforts¹⁷¹. The first studies in different cancer types, including lung and pancreatic cancer, melanoma, and urothelial carcinoma, point towards a tumor-promoting role of microenvironmental autophagy mainly by providing the tumor cells with essential amino acids to sustain their energy levels and metabolic integrity¹⁷²⁻¹⁷⁵.

7. The endocytic pathway

The endocytic pathway of mammalian cells consists of distinct membrane compartments which internalize molecules from the plasma membrane and either recycle them back to the plasma membrane or sort them for degradation¹⁷⁶. Therefore, lysosomal degradation is the final step of both the autophagic and the endocytic system. The endocytic system is complex and the sorting of the cargo is a tightly regulated process¹⁷⁷. The different compartments of the endocytic system have specific roles in the processing, sorting, and degradation of the internalized cargo which include early and recycling endosomes, late endosomes, and the lysosomes (figure 5)¹⁵⁴.

7.1 Multivesicular bodies

A specialized type of late endosomes are multivesicular bodies (MVB) which are essential for the internalization of nutrients, ligands, and membrane receptors¹⁷⁸. Within the MVB smaller vesicles that are called intraluminal vesicles (ILV) are formed by the invagination of the endosomal membrane with concurrent engulfing of cytoplasmic cargo¹⁷⁹. Interestingly, there is evidence suggesting that autophagosomes fuse with the MVB to form bigger vesicles that are called amphisomes and that this process is important for the efficiency of autophagic degradation^{178,180}. ILV have a size of 40 to 100nm and represent free vesicles with no connection with the vacuolar membrane. The incorporation of cargo from the outer membrane of the recycling endosome into the ILV is mediated by the endosomal sorting complex required for transport (ESCRT)^{181,182}.

8. Extracellular vesicles

When ILV do not degrade via fusion of the MVB with the lysosomes, they are released into the extracellular space. This is achieved after fusion of MVB with the

plasma membrane. The released vesicles, which range from 40 to 100 nm are called exosomes and play a key role in intercellular communication serving as vehicles for transferring proteins, lipids, and RNA between cells^{183,184}. Exosomes are part of a broad family of vesicles that are released extracellularly and are called extracellular vesicles (EV).

The current criteria to distinguish between the different EV populations are based on the size, the density, the subcellular origin, the function, and the molecular cargo¹⁸⁵. Possibly all cells, both healthy and malignant, release EV in a tightly regulated manner, and, interestingly, several types of EV can be released by a given cell¹⁸⁶.

Apart from exosomes, other vesicles that belong to the EV family are the microvesicles, the apoptotic bodies and the oncosomes and/or large oncosomes. Microvesicles are released by the outward budding of the plasma membrane and their size is small ranging from 0.1-1 μm . Apoptotic bodies are released also by membrane budding and their size ranges from 0.05-2 μm . Finally, oncosomes and large oncosomes have been reported to be released only by some tumor cells, like prostate cancer cells¹⁸⁷ and they range from 1-10 μm in size (figure 6)¹⁸⁸. EV can be taken up by the recipient cells through different mechanisms: macropinocytosis, phagocytosis, endocytosis, or fusion. They can also interact with receptors in the recipient cell membrane. EV contain cytosolic components (soluble proteins, DNA, mRNA, and non-coding RNAs (ncRNAs)) and express surface molecules of their cell of origin¹⁸⁸.

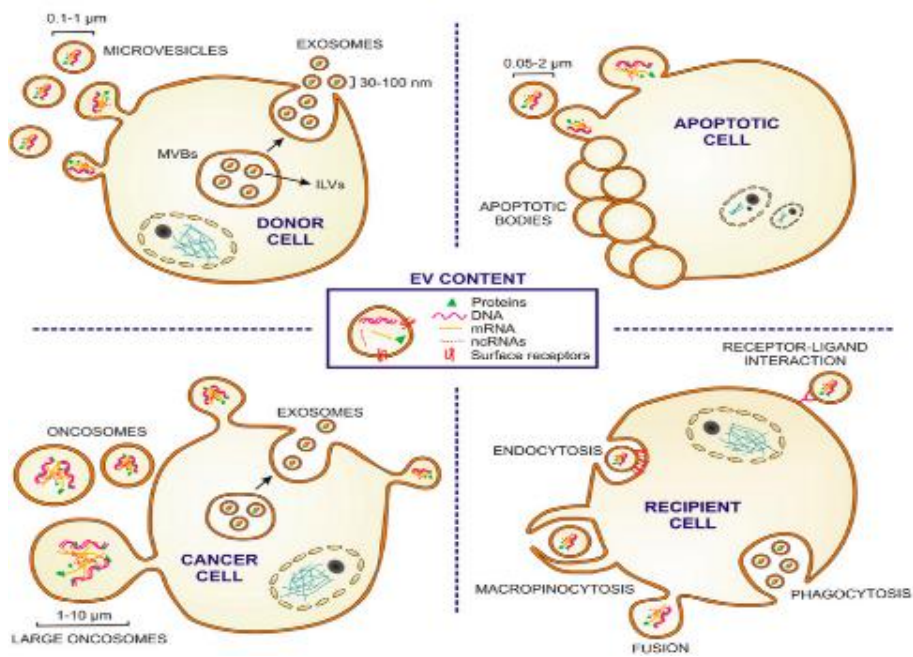


Figure 6: Extracellular vesicles: types, sizes, content, biogenesis, and uptake¹⁸⁸.

8.1 Pathways of exosome biogenesis

Exosomes are formed and released either in response to specific stimuli or continuously by a variety of cells including hematopoietic cells, MSC, as well as, cancer cells¹⁸⁹. Depending on the stimulus, the number and composition of the exosomes that are produced and released by a given cells varies¹⁹⁰⁻¹⁹². Exosome biogenesis starts with the plasma membrane invagination and continues with the cargo selection and formation of the ILV inside the MVB after the invagination of the MVB membrane¹⁸⁶. This process is tightly regulated and different pathways are involved in it. ESCRT-dependent and ESCRT-independent mechanisms work synergistically towards the completion of several steps of the process like protein sequestration and modification, processing and trafficking of the resulting vesicles, and fusion to the plasma membrane which is required for secretion^{193,194} (figure 7).

8.1.1 ESCRT-dependent pathway

There are many different molecules and enzymes involved in the exosome biogenesis and due to experimental challenges is unclear at which step the different molecules are involved. However, it is clear that more than twenty proteins are involved which belong to one of the four endosomal sorting complexes require for transport (ESCRT) namely ESCRT-0, ESCRT-I, ESCRT-II and ESCRT-III¹⁹⁴. Proteins of the ESCRT-0 complex are involved in the recognition and sequestration of the ubiquitylated cargo to specific domains of the endosomal membrane facilitating the first step of membrane invagination¹⁹⁵. After interaction with the ESCRT-I and -II complexes, the total complex will then combine with ESCRT-III, a protein complex that is involved in promoting the budding processes. Finally, following cleaving the buds to form ILV, the ESCRT-III complex separates from the MVB membrane with energy supplied by the sorting protein vacuolar protein sorting-associated protein 4 (Vps4).

ALG-2-interacting protein X (Alix) interacts with several ESCRT proteins, as well as, syndecan and syntenin and that way facilitates the endosomal budding and the selection of the cargo respectively. Syndecans are transmembrane proteins that represent the main source of heparan sulfate (HS) in cell membranes. Syndecans interact with syntenin, which, in turn, interacts with CD63, an important tetraspanin present on exosomes, and Alix¹⁹⁶. Heparinase is an enzyme that regulates¹⁹⁶. Finally, heparanase is an enzyme that cleaves syndecan's heparan sulfate chains and regulates the intraluminal budding of syntenin and syndecan into endosomes. It also controls the loading of these two proteins on the released exosomes¹⁹⁷.

8.1.2 ESCRT-independent pathway

The ESCRT-independent pathway is an alternative way to sort exosomal cargo into MVB and depends on raft-based microdomains. For example, sphingomyelin can be hydrolyzed into phosphorylcholine and ceramide. Ceramide promotes membrane budding contributing to this alternative exosome production¹⁹⁸. Another pathway is the tetraspanin-dependent pathway which involves CD63, which belongs to the superfamily of tetraspanins and along with partner molecules form tetraspanin-enriched microdomains which contribute to exosome formation¹⁹³.

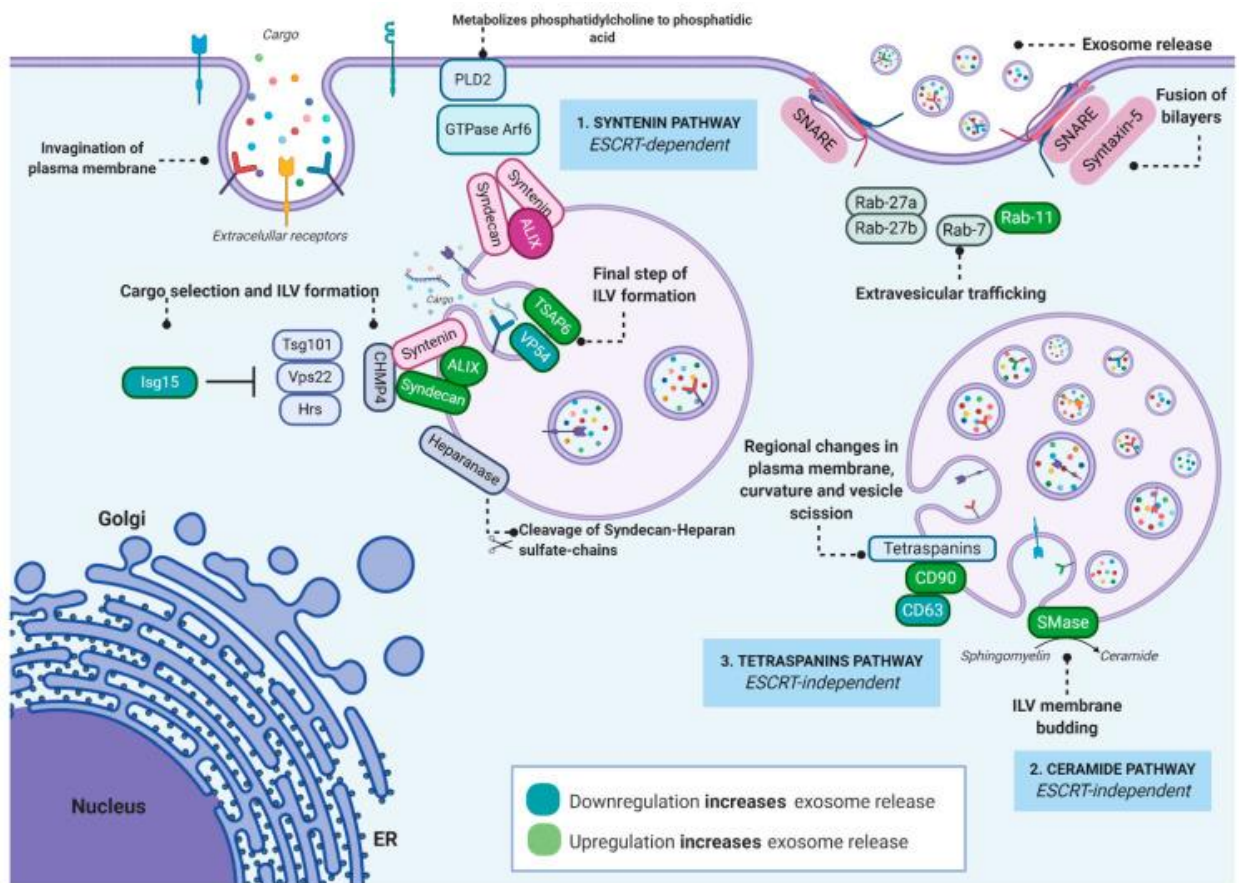


Figure 7: Different pathways of exosome biogenesis¹⁹⁴.

8.2 Extracellular vesicles and cancer

EV and particularly exosomes, as means of communication between cells, have been extensively studied in the context of cancer. Most studies focus on cancer-released exosomes and their effect on the tumor microenvironment. For example, cancer-derived exosomes promote the differentiation of fibroblasts to myofibroblasts that in turn promote tumor growth¹⁹⁹. However, several studies have also been focusing on EV released by the microenvironment.

Cancer-associated fibroblasts (CAF) release EV with specific cargo which can influence the migration and invasion of breast cancer cells, as well as, lead to metabolic reprogramming in the target cells^{200,201}. Furthermore, it was demonstrated that BM-MSC can support multiple myeloma cells, which are malignant plasma cells, via the release of exosomes which carry lower amounts of the tumor suppressor microRNA (miR) – 15a and, therefore, promote tumor growth *in vivo*²⁰². Furthermore, EV are key players in microenvironmental-derived therapy resistance of tumor cells by transferring proteins which increase tumor cell survival and DNA repair. In the tumor cells themselves, microvesicles can also increase therapy resistance by reducing intracellular drug concentrations and removing pro-apoptotic proteins²⁰³. Specifically, cancer cells resistant to chemotherapeutic drugs found to release more microvesicles which contained significantly bigger amount of these drugs compared to cancer cells sensitive to chemotherapy. This suggests that chemotherapeutic drugs may be extruded from cells via microvesicles²⁰⁴. Lastly, MSC-derived exosomes enhance angiogenesis of tumors by increasing VEGF expression in tumor cells by activating the extracellular signal-regulated kinase 1/2 (ERK1/2) and p38 mitogen-activated protein kinase (MAPK) pathways²⁰⁵.

It is evident from the nature of the autophagic, the endolysosomal, and the exosome biogenesis pathways which all involve vesicular trafficking and fusion events that an intricate relationship exists among them at different stages. One example is the formation of the amphisomes that were mentioned above which are formed from the fusion of autophagosomes with endosomes and MVB. Another illustration of this is the fact that MVB can be degraded via autophagy²⁰⁶ and therefore autophagy can regulate exosome biogenesis and EV degradation. In turn, EV can induce intracellular autophagy to the target/recipient cell, thus, acting in a cytoprotective manner²⁰⁷.

The interplay of exosomes and autophagy might be important also in the presence of cancer. Under the hypoxic and nutrient-deprived conditions of the tumor microenvironment autophagy promotes the survival of tumor cells²⁰⁸, while hypoxia induces exosome production and alters their proteomic and nuclear acid profiles²⁰⁹. Endoplasmic reticulum (ER) stress can also trigger autophagy in cancer cells²¹⁰ and simultaneously increases exosome release²¹¹. Further, both exosomes and autophagy have been found to mediate therapy resistance^{212,213}. Lastly, tumor-derived exosomes induce autophagy in an autocrine manner, thus, promoting tumor growth²¹⁴.

9. PLEKHM1: a hub between autophagy and the endolysosomal *system*

The autophagic and the endocytic pathways require the fusion of the lysosome with the autophagosome or the MVB, respectively. Specific proteins facilitate the trafficking and fusion of these vesicles. One such protein is the pleckstrin homology domain-containing family M member 1 (PLEKHM1). Mutation of *PLEKHM1* in rats and humans may lead to an osteopetrotic phenotype²¹⁵. Specifically, PLEKHM1 controls the release of enzymes from secretory lysosomes, which are contained in BM osteoclasts, in a way that aids the degradation of bone during the bone remodeling

process. In the absence of PLEKHM1 the trafficking of the aforementioned lysosomes is impaired. Therefore, the bones become thicker and more fragile (osteopetrosis).

Additionally, PLEKHM1 is associated with other cellular functions including lysosomal distribution, epidermal growth factor receptor (EGFR) degradation, major histocompatibility complex (MHC) molecules recycling, and autophagy completion¹⁶². Regarding the latter, PLEKHM1 serves as an autophagy adaptor protein and mediates the fusion of autophagosomes with lysosomes¹⁶² at the latest steps of this process. Therefore, PLEKHM1 contributes to the degradation of the damaged organelles and protein aggregates¹⁵³ and it is regulated via phosphorylation by the mammalian target of rapamycin (mTOR) and MAPK pathway²¹⁶ but the function of this regulation is yet to be defined. Additionally, PLEKHM1 is involved in the fusion and trafficking of endosomes^{162,217,218} including MVB which upon fusion with the plasma membrane release exosomes into the extracellular space.

Hypothesis

Given the role of PLEKHM1 in quality control mechanisms in osteoclasts, we hypothesized, that PLEKHM1 in the cells of the BMM might play a role in leukemia progression.

Materials and Methods

1. Mice and Genotyping

All animal experiments were approved by the local government (Regeierungspräsidium Darmstadt, Germany). 8–10 week-old (used as recipients) or 5–6 week-old (used as donors) C57BL/6 mice were purchased from Charles River Laboratories (Sulzfeld, Germany). 8-10 week-old *Plekhm1* KO mice were used for all experiments.

Plekhm1 gene: Primers and Polymerase Chain Reaction (PCR) conditions

Primers:

Wild type allele: 390 base pairs (bp)

Forward: 5'-CACTGAGCCATCTCACCAGCC-3'

Reverse: 5'-CCCAAAGTGCCTGTTTACAC-3'

KO allele: 274 bp

Forward: 5'-AGAGGCTATTCGGCTATGACTG-3'

Reverse: 5'-GCAAGGTGAGATGACAGGAGAT-3'

PCR conditions:

1. 95°C 2min
2. 95°C 30sec
3. 60°C 30sec
4. 72°C 30sec

Repeat steps 2-4 30 times

5. 72°C 5min
6. 4°C hold

2. Virus production and titration

3×10^6 293T cells were seeded on 6 cm plates and 18 hours later 4 ml of fresh medium containing 25µM of chloroquine was added. Initially, a master mix with 10µg of DNA (BCR-

ABL1+ plasmid), 5 µg Ecopack, and 2M CaCl₂ was made. HBS (280mM NaCl, 50mM HEPES, 1.42mM Na₂HPO₄ pH 7.05) sterilized by 0.2 µm filtering was added to the master mix dropwise while vortexing. The final mixture was added to each plate dropwise. 8 hours later the medium was changed with without chloroquine. 48 hours later the virus was harvested and filtered through a 0.2 µm filter and stored in aliquots of 2ml at -80 °C. Titration: NIH/3T3 cells were seeded at 3 ×10⁵ per 6 cm plate. After 18 hours, the cells were transduced with the virus in a 1:3, 1:10, 1:30, and 1:100 dilution and incubated at 5% CO₂ / 37 °C in an incubator for 48 hours. After trypsinization, the cells were washed and resuspended in 500 µl of phosphate-buffered saline (PBS) and analyzed by flow cytometry. (Fortessa Flow Cytometer). The data were further analyzed and edited using the FlowJo software to calculate the percentage of successfully transduced GFP⁺ cells.

3. Bone marrow (BM) transduction/transplantation

3.1 CML

For the induction of chronic myeloid leukemia (CML)-like myeloproliferative neoplasia (MPN) donor BM cells were harvested from mice which had been treated with 5-fluorouracil (5-FU) (Cat. No. F6627, Sigma-Aldrich, Darmstadt, Germany) (200mg/kg) 4 days earlier and placed in sterile cold PBS + 2% FBS. For harvesting, the BM was flushed from the bones (femurs and tibiae) of the mice with DMEM + 10% FBS + 1% Pen-Strep + 1% L-Glutamine using a 25G needle and syringe under sterile conditions. The cells were centrifuged at 1000 rpm for 10 min and the pellet was resuspended in 1 ml of ammonium-chloride-potassium ACK lysis buffer (Cat. No. A1049201, ThermoFisher Scientific, Waltham, MA) for 5 min at room temperature for the lysis of the red blood cells. The ACK lysis buffer was diluted by adding 10ml of medium and the cells were pelleted down again. The final pellet was resuspended in 1ml of medium and the cells were counted. Depending on their number the cells were cultured either in 1 or 2 10cm dishes in RPMI, 10% fetal bovine serum (FBS), 1% penicillin/streptomycin and 1% L-glutamine supplemented with 50ng/ml stem cells factor (SCF) (Cat. No, 250-03, PeproTech, London, UK) (50 ng/ml), interleukin (IL)-3 (Cat. No. 213-

13, PeproTech, London, UK) (6 ng/ml), and IL-6 (Cat. No. 216-16, PeproTech, London, (10 ng/ml) overnight. The next day, the cells were collected and resuspended in 4ml of the above medium and transduced with 4ml of previously titrated retrovirus expressing MSCV IRES GFP BCR-ABL1 by centrifugation at 2500 rpm for 90 min at 32 °C with 5µg/ml polybrene and 50mM HEPES (Cat. No. 15630080, ThermoFisher Scientific, Waltham, MA). Next, fresh medium was added and the cells were returned to the incubator overnight. The following day, the process of virus transduction was repeated and again the cells were placed in a 37 °C / 5% CO₂ incubator for 2-4 hours. Finally, the cells were counted and transplanted intravenously (i.v.) without sorting into sub-lethally irradiated recipient mice (2x450 cGy) at a dose of 2.5x10⁵ cells per recipient in Hanks balanced salt solution (HBSS) solution^{219,220}. The mice were monitored daily and any abnormalities in their posture, health status, and behavior were noted.

3.2 AML

For the induction of acute myeloid leukemia (AML), donor BM cells were harvested from 5-FU treated WT mice, transduced twice with cryopreserved retrovirus expressing MSCV-IRES GFP MLL-AF9 as above, and transplanted i.v. into sub-lethally irradiated recipient mice (2x450 cGy) at a dose of 5x10⁵ cells per recipient²²¹ in HBSS solution. The mice were monitored daily and any abnormalities in their posture, health status, and behavior were noted.

3.3 BALL - Primary transplant

For the induction of BCR-ABL1⁺ B-cell acute lymphoblastic leukemia (B-ALL) BM cells were harvested from non-5-FU treated WT mice, transduced once with MSCV-IRES GFP BCR-ABL1-expressing retrovirus, and transplanted i.v into sub-lethally (2x450 cGy) irradiated recipient mice at a dose of 1x10⁶ cells per recipient in HBSS solution. The mice were monitored daily and any abnormalities in their posture, health status, and behavior were noted. The mice were euthanized when they were moribund.

3.4 BALL - Secondary transplant

For the induction of B-ALL in secondary recipient mice, unsorted BM cells from WT or *Plekhm1* KO primary recipient mice with established B-ALL were harvested on day 20 after

transplantation, counted, and transplanted i.v. at a dose of 2×10^6 cells per recipient into sub-lethally (2×450 cGy) irradiated recipient WT mice in HBSS solution. The mice were monitored daily and any abnormalities in their posture, health status, and behavior were noted.

3.5 Preincubation of BCR-ABL1-transduced BM cells with sEV

BM cells were harvested as above ("BALL – Primary transplant") from non-5-FU treated WT mice and transduced with BCR-ABL1. Subsequently, the cells were incubated with sEV prepared from the supernatants of WT or *Plekhh1* KO MSC (see sEV isolation) for 1h in RPMI, 1% penicillin/streptomycin, and 1% L-glutamine without serum (FBS). The ratio that was used was 1:5 donor (MSC) to recipient (BCR-ABL1-transduced) cells.

4. Homing

BM cells were harvested from non-5-FU treated WT mice and transduced once with retrovirus expressing MSCV-IRES GFP BCR-ABL1. Subsequently, the cells were incubated overnight in RPMI, 10% FBS, 1% penicillin/streptomycin, and 1% L-glutamine supplemented with IL-7 (Cat. No. 217-17, PeproTech, London, UK) (10 ng/ml). Finally, the cells were transplanted i.v. into sub-lethally (2×450 cGy) irradiated recipient WT or *Plekhh1* KO mice at a dose of 3×10^6 cells per recipient in HBSS. 18 hours after transplantation, the BM cells of the recipient mice were analyzed for the percentage of GFP⁺ (BCR-ABL1)⁺ BP-1⁺ cells by flow cytometry.

5. Analysis of diseased mice and tumor burden

Leukemia progression was assessed by both complete blood count (CBC) analysis (Scil Animal Care Company, Viernheim, Germany) and the percentage of GFP⁺ (BCR-ABL1)⁺ BP-1⁺ in the case of BCR-ABL1⁺ B-ALL, GFP⁺ (BCR-ABL1)⁺ CD11b⁺ cells in the case of CML-like MPN, and GFP⁺ (MLL-AF9⁺) Gr-1⁺ cells in the case of AML, in the peripheral blood of the diseased mice by flow cytometry (BD Fortessa, Heidelberg, Germany).

6. Flow cytometry

For the hematological profile of WT or *Plekhh1* KO mice antibodies to the following markers were used: CD11b (Cat. No. 55312, BD Biosciences Franklin Lakes, NJ, USA) (myeloid cells), Ter119 (Cat. No. 561032, BD Biosciences Franklin Lakes, NJ, USA) (erythroid cells), CD5

(Cat. No. 553019, BD Biosciences Franklin Lakes, NJ, USA) (T lymphocytes), B220 (Cat. No. 103207, BioLegend, San Diego, CA, USA) (B lymphocytes), F4/80 (Cat. No. 565409, BD Biosciences Franklin Lakes, NJ, USA) (macrophages), Gr-1 (Cat. No. 557661, BD Biosciences Franklin Lakes, NJ, USA), c-Kit (Cat. No. 553356, BD Biosciences Franklin Lakes, NJ, USA), Sca1 (Cat. No. 108114, BioLegend, San Diego, CA, USA), CD48 (Cat. No. 103418, BioLegend, San Diego, CA, USA) and CD150 (Cat. No. 115903, BioLegend, San Diego, CA, USA). LKS cells were defined as Lin⁻ (Gr-1, Ter119, CD5, B220, F4/80)⁻ c-Kit⁺ Sca1⁺ and LKS SLAM cells as Lin⁻ c-Kit⁺ Sca1⁺ CD48⁻ CD150⁺. For the detection of apoptotic cells AnnexinV (Cat. No. 640941, BioLegend, San Diego, CA, USA) and 4',6-diamidino-2-phenylindole (DAPI) (Cat. No. 12453, Merck, Darmstadt, Germany) were used. AnnexinV⁺ DAPI⁻ cells were considered as early and AnnexinV⁺ DAPI⁺ cells as late apoptotic cells. For cell cycle analysis BM cells were stained with BP-1 antibody for 30 min at 4 °C in the dark, permeabilized with cold methanol for 10 minutes and stained overnight with Ki-67 (Cat. No. 652406, BioLegend, San Diego, CA, USA) and DAPI. The cell cycle tool in FlowJo_v10.6.2 software was used to distinguish the G1, S and G2 phases. For the detection of the different B-cell fractions the following combination of markers was used²²²:

A: B220^{low}CD43^{high}BP1^{neg}HSA^{neg}

B: B220^{low}CD43^{high}BP1^{neg}HSA^{pos}

C: B220^{low}CD43^{high}BP1^{high}HSA^{pos}

D: B220^{high}CD43^{neg}IgM^{neg}

E: B220^{high}CD43^{neg}IgM^{mid}

F: B220^{high++}CD43^{neg}IgM^{high/mid}

For the detection of the B-cell surface markers the following antibodies were used: CD43 (Cat. No. 143209, BioLegend, San Diego, CA, USA), HSA (CD24) (Cat. No. 138505, BioLegend, San Diego, CA, USA), IgM (Cat. No. 561285, BD Biosciences Franklin Lakes, NJ, USA), CD19 (Cat. No. 115531, BioLegend, San Diego, CA, USA) and B220 (Cat. No. 103207, BioLegend, San Diego, CA, USA).

7. Quantitative real-time PCR

BM cells from WT or *Plekhh1* KO mice were collected on day 20 after transplantation, centrifuged (at 1200 rpm for 10 minutes), and lysed in TRIzol reagent (Cat. No. 15596026, ThermoFisher, Darmstadt, Germany). For the isolation of RNA, chloroform was added, and the RNA was purified using an mRNA purification kit (Qiagen, Düsseldorf, Germany) according to the manufacturer's instructions. The RNA concentration was measured using a NanoDrop (ThermoFisher, Darmstadt, Germany), and equal amounts (200-300ng) of RNA were reverse transcribed into cDNA using the ProtoScript First Strand cDNA Synthesis kit (New England Biolabs, Ipswich, MA). A master mix was prepared with Power SYBR Green (Cat. No. A25742, Thermo Fisher Scientific, Darmstadt) with 10 μ M forward and 10 μ M reverse primers in triplicate with an RNA amount of 10 ng or higher. The average Ct value was calculated and normalized to the Ct values of GAPDH. Delta Ct and Delta Delta Ct values were calculated and represented as either Delta Ct or as relative expression. If needed, the fold change of the *Plekhh1* KO samples to WT was calculated. The primers used were as follows: *Pax5* forward: AATCGCTGAGTACAAACGCCAA reverse: TCCGAATGATCCTGTTGATGGA, *Ikzf1* forward: TCGGGAGAGAAAATAATGG reverse: AGGCCGTTCCACCAGTATGAC, *Ebf1* forward: AGATCTGGTTGAAGCCCTGTATGG reverse: CATGTCACATCTCAGATCCTGTGTTCT.

8. Osteoclast isolation and differentiation

Femora and tibiae from 4-6 week old mice were aseptically removed and BM cells were flushed with α -MEM using a 25G needle and syringe. The cells were collected in a 50ml tube, centrifuged at 1000 rpm for 5 min, resuspended in fresh medium, and strained through a 70 μ m filter. Finally, the cells were cultured in a 10 cm dish with 10 ml of α -MEM containing 10% FBS, 1% penicillin/streptomycin, and 1% L-glutamine in a 37 °C / 5% CO₂ incubator overnight. Subsequently, non-adherent cells were gently removed with a 10 ml pipette and added to a 50 ml tube. The dish was gently washed one more time with 10 ml of medium, and this was added to the same 50 ml tube. After centrifugation at 1000 rpm for 5 min, the supernatant was removed, and the pellet was resuspended in 5 ml of medium. Additionally, 5 more ml were used to rinse the tube. In a new 50 ml, tube 15 ml of Ficoll-Paque PLUS (Cat. No. 17-1440-

02, Fisher Scientific, Stockholm, Sweden) were added, and gently the 10 ml of cell suspension were layered on top of the Ficoll-Paque PLUS. The cells were centrifuged at 2500 rpm for 30 min at room temperature with no break. The interphase, which contains the mononuclear cells, was collected in a 50 ml tube using a 10 ml pipette. The volume was brought up to 30 ml with complete medium and the cells were centrifuged at 1000 rpm for 5 min. Finally, the supernatant was removed and the cells were resuspended in complete medium (2ml / mouse). 50,000 cells were plated in a well of a 96-well plate and then treated with 50ng/ml macrophage colony-stimulating factor (MCSF) for 48-72 hours (BM macrophages). Then, the cells were treated for an additional 4-6 days with 50ng/ml MCSF and 50ng/ml receptor activator of nuclear factor kappa-B ligand (RANKL) (Cat. No. 462-TEC-010, R&D systems, Minneapolis, MN, USA)²²³. From day 6, multinuclear cells (osteoclasts) were visible under the light microscope.

9. Osteoclast resorption assay

Bovine cortical bone slices (boneslices.com, Jelling, Denmark) of 6 mm diameter and 0.4 mm thickness were placed in a 96-well plate (1 bone slice per well), and the differentiation to osteoclasts, as described above, was performed on top of the slices. The pits generated in the bone slices by the osteoclasts were stained using 1% toluidine blue solution (Cat. No. 89640, Merck KGaA, Darmstadt, Germany) and were visualized under the light microscope²²⁴. The area of the pits was measured using the Image J software.

10. Proliferation of BCR-ABL1⁺ BA/F3 cells on osteoclasts

BCR-ABL1⁺ BA/F3 cells were cultured in a 96-well plate (10,000 cells/well) on top of previously *in vitro* differentiated WT or *Plekhh1* KO osteoclasts, as described above. The cells were counted for 4 days using trypan blue (Cat. No. T8154, Merck KGaA, Darmstadt, Germany) to distinguish live from dead cells.

11. Preparation of mesenchymal stromal cells

Femora and tibiae from WT or *Plekhh1* KO mice were harvested and stored in ice-cold PBS + 2% FBS. Pelvic bones were also kept in ice-cold PBS (used for controls). The bones were

crushed gently using a sterile pestle and mortar, and cut in small pieces using scissors until they resembled a paste. The crushed bones were washed 3 times using HBSS⁺ (HBSS supplemented with 2% FBS, 10mM HEPES and 1% penicillin/streptomycin), collected in 50ml falcons, and incubated in 15ml of DMEM + 0.2% collagenase A (Cat. No. 10103586001, Merck KGaA, Darmstadt, Germany) at 37°C for 1 hour while shaking (110rpm). For the flow cytometry controls the pelvic bones were crushed, suspended in 3-4 ml of PBS + 2% FBS and the suspension was aspirated, filtered through a 70µm filter and kept on ice. After digestion with collagenase A, the cell suspension was filtered through a 70µm filter and was put on ice to quench the collagenase activity. The remaining bones were transferred to the mortar and crushed by use of the pestle. 5ml of HBSS⁺ was added, and the cell suspension was filtered through a 70µm filter; the whole process was repeated 5 times. The cell suspension was combined with the one from the previous step. All cell suspensions (from WT mice, *Plekha1* KO mice and controls) were centrifuged at 800 rpm at 4°C for 10 minutes. The supernatant of all samples was aspirated, and the red blood cells were lysed using 1ml of ACK lysis buffer for 5 minutes at room temperature (RT). The cells were washed by adding 9 ml of HBSS⁺, and the cell suspensions were filtered through a 70µm filter and centrifuged at 800 rpm at 4°C for 10 minutes. The supernatant was aspirated and the cells were stained. For the main samples the digested bones were stained with antibodies against CD45 (Cat. No. 553081, BD Biosciences Franklin Lakes, NJ, USA), Ter119 (Cat. No. 561032, BD Biosciences Franklin Lakes, NJ, USA), PDGFR α (Cat. No. 17-1401-81, Thermo Fisher Scientific, Darmstadt, Germany) and Sca1 (Cat. No. 108114, BioLegend, San Diego, CA, USA), and CD45⁻ Ter119⁻ PDGFR α ⁺ Sca1⁺ mesenchymal stromal cells (MSC) were obtained by sorting (BD FACSAria Fusion Cell Sorter, Franklin Lakes, NJ, USA)²²⁵. For the flow cytometry controls the cell pellet was resuspended in 1ml of HBSS⁺ and it was divided into 3 tubes: unstained in which no antibodies were added, stained control #1 or -PDGFR α in which 1 µl of CD45 and 1µl of Sca1 were added and stained control #2 or -Sca1 in which 1 µl of CD45 and 1µl of PDGFR α were added. The samples were incubated at 4°C for 1 hour in the dark. Subsequently, the stained samples were washed with 10 ml of HBSS⁺ for the main samples (WT and KO) and 1 ml for

the control samples. The samples were centrifuged at 800rpm for 10 minutes. The cells from WT, *Plekhh1* KO mice, and flow cytometry control samples were resuspended in 1 ml of HBSS⁺ and propidium iodide (PI) solution (2µg/ml) (Cat. No. P4170, Sigma-Aldrich, Darmstadt, Germany) was added. The unstained cells were resuspended in HBSS⁺ only. Finally, MSC were isolated by sorting (BD FACSAria Fusion Cell Sorter, Franklin Lakes, NJ, USA).

12. Mesenchymal stromal cell culture

Depending on number of cells that were sorted, the MSC were cultured in a 48-, 24-, 12- or 6-well plate in α -MEM with 20% FBS, 1% penicillin/streptomycin and 1% L-glutamine. The medium was supplemented with 100 µg/ml of primocin (InvivoGen, Toulouse, France) until passage 2 to prevent cell contamination. The cells were split 2 times a week in a 1:2 ratio using 0.25% trypsin (Cat. No. 25200056, ThermoFisher Scientific, Darmstadt, Germany). MSC were not cultured or used for downstream applications beyond passage 6.

13. Colony forming unit fibroblast assay (CFU-F)

2,000 WT or *Plekhh1* KO MSC, obtained as described above²²⁵, were plated in 10cm dishes. Half the volume of the medium was carefully removed and substituted with fresh medium twice a week for a total of 10 days. Subsequently, the medium was removed and the cells were fixed with 4% paraformaldehyde (PFA) (Cat. No. sc-281692 Santa Cruz, Heidelberg, Germany) for 15 min at RT. The cells were stained with 1% crystal violet (Cat. No. HT901, Sigma-Aldrich, Darmstadt, Germany) solution (in 20% methanol) at RT for 30 minutes. The colonies were counted and images were taken²²⁵.

14. Differentiation of MSC

6,000 WT or *Plekhh1* KO MSC were seeded in 48-well plates. Subsequently, the MSC were differentiated into adipocytes using adipocyte differentiation and maintenance medium (Cat. No. PT3102A, PT3102B, Lonza, Cologne, Germany) or into osteoblasts using α -MEM containing 20 % FBS, 1% penicillin/streptomycin and 1% L-glutamine supplemented with 50 µg/ml ascorbic acid (Cat. No. A5960, Sigma-Aldrich, Darmstadt, Germany), 10 mM β -

glycerophosphate (Cat. No. G9422, Sigma-Aldrich, Darmstadt, Germany) and 10 mM dexamethasone (Cat. No. 50022, Merck, Darmstadt, Germany) for 10 days. The differentiated cells were fixed and stained with Von Kossa (1% silver nitrate – Cat. No. S8157 Sigma-Aldrich, Darmstadt, Germany) or alizarin red S (Cat. No. A5533, Sigma-Aldrich, Darmstadt, Germany) solution for detection of calcium deposits or with oil red O solution for the detection of lipid droplets²²⁵.

15. Immunofluorescence

WT or *Plekhm1* KO MSC were cultured on 12 mm coverslips in 24 well plates until they reach 60% confluency. Subsequently, the cells were washed with PBS twice and fixed using 4% PFA (Santa Cruz, Heidelberg, Germany) for 15 minutes at RT. The cells were incubated in saponin-based blocking solution (PBS, 5mM MgCl₂, 0.1% saponin, 5% FBS) for 30 minutes at RT, and, subsequently, the cells were stained for 1h with the respective antibodies as follows. For the detection of multivesicular bodies (MVB) the cells were stained with anti-CD63 (Cat. No. sc-5275, Santa Cruz, Heidelberg, Germany) antibody at a 1:300 dilution in blocking solution for 1 hour at RT. For the detection of syndecan-1 the cells were incubated with anti-syndecan-1 (Cat. No. ab60199, Abcam, Cambridge, UK) at a 1:300 dilution in blocking solution for 1 hour at RT. Phalloidin (Cat. No. A22287, Thermo Fisher Scientific, Darmstadt, Germany) was used to stain actin filaments. For autophagy studies anti-LC3 (Cat. No. M152-3, MBL International, Woburn, MA, USA) and anti-LAMP1 (ab208943, Abcam, Cambridge, UK), both at a 1:300 dilution in blocking solution, were used for 1 hour at RT. The secondary antibodies, anti-rabbit (Cat. No. A22287, Thermo Fisher Scientific, Darmstadt, Germany) or anti-mouse (Cat. No. A11029, Thermo Fisher Scientific, Darmstadt, Germany), were used at a 1:400 dilution in blocking solution for 1 hour at RT. Nuclei were counterstained with DAPI (5 µg/ml) and the slides were mounted using mowiol 4-88 reagent (Sigma-Aldrich, Darmstadt, Germany) mounting medium. Images were acquired using a confocal laser scanning microscope (CSLM) (Leica, Wetzlar, Germany) and analyzed using Image J software.

16. Preparation of extracellular vesicles (EV)

WT or *Plekhm1* KO MSC were washed twice with PBS and incubated in α -MEM containing 1% penicillin/streptomycin and 1% L-glutamine without FBS for 24 hours. Subsequently, the conditioned medium (CM) was collected and centrifuged at 300 x g for 10 minutes at 4°C to discard the dead cells and the supernatant was centrifuged at 2,000 x g for 20 minutes to remove the cell debris. Next, the supernatant was centrifuged at 10,000 x g for 1 hour to precipitate the large EV¹⁸⁷. The remaining supernatant was then transferred to fresh 50ml tubes, balanced for weight and further centrifuged for 90 minutes at 100,000 x g to isolate the small EV (sEV). The pellet was resuspended in PBS (for imaging flow cytometry analysis and functional *in vitro* assays), HBSS for *in vivo* functional assays and RIPA buffer (see “Immunoblotting”) for immunoblot analysis. The PBS and HBSS solutions that were used during the isolation process were filtered with a 0.2 μ m filter.

17. Immunoblotting

MSC, sEV prepared from MSC or BCR-ABL1⁺ BA/F3 cells were lysed in RIPA buffer (50 mM Tris HCl pH 7.4, 150 mM NaCl, 1% Triton X-100, 1% Na DOC, 0.1% SDS, 1 mM EDTA), supplemented with fresh protease and phosphatase inhibitors (Sigma-Aldrich, Darmstadt, Germany). Lysates were centrifuged at 14000 rpm for 20 minutes at 4°C, and the protein concentration was measured using the Bradford protein assay (Cat. No. 50000006, Bio-Rad, Hercules, CA, USA). The proteins were denatured and run on 4-12% Bis-Tris polyacrylamide gels (ThermoFisher Scientific, Darmstadt, Germany), and, subsequently, transferred to methanol-activated PVDF membranes (ThermoFisher Scientific, Darmstadt, Germany). In the case of MSC and BCR-ABL1⁺ BA/F3 cells, equal amounts of protein were used, while, in the case of sEV, protein amounts from an equal number of donor MSC were used for immunoblotting. The membranes were incubated at 4°C overnight with the following antibodies for the detection of the respective proteins: pFAK (Tyr397) (Cat. No. 3283, Cell Signaling, Frankfurt am Main, Germany) at 1:500 in TBS-T, FAK (Cat. No. 610087, BD Biosciences Franklin Lakes, NJ, USA) at 1:1000 in 5% milk, AKT (Cat. No. 9272, Cell

Signaling, Frankfurt am Main, Germany) at 1:1000 in 5% milk, syntenin (Cat. No. sc-515538, Santa Cruz, Heidelberg, Germany) at 1:500 in 5% milk, syndecan-1 (Cat. No. ab60199, Abcam, Cambridge, UK) at 1:500 in 5% milk, GM130 (Cat. No. PA1-077, Thermo Fisher Scientific, Darmstadt, Germany) at 1:1000 in 5% milk, phospho-p65 (Cat. No. 3033 Cell Signaling, Frankfurt am Main, Germany) at 1:1000 in TBS-T, p65 (Cat. No. 8242, Cell Signaling, Frankfurt am Main, Germany) at 1:1000 in 5% milk, GAPDH (Cat. No. sc-32233, Santa Cruz, Heidelberg, Germany) at 1:2000 in 5% milk and vinculin (Cat. No. MA5-11690, Thermo Fisher Scientific, Darmstadt, Germany) at 1:2000 in 5% milk. Secondary horseradish-peroxidase (HRP)-conjugated (Cell Signaling, Frankfurt am Main, Germany) antibodies were used at 1:3000 in 5% milk. The membranes were developed using X-ray films (Fujifilm, Düsseldorf, Germany) and band intensities were quantified using Image J software.

18. Mass Spectrometry

sEV sample preparation for mass spectrometry

sEV were prepared as described in the “Preparation of extracellular vesicles” section, and the final pellet was dissolved in 0.2 µm filtered PBS. Sample preparation was performed using the in StageTip (“iST”) method, described in ²²⁶, with minor modifications. Briefly, the sEV were lysed, reduced and alkylated in sodium deoxycholate (SDC) buffer (2% SDC, 50mM Tris pH 8.5, 1mM tris (2-carboxyethyl) phosphine, 4mM chloroacetamide). The proteins were boiled for 10 minutes at 95°C, digested by adding one volume of 50mM Tris pH 8.5 containing 500ng LysC/Trypsin and incubated overnight at 37°C. The digestion was stopped with isopropanol/1% trifluoroacetic acid (TFA), and the peptides were purified on SDB-RPS stage tips (3M Empore) and centrifuged at 3500 x g for 5 minutes. Next, isopropanol/1%TFA was added, the samples were centrifuged at 3500 x g for 3 minutes, and, finally, 0.2% TFA in water was added. After final centrifugation the peptides were eluted in 80% acetonitrile (ACN)/1.25% ammonia and dried by vacuum centrifugation before reconstitution in 2% ACN, 0.1% TFA for LC-MS/MS analysis.

LC-MS analysis

Tryptic peptides derived from isolated sEV were analysed on a Q Exactive HF coupled to an easy nLC 1200 (ThermoFisher Scientific, Waltham, MA) using a 35 cm long, 75µm ID fused-silica column packed in house with 1.9 µm C18 particles (Reprosil pur, Dr. Maisch), and kept at 50°C using an integrated column oven (Sonation). Peptides were eluted by a non-linear gradient from 1.5-40% acetonitrile over 220 minutes and directly sprayed into the mass-spectrometer equipped with a nanoFlex ion source (ThermoFisher Scientific, Waltham, MA). Full scan MS spectra (300-1650 m/z) were acquired in profile mode at a resolution of 60,000 at m/z 200, a maximum injection time of 20 ms and an AGC target value of 3×10^6 charges. Up to 15 most intense precursors per full scan were isolated using a 1.6 Th window and fragmented using higher energy collisional dissociation (HCD, normalized collision energy of 27). MS/MS spectra were acquired in centroid mode with a resolution of 15,000, a maximum injection time of 25 ms and an AGC target value of 1×10^5 . Single charged ions, ions with a charge state above 5 and ions with unassigned charge states were not considered for fragmentation and dynamic exclusion was set to 30s.

Mass spectrometry data processing

MS raw data processing was performed with MaxQuant (v 1.6.10.43) and its built-in label-free quantification algorithm MaxLFQ applying default parameters^{227,228}. Acquired spectra were searched against the mouse reference proteome (Taxonomy ID 10090) downloaded from UniProt (10-12-2018; 62309 sequences including isoforms) and a collection of common contaminants (244 entries) using the Andromeda search engine integrated in MaxQuant²²⁹. Identifications were filtered to obtain false discovery rates (FDR) below 1% for both peptide spectrum matches (PSM; minimum length of 7 amino acids) and proteins using a target-decoy strategy²³⁰. “Match-between-runs” was enabled applying default settings.

Mass spectrometry data statistical analysis

Filtering and statistical analysis of the MaxQuant output (“ProteinGroups.txt”) was performed in Perseus (v 1.6.7.0). Proteins not passing the protein-FDR cut-off (“only identified by site”)

and/or identified in the reversed or contaminants databases were removed and only proteins with at least 2 values per experimental group (WT and KO) were used for statistical analysis. Significant proteins were defined after a Student's *t*-test applying a p-value cut-off (<0.05) and fold-change threshold (log₂ratio larger than ±0.58).

Preparation of leukemia cells for mass spectrometry

Leukemic mice were sacrificed on day 20 after transplantation, and bone marrow cells were harvested and centrifuged at 1000 x g for 10 minutes. 80% of leukocytes were positive for both GFP and BP-1 in both mouse groups. Cell pellets were dissolved in lysis buffer (2% SDS, 10mM TCEP, 40mM CAA, 50mM Tris pH 8.5), boiled for 10 minutes at 95°C followed by 2 minutes of sonication and another 5 minutes of boiling at 95°C.

Proteins were precipitated using 4 volumes of ice-cold methanol, 1 volume of chloroform and 3 volumes ddH₂O. After centrifugation at 14,000 x g for 45min at 4°C, the upper aqueous phase was aspirated, and 3 volumes of ice-cold methanol were added. Samples were mixed and proteins pelleted by centrifugation at 14,000 x g for 5 min at 4°C. The supernatant was discarded, and pellets were washed one additional time with ice-cold methanol. Protein pellets were dried at RT for further use. Proteins were resuspended in 8M urea, 50mM Tris pH 8.2, and the protein concentration was determined using the BCA assay (23225, Thermo Fisher Scientific, Waltham, MA). 50µg of protein from each sample were diluted to a final concentration of 4M urea using digestion buffer (50mM Tris pH 8.2) and incubated with LysC (Wako Chemicals, Neuss, Germany) at a 1:50 (w/w) ratio for 3 hours at 37°C. The sample was then further diluted to a final concentration of 1M urea using digestion buffer and incubated in a 1:100 (w/w) ratio with trypsin (V5113, Promega, Madison, WI) overnight at 37°C. Digests were acidified using trifluoroacetic acid (TFA) (to 0.5%), and peptides were purified using SepPak tC18 columns (WAT054955, Waters, Milford, MA) according to the manufacturer's protocol. Eluted peptides were dried, resuspended in TMT labelling buffer (0.2M EPPS pH 8.2, 20% acetonitrile), and the peptide concentration was determined by micro-BCA (23235, Thermo Fisher Scientific, Waltham, MA). Peptides were mixed with TMT10

reagents (90111, A37724, 90061, ThermoFisher Scientific, Waltham, MA) in a 1:2 (w/w) ratio (2µg TMT reagent per 1µg peptide). Reactions were incubated for one hour at RT and, subsequently, quenched by addition of hydroxylamine to a final concentration of 0.5% at RT for 15 min. After verification of labelling efficiency (>99%) and calculating necessary ratios for equal mixing by liquid chromatography – mass spectrometry (LC-MS), all samples were pooled, dried in a vacuum concentrator and fractionated using the Pierce High pH Reverse-Phase Peptide Fractionation Kit (84868, Thermo Fisher Scientific, Waltham, MA) into 8 fractions according to the manufacturer's instructions. Peptide fractions were dried and stored at -20°C until mass spectrometry analysis, for which they were resuspended in LC-MS grade water containing 2% ACN and 0.1% TFA.

All mass spectrometry proteomics data have been deposited in the ProteomeXchange Consortium Database²³¹ via the PRIDE partner repository²³² with the dataset identifier PXD027041 (Exosomal proteome) and PXD027044 (whole cell proteome).

19. Imaging flow cytometry

For imaging flow cytometry (IFCM) analysis, sEV samples were stained with anti-mouse CD81 antibodies (Miltenyi Biotec, Bergisch Gladbach, Germany) and incubated at room temperature for 2 hours. Subsequently, samples were diluted 1:5 with PBS and analyzed on the AMNIS ImageStreamX Mark II Flow Cytometer (AMNIS/Luminex, Seattle, WA, USA), as previously described^{233,234}, following the recommendations of the MIFlowCyt-EV guidelines²³⁵. Unstained MSC-EV preparations, antibodies diluted in PBS and samples supplemented with 1% NP40 (Calbiochem, San Diego, CA, USA) were analyzed as controls. Acquisition time was set to 5 minutes per well. Data were acquired at 60x magnification, at a low flow rate, and with the 'removed beads option' disabled. For the calibration of the IFCM device, MESF beads for PE were used (Bangslab, Hirschberg an der Bergstrasse, Germany). Data were analyzed as described previously using the IDEAS software (version 6.2)^{233,236}.

20. *In vitro* treatment of BCR-ABL1⁺ BA/F3 cells

BCR-ABL1⁺ BA/F3 cells were exposed to sEV derived from WT pr *Plekhm1* KO MSC for 40 minutes or 6 hours in a 1:5 ratio (donor (MSC) to recipient (BCR-ABL1⁺ BA/F30 cells)) in the presence or absence of 20 μ M dynasore (Cat. No. S8047 Selleckchem, Houston, TX, USA) in RPMI, 5% FBS, 1% penicillin/streptomycin, and 1% L-glutamine. Subsequently the cells were collected and lysed in RIPA buffer for immunoblot analysis.

21. *In vitro* treatment of MSC with TNF α or coculture with BCR-ABL1⁺ BA/F3 cells

12,000 MSC were cultured in α -MEM, 5% FBS, 1% penicillin/streptomycin, and 1% L-glutamine in a 24 well plate and either treated with TNF α (15ng/ml) for 24 hours or cultured in the presence of 100,000 BCR-ABL1⁺ BA/F3 cells for 6 or 24 hours. The BCR-ABL1⁺ BA/F3 cells were separated from the MSC by a transwell with a 0.4 μ m pore as described in the schematic in figure 19A.

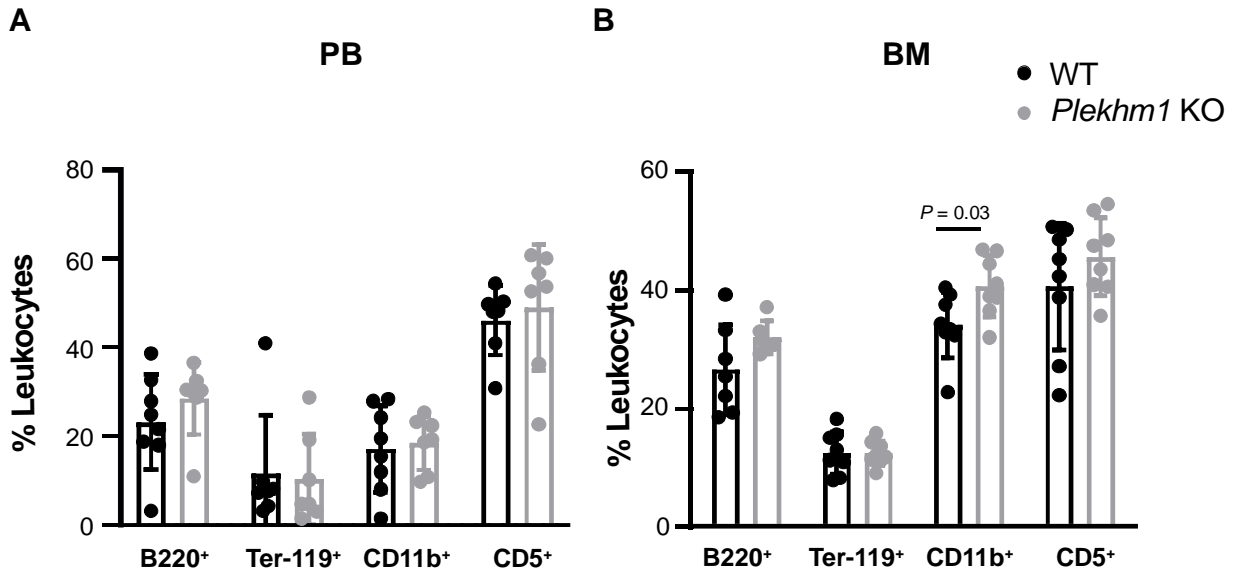
22. Statistical Analysis

For each experiment three to nine biological replicates were included (except for the data in figure 17A). Data are represented as mean \pm SD, and data were considered statistically significant, when $P \leq 0.05$. GraphPad Prism Software (Prism 9.0) was used for the generation of all graphs and for statistical analyses. Statistical significance was calculated using the Student's t-test or one-way or two-way ANOVA. For post hoc analysis the Tukey Test was employed to determine statistical significance between multiple comparisons. For survival analyses by Kaplan-Meier curves the Log-rank (Mantel-Cox) test was used to determine statistical significance.

Results

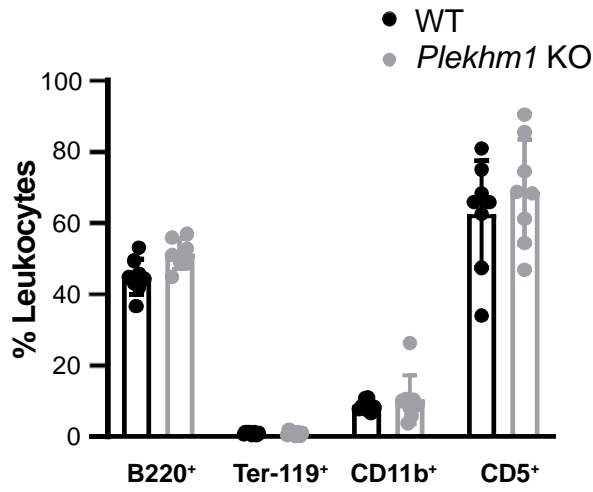
1. *Plekhm1* KO and WT mice have comparable hematological profiles

Given that the role of PLEKHM1 in the context of leukemia, but, also in normal hematopoiesis has not been studied before, we first characterized the hematological profile of *Plekhm1* KO mice compared to wild-type C57BL/6N mice (hereafter WT). To study the murine profile of hematopoietic cells, the following markers which identify differentiated blood cells were used: B220 to identify B lymphocytes, Ter-119 for erythroid cells, CD5 for T lymphocytes, and CD11b for myeloid cells. To study HSC first, the differentiated cells were removed using the above markers, the so-called lineage cocktail, with antibodies against these markers (negative selection), combined with positive selection for markers known to be expressed on HSC such as c-Kit and Sca-1 (LKS). LKS cells that are selected with the above strategy are a heterogeneous population that also contains multipotent progenitors in addition to HSC. To obtain HSC of higher purity an additional marker selection strategy was used to detect LKS CD150⁺ CD48⁻ (LKS SLAM) which are considered more representative of multipotent long-term (LT)-HSC²³⁷. *Plekhm1* KO and WT mice showed similar levels of B220⁺, Ter-119⁺ and CD5⁺ cells in the PB (Figure 8A), BM (Figure 8B), and spleen (Figure 8C). In contrast, CD11b⁺ cells were similar in the PB (Figure 8A) and spleen (Figure 8C), but, significantly higher in the BM (Figure 8B) of the *Plekhm1* KO mice. LKS (Figure 8D) and LKS-SLAM (LKS⁺ CD48⁻ CD150⁺) cells (Figure 8E) were detectable only in the BM and spleen of these mice where they were also found to be similar. More details on the markers defining the lineage positive cells are provided in the respective materials and methods section (“flow cytometry”).



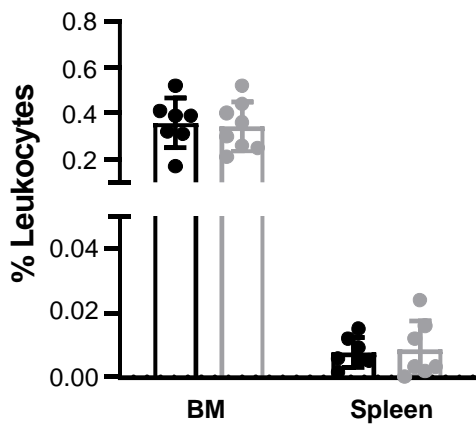
C

Spleen



D

LKS



E

LKS SLAM

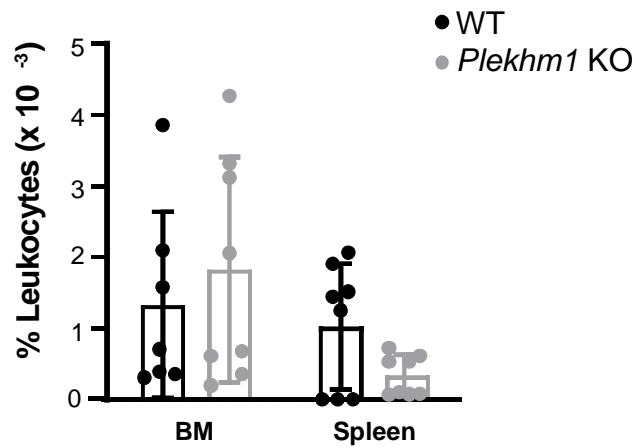


Figure 8: A-C) Percentage of B220⁺, Ter119⁺, CD11b⁺ or CD5⁺ cells in PB (A), BM (B) or spleen (C) of healthy WT (black) or *Plekhhm1* KO (grey) mice (WT n = 7-8; *Plekhhm1* KO n = 6-8; t-test). (D) Percentage of LKS in BM, spleen and PB of healthy WT (black) or *Plekhhm1* KO (grey) mice (WT n = 7; *Plekhhm1* KO n = 7-8; t-test). (E) Percentage of LKS SLAM cells in BM and spleen of healthy WT (black) or *Plekhhm1* KO (grey) mice (WT n = 7-8; *Plekhhm1* KO n = 8; t-test).

2. PLEKHM1 deficiency in the bone marrow microenvironment differentially influences specific leukemias

To elucidate the role of PLEKHM1 in the leukemic BMM, we induced different types of leukemia in WT or *Plekhhm1* KO recipient mice. Specifically, we induced CML-like myeloproliferative neoplasia (MPN), AML, and BCR-ABL1⁺ B-ALL using the retroviral transduction/transplantation model²¹⁹.

i. Chronic myeloid leukemia (CML)-like myeloproliferative neoplasia (MPN)

To induce CML-like MPN we transplanted 2.5×10^5 BCR-ABL1-transduced BM cells from 5-fluorouracil (5-FU)-treated donor mice into sub-lethally (2 x 450cGy) irradiated recipient WT or *Plekhhm1* KO mice. The mice were periodically bled to assess the tumor load. Leukemia cells are detected as GFP⁺ (BCR-ABL1⁺) CD11b⁺, whereby GFP is used to detect the presence of the *BCR-ABL1* oncogene and CD11b to detect myeloid cells. The percentage of GFP⁺ (BCR-ABL1⁺) CD11b⁺ cells was reduced in the PB of *Plekhhm1* KO compared to the WT mice (Figure 9A) and a modest, but, significant increase in the survival of these mice was observed (Figure 9B).

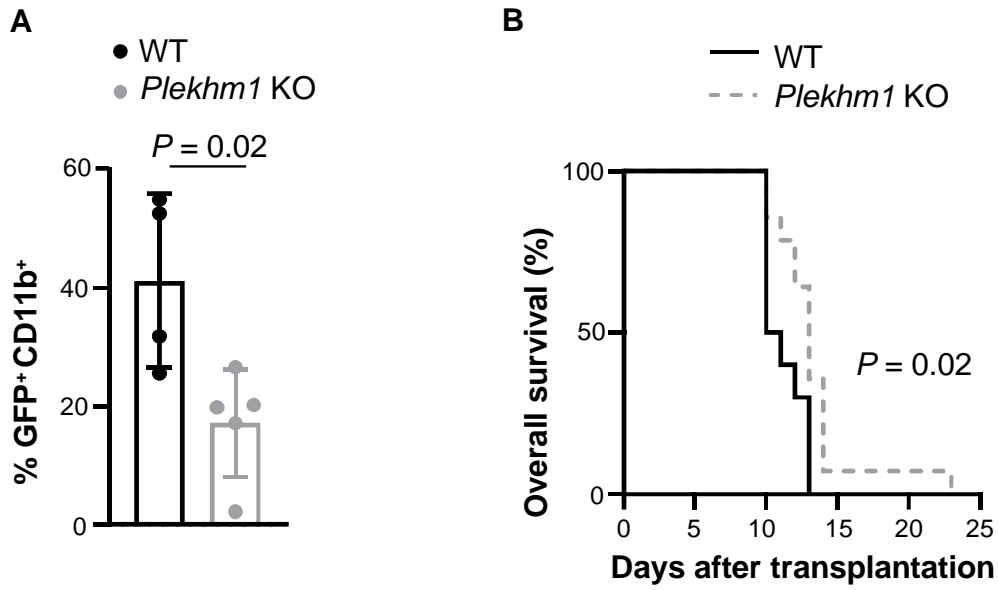


Figure 9: A) Percentage of GFP⁺ (BCR-ABL1⁺) CD11b⁺ cells in peripheral blood of WT (black) or *Plekhh1* KO (grey) recipient mice on day 12 after transplantation of BCR-ABL1-transduced BM in the CML model (WT n = 4; *Plekhh1* KO n = 5; *t*-test). B) Kaplan-Meier-style survival curve of WT (black solid line) or *Plekhh1* KO (grey dashed line) recipient mice transplanted with 5-fluorouracil (5-FU) treated BCR-ABL1-transduced bone marrow in the CML model (WT n = 10; *Plekhh1* KO n = 14; Log-rank test).

ii. Acute myeloid leukemia (AML)

In the case of acute myeloid leukemia (AML), we transplanted 5×10^5 5-fluorouracil (5-FU)-treated donor BM cells, transduced with MLL-AF9-expressing retrovirus, into sub-lethally ($2 \times 450\text{cGy}$) irradiated recipient WT or *Plekhh1* KO mice. In this case we detected the leukemia cells as GFP⁺ (MLL-AF9⁺) Gr-1⁺, whereby GFP is used to detect the presence of the *MLL-AF9* oncogene and Gr-1 to detect myeloid cells. We did not observe any differences in the percentage of GFP⁺ (MLL-AF9⁺) Gr-1⁺ cells (Figure 10A), which represent the tumor burden in this model, or, in the survival of the respective group of mice (Figure 10B).

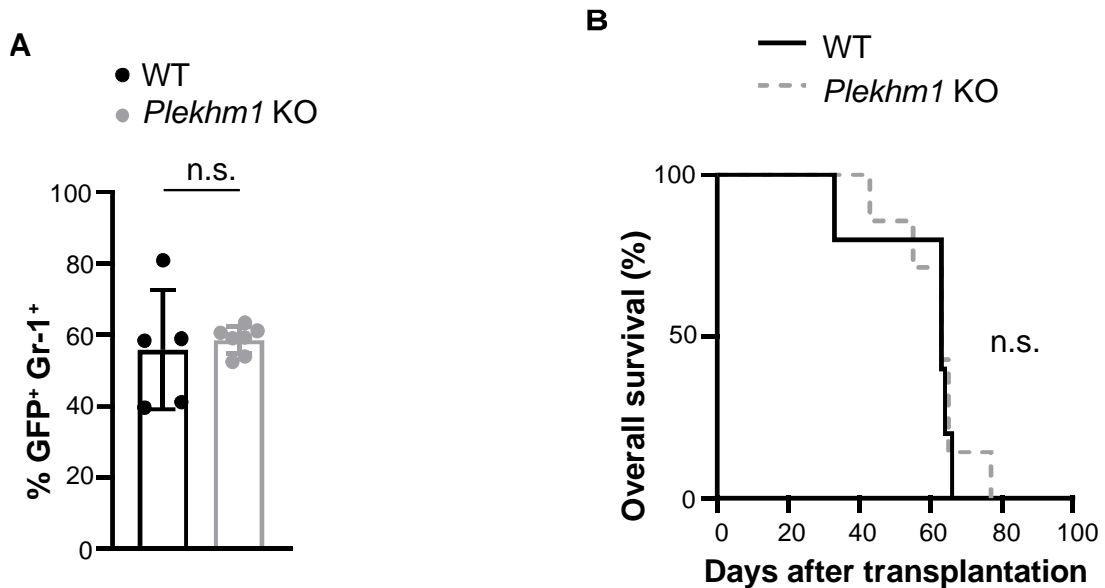


Figure 10: A) Percentage of GFP⁺ (MLL-AF9⁺) Gr-1⁺ cells in peripheral blood of WT (black) or *Plekhh1* KO (grey) recipient mice on day 20 after transplantation of MLL-AF9-transduced BM in the AML model (WT n = 5; *Plekhh1* KO n = 7; *t*-test). B) Kaplan-Meier-style survival curve of WT (black solid line) or *Plekhh1* KO (grey dashed line) recipient mice transplanted with 5-fluorouracil (5-FU) treated MLL-AF9-transduced bone marrow (WT n = 5; *Plekhh1* KO n = 7; Log-rank test).

iii. BCR-ABL1⁺ B-cell acute lymphoblastic leukemia (B-ALL)

Finally, we transplanted 1×10^6 BCR-ABL1-transduced BM cells from non-5-FU treated donor mice into sub-lethally (2×450 cGy) irradiated recipient WT or *Plekhh1* KO mice. Firstly, we observed an increased number of leukocytes in the PB of the mice at day 20 post-transplantation (Figure 11A). At the same time point the tumor burden, which was detected as GFP⁺ (BCR-ABL1⁺) BP-1⁺ cells, with BP-1 being a marker of pre-B cells, in the PB of the *Plekhh1* KO mice was significantly higher (Figure 11B). This translated to reduced survival of the *Plekhh1* KO recipient mice compared to WT (Figure 11C).

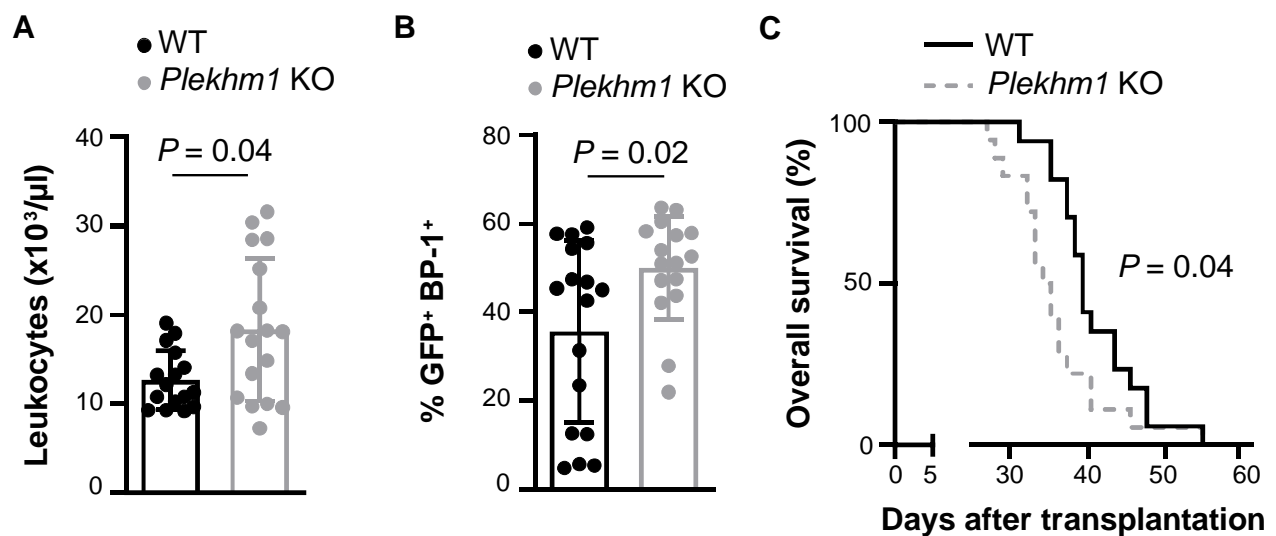


Figure 11: A) Leukocyte counts in PB of WT (black) or *Plekhh1* KO (grey) recipient mice on day 20 after transplantation with BCR-ABL1⁺-transduced BM in the B-ALL model (WT n = 16; *Plekhh1* KO n = 17; t-test). B) Percentage of GFP⁺ (BCR-ABL1⁺) BP-1⁺ cells in PB of WT (black) or *Plekhh1* KO (grey) recipient mice transplanted with BCR-ABL1-transduced BM on day 20 after transplantation. (WT n = 17; *Plekhh1* KO n = 16; t-test). C) Kaplan-Meier-style survival curve for WT (black solid line) or *Plekhh1* KO (grey dashed line) recipient mice with BCR-ABL1⁺ B-ALL (WT n = 17; *Plekhh1* KO n = 18; Log-rank test).

3. PLEKHM1 deficiency in the BMM does not alter the homing capacity of BCR-ABL1⁺ B-ALL cells

Next, we tested whether the reason for disease aggressiveness in the *Plekhm1* KO recipients was due to increased homing efficiency of BCR-ABL1⁺ (GFP⁺) BP-1⁺ to a PLEKHM1 deficient BM or spleen. We observed a similar percentage of BCR-ABL1⁺ (GFP⁺) BP-1⁺ leukemia-initiating cells (LIC) in both BM and spleen of WT and *Plekhm1* KO recipients 18 hours post-transplantation (Figure 12A) suggesting that the increased aggressiveness cannot be attributed to an increased homing efficiency.

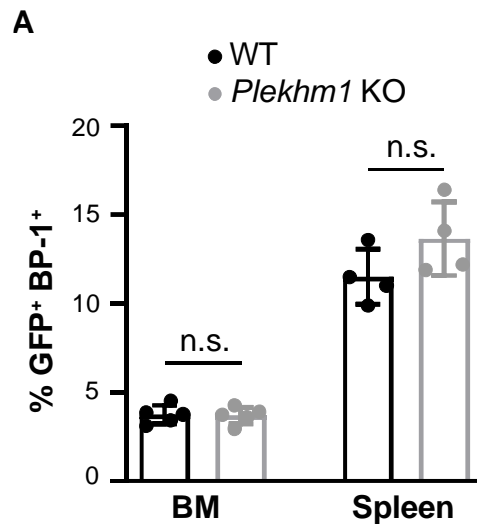


Figure 12: A) Percentage of GFP⁺ (BCR-ABL1⁺) BP-1⁺ cells of total leukocytes which homed to the BM or spleen of WT (black) or *Plekhm1* KO (grey) recipient mice 18 hours after transplantation (BM: WT n=5; *Plekhm1* KO n=5; Spleen: WT n=4; *Plekhm1* KO n=4; *t*-test).

4. Characterization of B-ALL cells in the *Plekhm1* KO BMM

To investigate what caused the more aggressive phenotype of B-ALL cells in the *Plekhm1* KO mice we isolated BCR-ABL1⁺ (GFP⁺) BP-1⁺ from the BM of WT or *Plekhm1* KO recipient mice on day 20 after transplantation and characterized them.

i. Apoptosis and cell cycle

Analysis of GFP⁺ (BCR-ABL1⁺) BP-1⁺ cells' apoptotic status using 4',6-diamidino-2-phenylindole (DAPI) and Annexin V staining, revealed a decreased percentage of early apoptotic cells (DAPI⁻ AnnV⁺) in the BM of *Plekhm1* KO recipient mice (Figure 13A) compared to the WT counterparts. However, late apoptotic cells (DAPI⁺ AnnV⁺) were similar between the two groups (Figure 13B). Cells from the BM of *Plekhm1* KO mice also showed a significant increase in the G₀ phase of the cell cycle as it was revealed by Ki67 staining (Figure 13C). Ki-67 is a cellular marker of proliferation that is present during all the active phases of the cell cycle (G₁, S, G₂, and mitosis), but is absent in resting (quiescent) cells (G₀)²³⁸. However, DAPI staining which is used to stain DNA and whose intensity increases in the S phase of the cell cycle due to duplication of the DNA, showed no further differences in the G₁, S and G₂ phases of the cell cycle (Figure 13D). This suggests that absence of PLEKHM1 might affect the entering of the cells in the cell cycle but not the progression from one phase to the next, once the cells have entered the cycle.

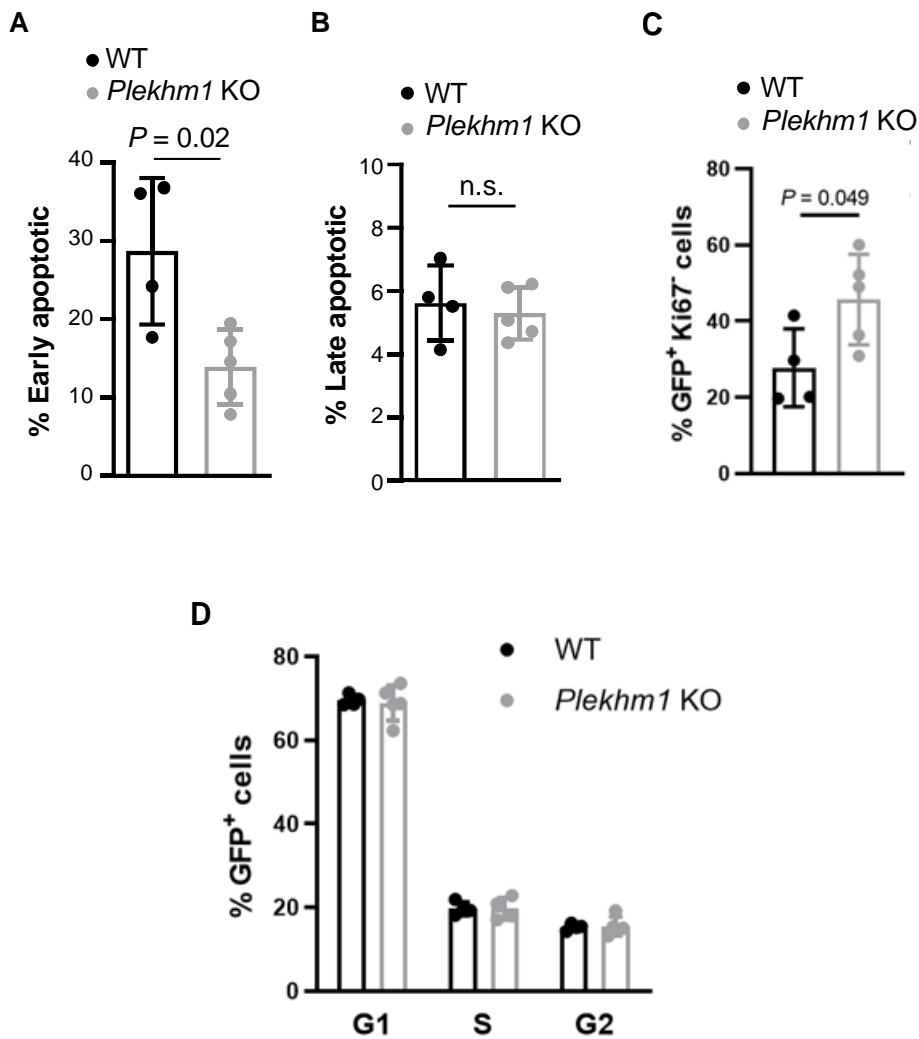


Figure 13: A) Percentage of GFP⁺ (BCR-ABL1⁺) BP-1⁺ early apoptotic (DAPI⁻ AnnexinV⁺) cells in the BM of WT (black) or *Plekhm1* KO (grey) mice (WT n=4; *Plekhm1* KO n=5; *t*-test). B) Percentage of GFP⁺ (BCR-ABL1⁺) BP-1⁺ late apoptotic (DAPI⁺ AnnexinV⁺) cells in the BM of WT (black) or *Plekhm1* KO (grey) recipient mice on day 20 after transplantation (WT n = 4; *Plekhm1* KO n = 5; *t*-test). C) Percentage of GFP⁺ (BCR-ABL1⁺) cells in the G₀ phase of the cell cycle in the bone marrow of WT (black) or *Plekhm1* KO (grey) mice (WT n = 4; *Plekhm1* KO n = 5; *t*-test). D) Percentage of GFP⁺ (BCR-ABL1⁺) cells in the G₁, S, and G₂ phases of the cell cycle in the BM of WT (black) or *Plekhm1* KO (grey) mice (WT n = 4; *Plekhm1* KO n = 5; *t*-test).

ii. B-cell markers on B-ALL cells from WT or *Plekhh1* KO mice

B lymphocytes originate in the BM after differentiation from HSC and go through a series of differentiation steps until they finally egress from the BM to the periphery. During these stages, which are regulated by interactions with the BMM^{38,239}, B cells are characterized by the sequential expression of specific surface markers which are involved in signal transduction and play a role in the developmental fate of B cells²⁴⁰(figure 14).

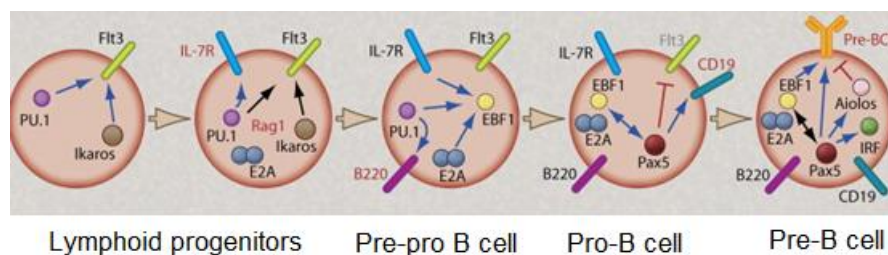
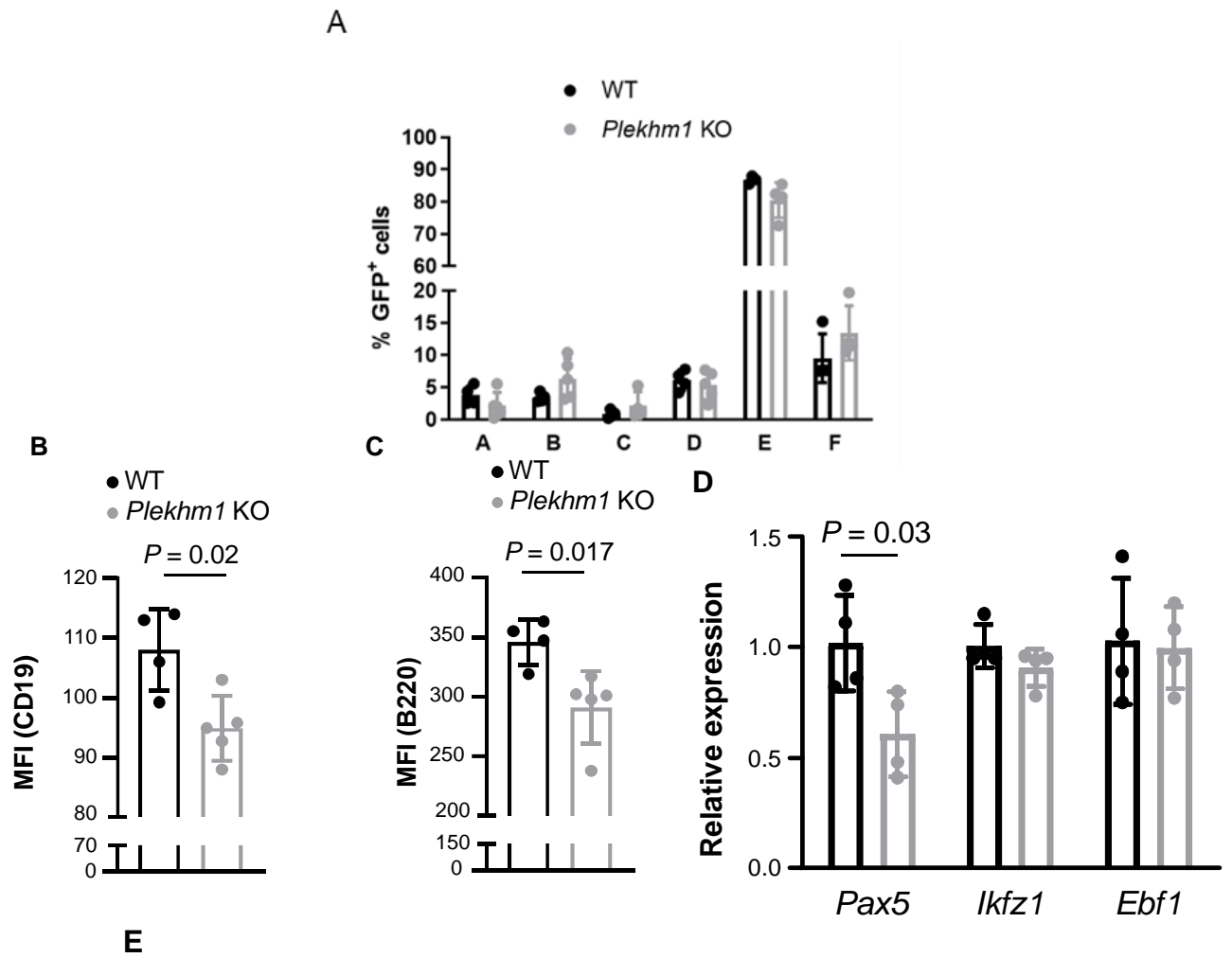


Figure 14: Expression of surface markers and presence of key transcription factors in the different stages of B-cell development. Flt3: definitive marker of lymphoid progenitors, PU.1: TF functions early in the progression toward B cell specification. Ikaros: transcriptional regulator implicated in early lymphoid specification. IL-7R: IL-7R-modulated transcription factors control the induction of the B cell-lineage-specification factor EBF1. Cell committed to the B cell lineage can be identified by expression of CD19, a target of the lineage-commitment factor Pax5²⁴⁰.

The increased B-ALL aggressiveness in *Plekhh1* KO mice in combination with the increased percentage of B-ALL LIC in G₀ phase, as well as their increased viability in *Plekhh1* KO mice led to the question whether these cells were characterized reduced differentiation or maturation stage compared to the WT counterparts. Therefore, we used a combination of markers, specifically CD43 (leukosialin, S7), BP-1 and heat stable antigen (HSA) (30F1), B220, and IgM which have been previously used to identify different fractions of B cells during development²²². Specifically, the following fractions (with the corresponding markers) were used **A**: B220^{low}CD43^{high}BP1^{neg}HSA^{neg},

B: B220^{low}CD43^{high}BP1^{neg}HSA^{pos}, **C:** B220^{low}CD43^{high}BP1^{high}HSA^{pos}, **D:** B220^{high}CD43^{neg}IgM^{neg}, **E:** B220^{high}CD43^{neg}IgM^{mid} and **F:** B220^{high++}CD43^{neg}IgM^{high/mid}.

There were no differences in the different B-cell fractions (fractions A-F) in the GFP⁺ BM cells between WT and *Plekhh1* KO mice with B-ALL as these are defined by these markers' combination (see Materials and Methods) (Figure 15A). However, when we looked at single markers we noticed that CD19 (Figure 15B) and B220 (Figure 15C), both B-cell specific markers that control B-cell development^{241,242}, were found to be decreased in the GFP⁺ BM cells from *Plekhh1* KO compared to WT mice. Furthermore, expression levels of the paired box 5 (*Pax5*) gene which encodes for a transcription factor with a key role in B-lymphocyte development¹⁶ and regulates CD19 expression²⁴³, were reduced in BM cells from *Plekhh1* KO mice (Figure 15D). We also tested expression levels of two other genes that code for transcription factors (TF) which play a regulatory role in B-cell development and have been linked to B-ALL: *Ikaros* (*IKZF1*) and *Early B-cell factor 1* (*EBF1*)^{244,245}. However, we could not detect any differences between the two conditions (Figure 15D). However, in agreement with the acquisition of a more primitive phenotype further analysis with proteomics revealed decreased expression of the immunoglobulin heavy constant alpha 1 (IGHA1) and immunoglobulin kappa constant (IGKC) chains in GFP⁺ (BCR-ABL1⁺) BP-1⁺ cells derived from *Plekhh1* KO mice (Figure 15E) which are both components of the B-cell receptor of mature B-lymphocytes²⁴⁶.



E

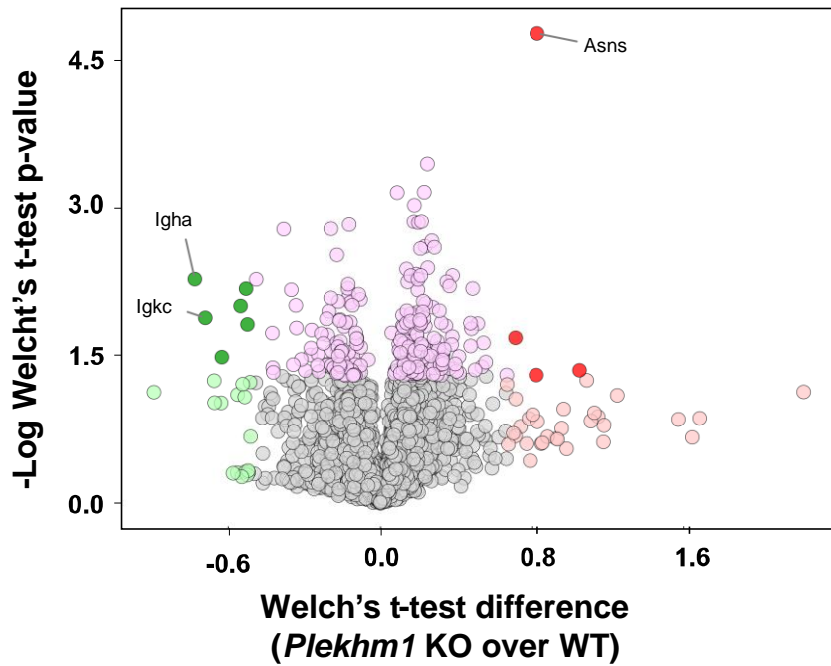


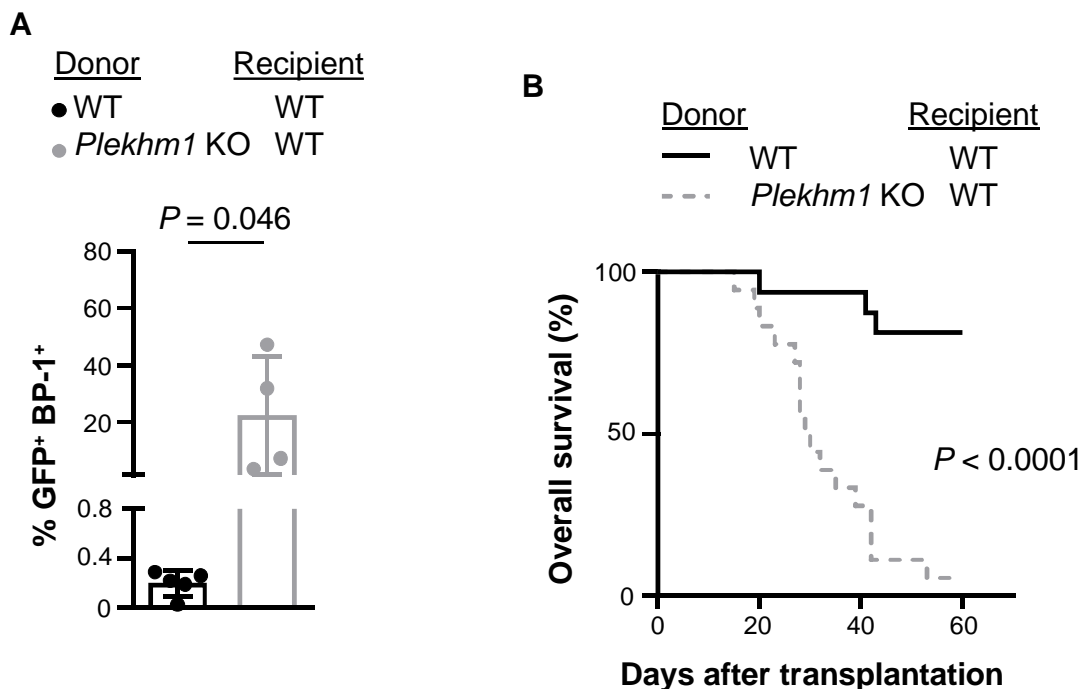
Figure 15: A) Percentage of GFP⁺ (BCR-ABL1⁺) cells from the BM of WT (black) or *Plekhhm1* KO (grey) mice in the different B-cell fractions (fractions A-F) (WT n = 3-4; *Plekhhm1* KO n = 4-5; *t*-test). B) Mean fluorescence intensity (MFI) of CD19 in GFP⁺ (BCR-ABL1⁺) cells in the BM of WT (black) or *Plekhhm1* KO (grey) mice with BCR-ABL1⁺ B-ALL on day 20 after transplantation (WT n = 4; *Plekhhm1* KO n = 5; *t*-test). C) Mean fluorescent intensity (MFI) of B220 in GFP⁺ (BCR-ABL1⁺) cells in the BM of WT (black) or *Plekhhm1* KO (grey) mice with BCR-ABL1⁺ B-ALL on day 20 after transplantation (WT n = 4; *Plekhhm1* KO n = 5; *t*-test). D) Relative expression of Pax5, IKZF1, and EBF1 in total BM of WT (black) or *Plekhhm1* KO (grey) mice with BCR-ABL1⁺ B-ALL on day 20 after transplantation (WT n = 4; *Plekhhm1* KO n = 4; *t*-test). E) Volcano plot showing protein expression in bone marrow cells from WT or *Plekhhm1* KO recipient mice with established B-ALL on day 20 after transplantation. Samples were normalized for protein content prior to mass spectrometry. The x-axis indicates the difference in protein abundance between *Plekhhm1* KO and WT mice, while the y-axis indicates the -log p value (Welch's *t*-test). Proteins on the right in dark red showed increased expression and proteins in dark green reduced expression in *Plekhhm1* KO mice compared to the WT (WT n = 4; *Plekhhm1* KO n = 5; *t*-test).

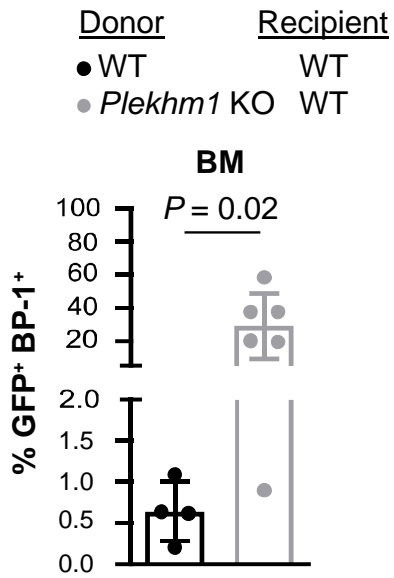
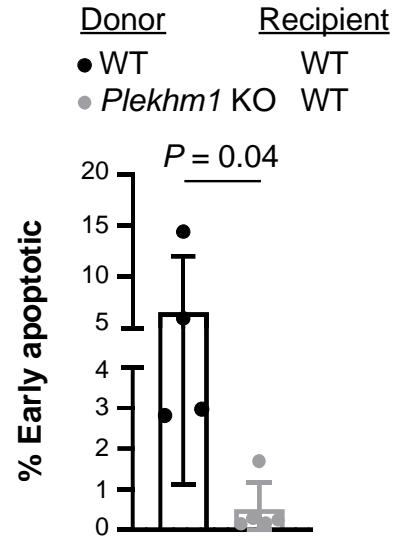
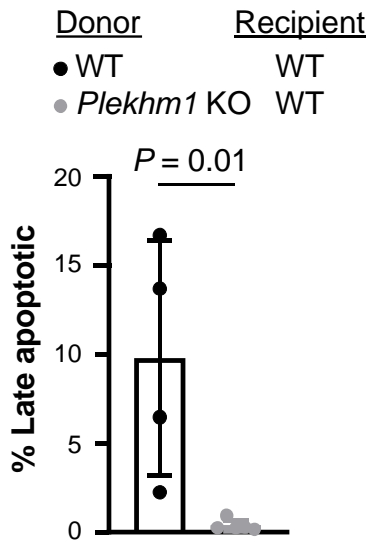
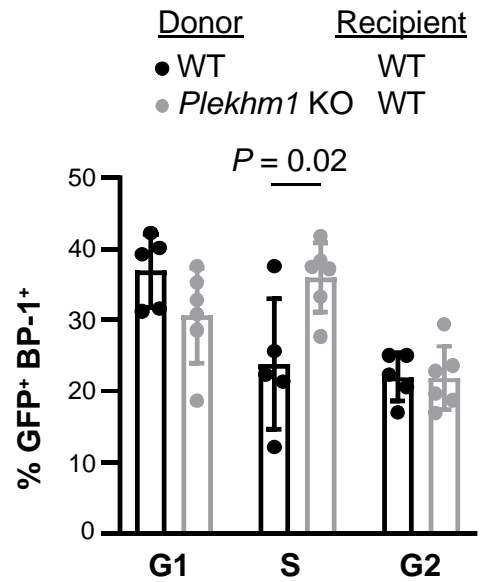
5. A *Plekhm1* KO microenvironment increases the number and/or function of B-ALL-initiating cells (LIC)

Leukemia stem cells are defined by their ability to give rise to disease upon transplantation into secondary recipients²⁴⁷. Therefore, we performed secondary transplantation assays to assess the number or function of these leukemia-initiating cells that are found in a WT or *Plekhm1* KO BMM on day 20 after transplantation. Here, we should note that the penetrance of the disease in secondary recipients is often less than 100% when WT mice are used as both donors and recipients. The above data suggest that B-ALL cells are more viable and can cause a more aggressive disease when they are derived from a *Plekhm1* KO compared to a WT microenvironment. At the same time absence of PLEKHM1 in the BMM seems to promote a more quiescent phenotype in B-ALL cells as evidenced by the increase in the G₀ phase of the cell cycle. Given that increased viability, dormancy, and differentiation blockade are all characteristics of “leukemia stem cells” (as is the case in other cancer stem cells) we questioned whether these characteristics can give a selective advantage to B-ALL-initiating cells as well.

To address this, we isolated B-ALL cells from the BM of WT or *Plekhm1* KO primary recipients on day 20 post-transplantation and transplanted them into secondary WT recipients. Interestingly, secondary recipient mice of *Plekhm1* KO BMM-exposed B-ALL cells had an increased tumor burden of GFP⁺ (BCR-ABL1⁺) BP-1⁺ in their peripheral blood (PB) on day 20 post-transplantation (Figure 16A). This was accompanied by an acceleration of B-ALL disease (Figure 16B) suggesting that PLEKHM1 deficiency in the BMM increases the number and/or function of BALL-initiating cells. Further characterization of the mice that received B-ALL cells previously exposed to a *Plekhm1* KO BMM revealed an increased number of BCR-ABL1⁺ BP-1⁺

cells in the BM (Figure 16C), which were more viable as they were characterized by decreased early (Figure 16D) and late (Figure 16E) apoptosis. B-ALL initiating cells previously exposed to a *Plekhh1* KO BMM were found to be more in the S phase of the cell cycle (Figure 16F), while, there was an increased number of cells which had not entered the cell cycle and were found in the G₀ phase (Figure 16G). While this seems contradictory it is possible that we are assessing two different populations and B-ALL initiating cells exposed to a *Plekhh1* KO BMM are more prone to quiescence, as indicated by an increase in the G₀ phase, but have entered the cell cycle they actually cycle faster compared to the B-ALL LIC exposed to a WT BMM.



C**D****E****F**

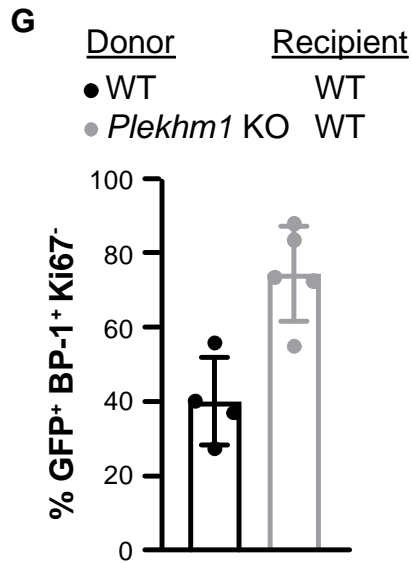


Figure 16: A) Percentage of GFP⁺ (BCR-ABL1⁺) BP-1⁺ cells in the peripheral blood of WT secondary recipient mice of total bone marrow cells from WT (black) or *Plekhh1* KO (grey) donor mice with established B-ALL. Cells were analyzed on day 20 after transplantation (WT n = 5; *Plekhh1* KO n = 4; *t*-test). B) Kaplan-Meier-style survival curve of WT secondary recipients of total bone marrow from WT (black solid line) or *Plekhh1* KO (grey dashed line) donor mice with established B-ALL (WT n = 16; *Plekhh1* KO n = 17; Log-rank test). C) Percentage of GFP⁺ (BCR-ABL1⁺) BP1⁺ cells in the bone marrow of WT secondary recipients of total bone marrow from WT (black) or *Plekhh1* KO (grey) donor mice with established B-ALL. Cells were analyzed on day 20 after transplantation (WT n = 4; *Plekhh1* KO n = 6; *t*-test). D) Percentage of GFP⁺ (BCR-ABL1⁺) BP-1⁺ early apoptotic (DAPI⁻ AnnV⁺) cells in the bone marrow of WT secondary recipients of total bone marrow from WT (black) or *Plekhh1* KO (grey) donor mice with established B-ALL. Cells were analyzed on day 20 after transplantation (WT n = 4; *Plekhh1* KO n = 5; *t*-test). E) Percentage of GFP⁺ (BCR-ABL1⁺) BP1⁺ late apoptotic (DAPI⁺ AnnV⁺) cells in the bone marrow of WT secondary recipients of total bone marrow from WT (black) or *Plekhh1* KO (grey) donor mice with established B-ALL. Cells were analyzed on day 20 after transplantation (WT n = 4; *Plekhh1* KO n = 5; *t*-test). F) Percentage of GFP⁺ (BCR-ABL1⁺) BP-1⁺ cells in the G₁, S, and G₂ phases of the cell cycle in the bone marrow of WT secondary recipients of total bone marrow from WT (black) or *Plekhh1* KO (grey) donor mice with established B-ALL. Cells were analyzed on day 20 after transplantation (WT n = 5; *Plekhh1* KO n = 6; *t*-test). G) Percentage of GFP⁺ (BCR-ABL1⁺) BP-1⁺ cells in the G₀ phase of the cell cycle in the bone marrow of WT secondary recipients of total bone marrow from WT (black) or *Plekhh1* KO (grey) donor mice with established B-ALL. (WT n = 4; *Plekhh1* KO n = 5; *t*-test).

6. Characterization of the *Plekhh1* KO BMM

i. PLEKHM1 in osteoclasts is dispensable for the proliferation of B-ALL cells

Given the role of PLEKHM1 in the trafficking of secretory lysosomes in osteoclasts²¹⁵ we initially hypothesized that osteoclasts might play a role in the observed acceleration of B-ALL progression. Therefore, we differentiated osteoclasts from monocytes/macrophages isolated from WT or *Plekhh1* KO mice *in vitro* using macrophage colony-stimulating factor (M-CSF) and receptor activator of nuclear factor kappa-B ligand (RANKL) for 4-6 days²²³. These factors can induce differentiation of bone marrow hematopoietic precursor cells into bone-resorbing osteoclasts without the requirement for stromal cells of mesenchymal origin²⁴⁸. *Plekhh1* KO osteoclasts showed no impairment of their differentiation from monocytes *in vitro* and they had similar morphology compared to WT osteoclasts (Figure 17A). However, *Plekhh1* KO osteoclasts showed reduced resorptive activity as measured by the reduced surface area of pits that they formed on bone slices (Figure 17B and 17C). To investigate whether the differences in activity resulted in different interactions with B-ALL cells we co-cultured BCR-ABL1⁺ BA/F3 cells, a frequently used *in vitro* model for B-ALL¹³⁷, on WT or *Plekhh1* KO osteoclasts and measured their proliferation over the course of 4 days. There were no differences in the number of BCR-ABL1⁺ BA/F3 cells cultured on

top of *Plekhm1* KO osteoclasts compared to the WT counterparts throughout the 4 days (Figure 17D).

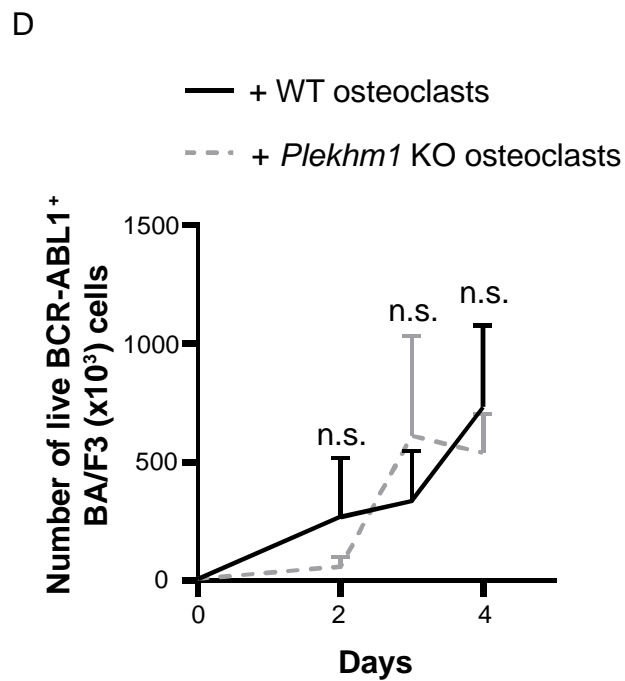
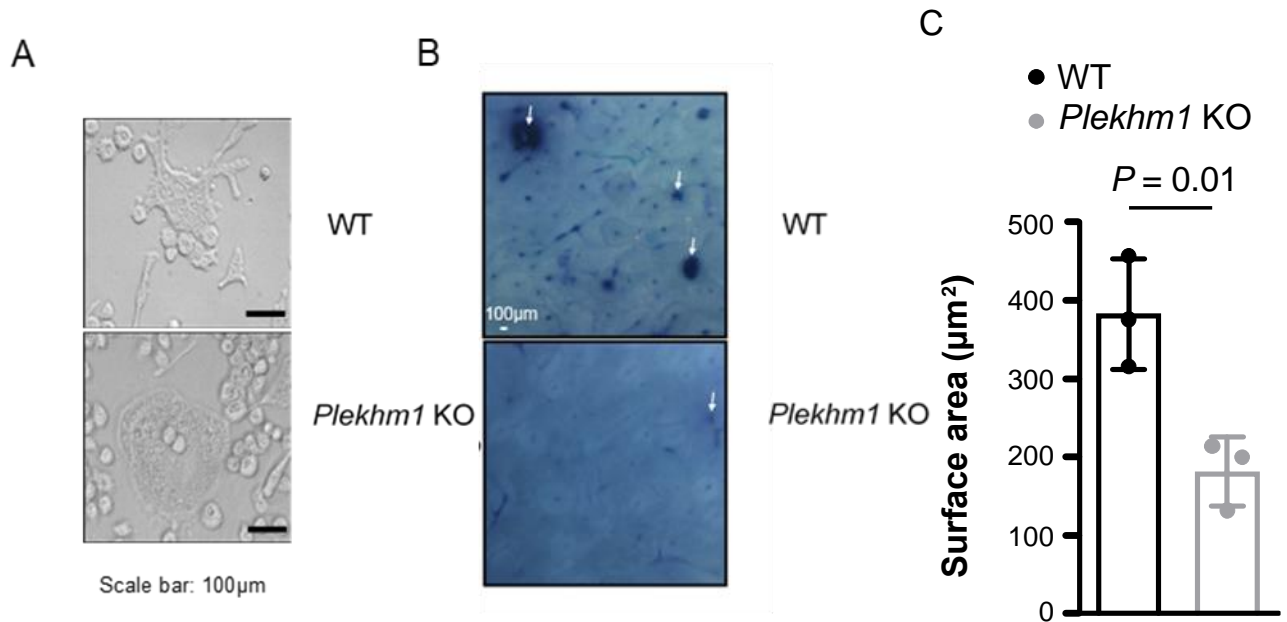


Figure 17: A) Microscopic pictures showing WT or *Plekhh1* KO osteoclasts. The scale bar depicts 100µm. B) Microscopic pictures showing toluidine-stained pits (white arrows) formed on bone slices by WT or *Plekhh1* KO osteoclasts C) Surface area of resorption pits formed by WT (black) or *Plekhh1* KO (grey) osteoclasts. Data are the results from triplicate plating of 3 independent biological replicates. D) Number of live BCR-ABL1⁺ BA/F3 cells plated on WT (black solid line) or *Plekhh1* KO (grey dashed line) osteoclasts. The data are representative of 3 independent experiments (two-way ANOVA).

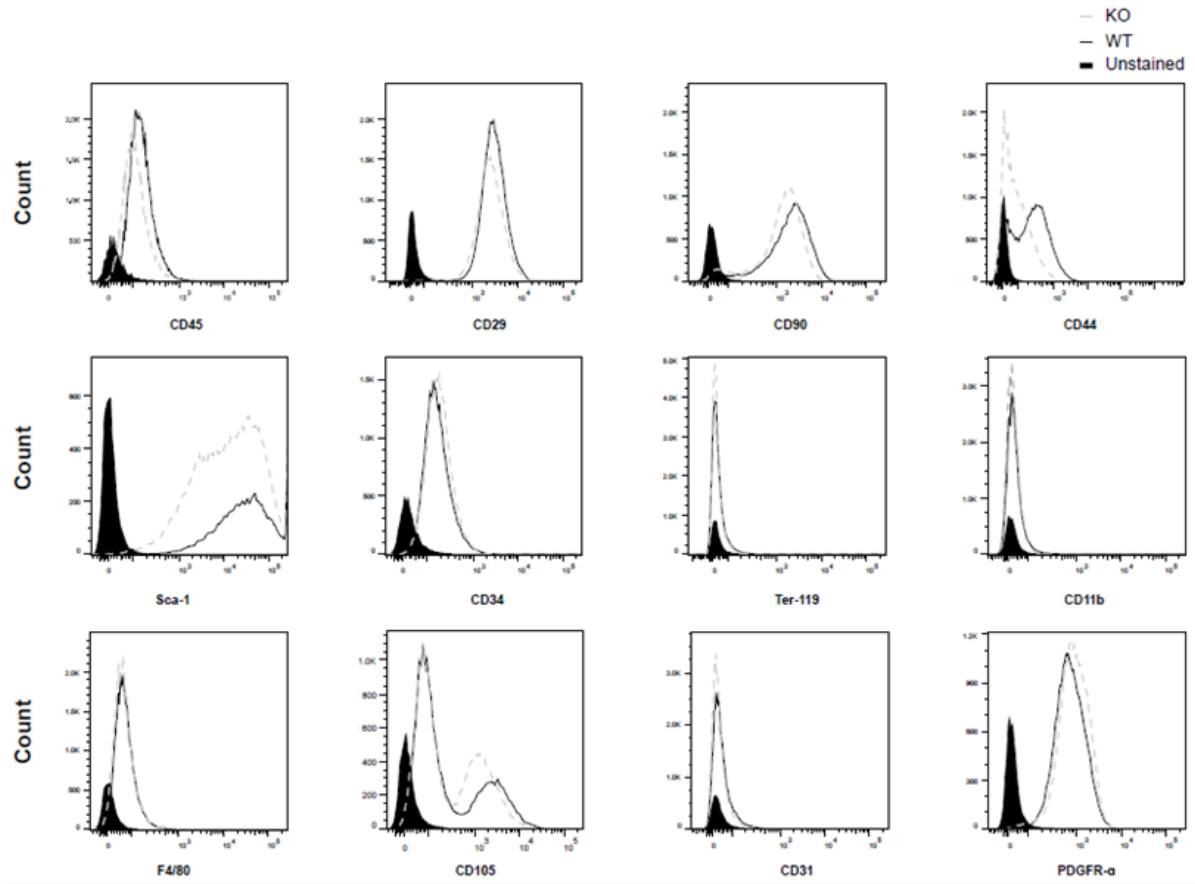
- ii. Differentiation to osteoblasts and adipocytes and vesicular trafficking are altered in *Plekhh1* KO mesenchymal stromal cells

The above results indicate that osteoclasts are likely not playing a direct role in the observed aggressiveness of B-ALL in *Plekhh1* KO recipient mice. As PLEKHM1 also is expressed in MSC²⁴⁹, which have a known role in B-ALL^{137,250}, we investigated whether MSC are involved in the establishment of the observed phenotype. To address this, we isolated CD45⁻ Ter-119⁻ PDGFR- α ⁺ Sca-1⁺ MSC²²⁵ from the BM of healthy WT or *Plekhh1* KO mice, which did not differ significantly with regards to their immunophenotype (Figure 18A). Of note, both WT and *Plekhh1* KO MSC were positive for previously described MSC markers including CD29, CD90, CD105, PRFGR-alpha and Sca-1. The cells were free of hematopoietic contamination as shown by lack of expression of CD45, CD34, and Ter-119. MSC can form colonies and differentiate to osteoblasts and adipocytes *in vitro* under the proper conditions. Therefore, we tested the colony-forming ability and the osteogenic differentiation potential, as assessed by Von Kossa and Alizarin Red stainings, of *Plekhh1* KO

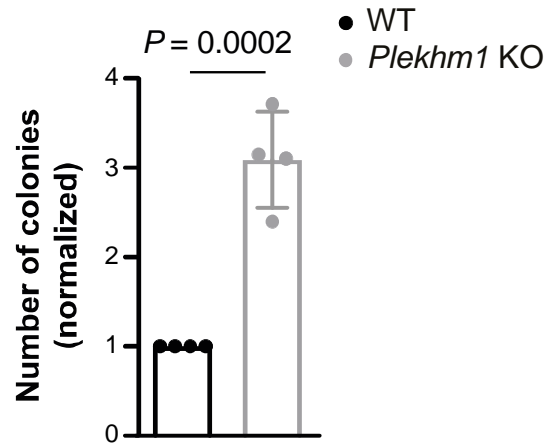
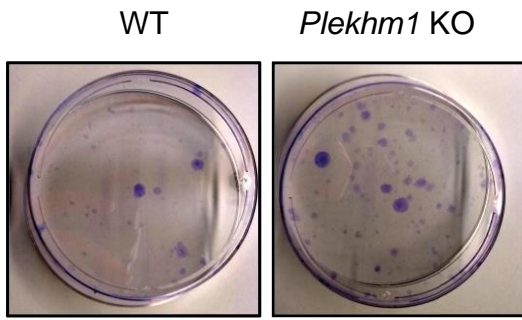
compared to WT MSC. Both colony-forming ability (Figure 18B) and osteogenic differentiation potential (Figure 18C) were higher in the *Plekhh1* KO compared to WT MSC. In contrast, the adipogenic differentiation potential of the *Plekhh1* KO MSC, as assessed by Oil Red O staining, was significantly reduced compared to the WT counterparts (Figure 18D). PLEKHM1 plays a role in vesicular trafficking and fusion of late endosomes with lysosomes²¹⁷. Therefore, we hypothesized that the reduced differentiation potential of *Plekhh1* KO MSC into adipocytes could be associated with an impairment in lipid droplet fusion as an indication of a more general impairment in vesicular trafficking. Therefore, we investigated whether the number of MVB, a subset of specialized late endosomes¹⁷⁸, was different between WT and *Plekhh1* KO MSC. Immunofluorescence staining for CD63, a specific MVB marker²⁵¹, showed an increased number of multivesicular bodies (MVB) in *Plekhh1* KO MSC compared to WT (Figure 18E). Of note immunofluorescence for LC3-positive vesicles (autophagosomes) or LAMP1-positive vesicles (lysosomes) showed no significant differences in their number or in their co-localization between WT and *Plekhh1* KO MSC (Figure 18F). This was indicative of similar autophagy basal levels between the two types of cells. Taken together, these results suggest that *Plekhh1* KO MSC have an increased capacity to form colonies and differentiate into the osteoblastic lineage

while harboring an increased number of CD63⁺ MVB, thus, affecting non-autophagic vesicular trafficking in MSC at baseline levels.

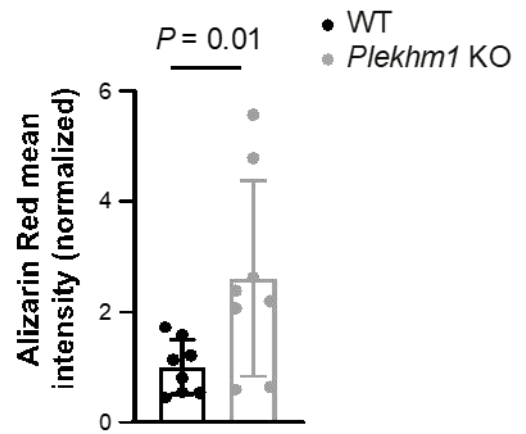
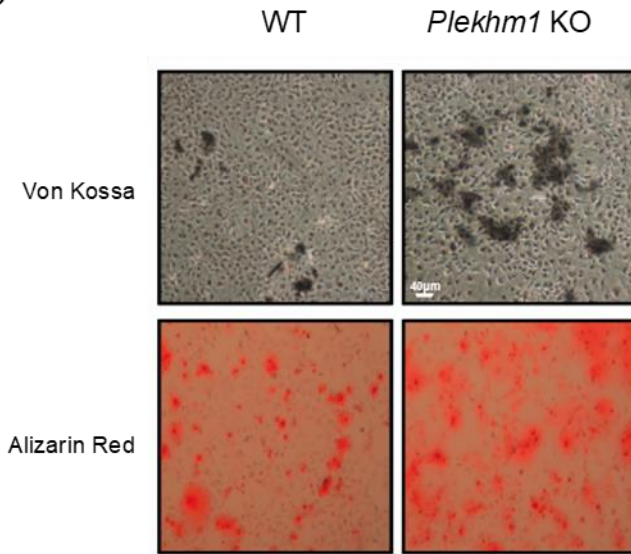
A



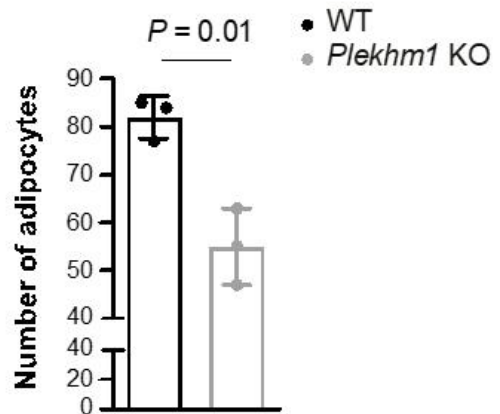
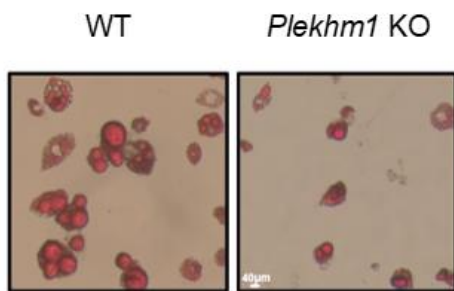
B



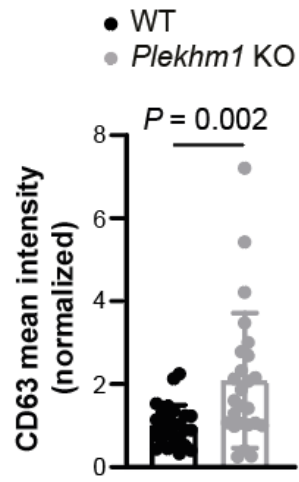
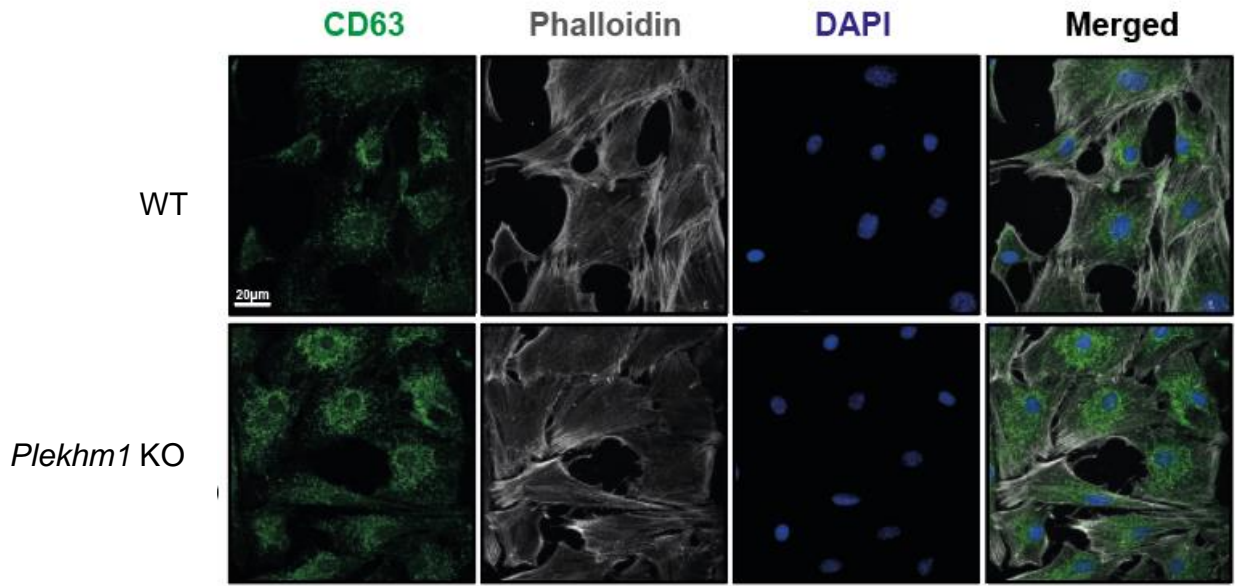
C



D



E



F

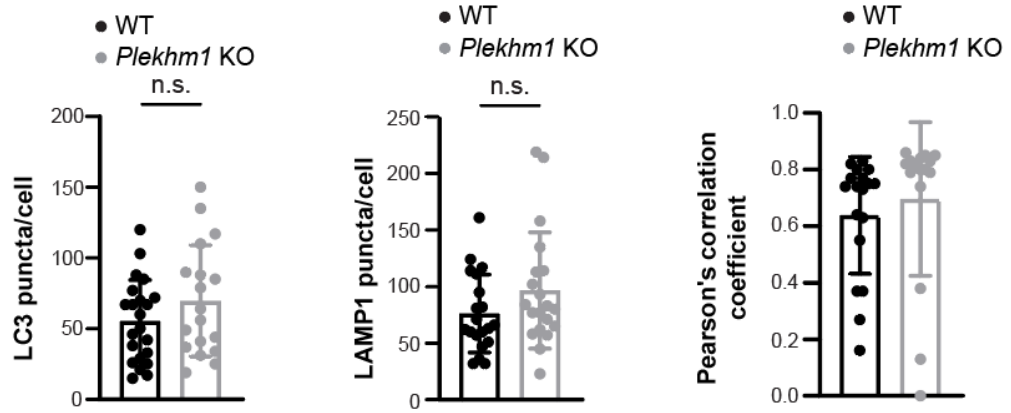
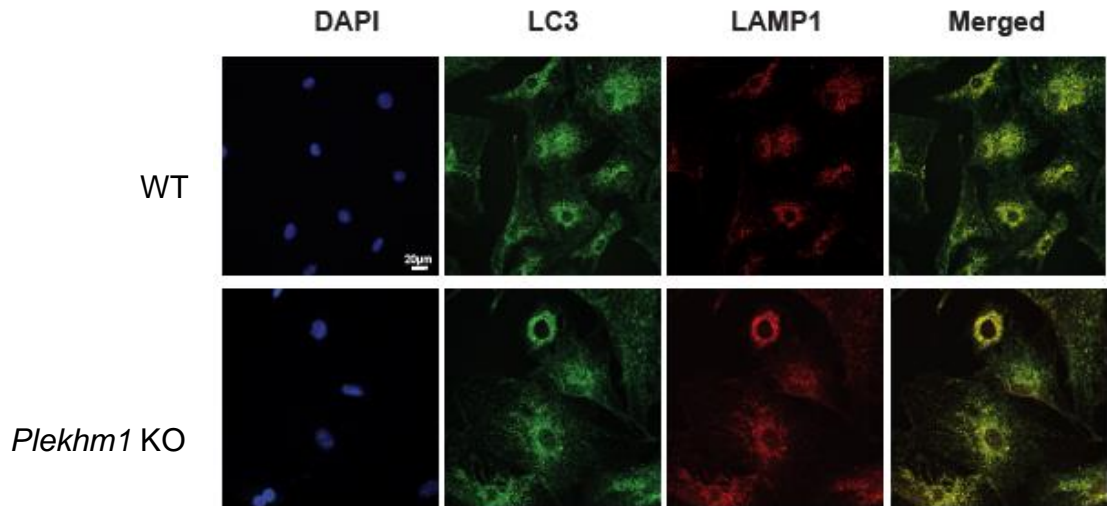


Figure 18: A) Surface marker expression of primary MSC derived from the BM of WT (black line) or *Plekhm1* KO (grey line) mice at passage 4. Unstained cell controls (black thick line) are included for comparison. B) Representative image of colonies derived from WT or *Plekhm1* KO MSC stained with crystal violet (left). Number of colonies formed by WT (black) and *Plekhm1* KO (grey) MSC (right). Data are the results of 4 independent experiments and the values are normalized to the WT for each independent experiment (*t*-test). C) Evaluation of osteogenic differentiation of WT or *Plekhm1* KO MSC. Von Kossa and Alizarin Red staining were used for the detection of the presence of calcium deposits (left). Scale bar depicts 40µm. Quantification of alizarin red staining intensity using ImageJ software normalized to the WT (right). Each dot represents a technical replicate from a total of 3 independent experiments (*t*-test). D) Evaluation of adipogenic differentiation of WT or *Plekhm1* KO MSC. Oil Red O staining was used for the detection of the presence of intracytoplasmic lipid-rich droplets (adipocytes) (left). Scale bar depicts 40µm. Number of adipocytes formed after differentiation of WT (black) or *Plekhm1* KO (grey) MSC (right). Data are results from 3 independent experiments (*t*-test). E) Representative immunofluorescence images of WT or *Plekhm1* KO MSC stained with an antibody against CD63 (green). The nuclei are counterstained with DAPI (blue) and the cytoplasm with phalloidin (grey) (top). Scale bar depicts 20µm. Quantification of CD63 fluorescence intensity of WT (black) or *Plekhm1* KO (grey) MSC (bottom). The values are normalized to the average value of WT. Data are results of 4 independent experiments (*t*-test). F) Representative immunofluorescence images of LC3 and LAMP1 staining their colocalization (top). Comparison of the number of LC3 (left) or LAMP1 (middle) puncta per cell between WT (black) and *Plekhm1* KO (grey) MSC measured with ImageJ software and quantification tool (bottom) (*t*-test). Comparison of the colocalization between LC3 and LAMP1 (right) between WT (black) versus *Plekhm1* KO (grey) MSC expressed as the Pearson's correlation coefficient and calculated using ImageJ software and coloc2 tool. Quantification was performed for 3 independent experiments with >15 cells quantified per condition. Scale bar depicts 20µm.

7. *Plekhh1* KO MSC release syntenin- and syndecan-1-enriched small extracellular vesicles (sEV)

i. PLEKHM1 does not affect the number of sEV released by MSC

MVB are involved in the release of intraluminal vesicles (ILV) to the extracellular space as exosomes²⁰⁷, and exosomes are critical mediators in the communication between leukemia cells and their environment^{116,252}. MVB are degraded after fusion with lysosomes¹⁷⁸ and there are reports on the involvement of autophagy- or vesicular trafficking-associated proteins for the regulation of EV cargo²⁵³. Therefore, given the increased amount of CD63⁺ MVB that were found in *Plekhh1* KO MSC we questioned whether the absence of PLEKHM1 affects the released exosomes. Using differential centrifugation, small extracellular vesicles (sEV), that are enriched in exosomes¹⁸⁷, were isolated from the conditioned medium of WT or *Plekhh1* KO MSC. We confirmed the successful isolation of sEV by the expression of the exosomal markers CD81 and flotillin-1 in the exosomal preparation, as well as by the absence of expression of the golgi matrix protein 130 kD (GM130)²⁵⁴ (Figure 19A). Given that the proliferation status of the donor cell has been shown to influence the release of exosome-like microvesicles²⁵⁵ we tested whether there were differences in the cell cycle between WT and *Plekhh1* KO MSC. However, we observed that the cell cycle of WT versus *Plekhh1* KO MSC was similar (Figure 19B). Additionally, there were no differences in the amount of CD81 protein in sEV derived from *Plekhh1* KO MSC compared to the WT (Figure 19C). Consistently, the number of CD81⁺ EV being detected by imaging flow cytometric analysis performed at the single EV level²³³ and normalized to the number of MSC, were similar, regardless of whether the EV were derived from WT or *Plekhh1* KO MSC (Figure 19D). In addition, molecules of equivalent soluble fluorochrome (MESF), describing the amount of antibody bound to CD81 per sEV,

were also similar between sEV derived from WT versus *Plekhm1* KO MSC (Figure 19E). Taken together, these results indicate that PLEKHM1 does not affect the number of CD81⁺ sEV released by BM-derived MSC.

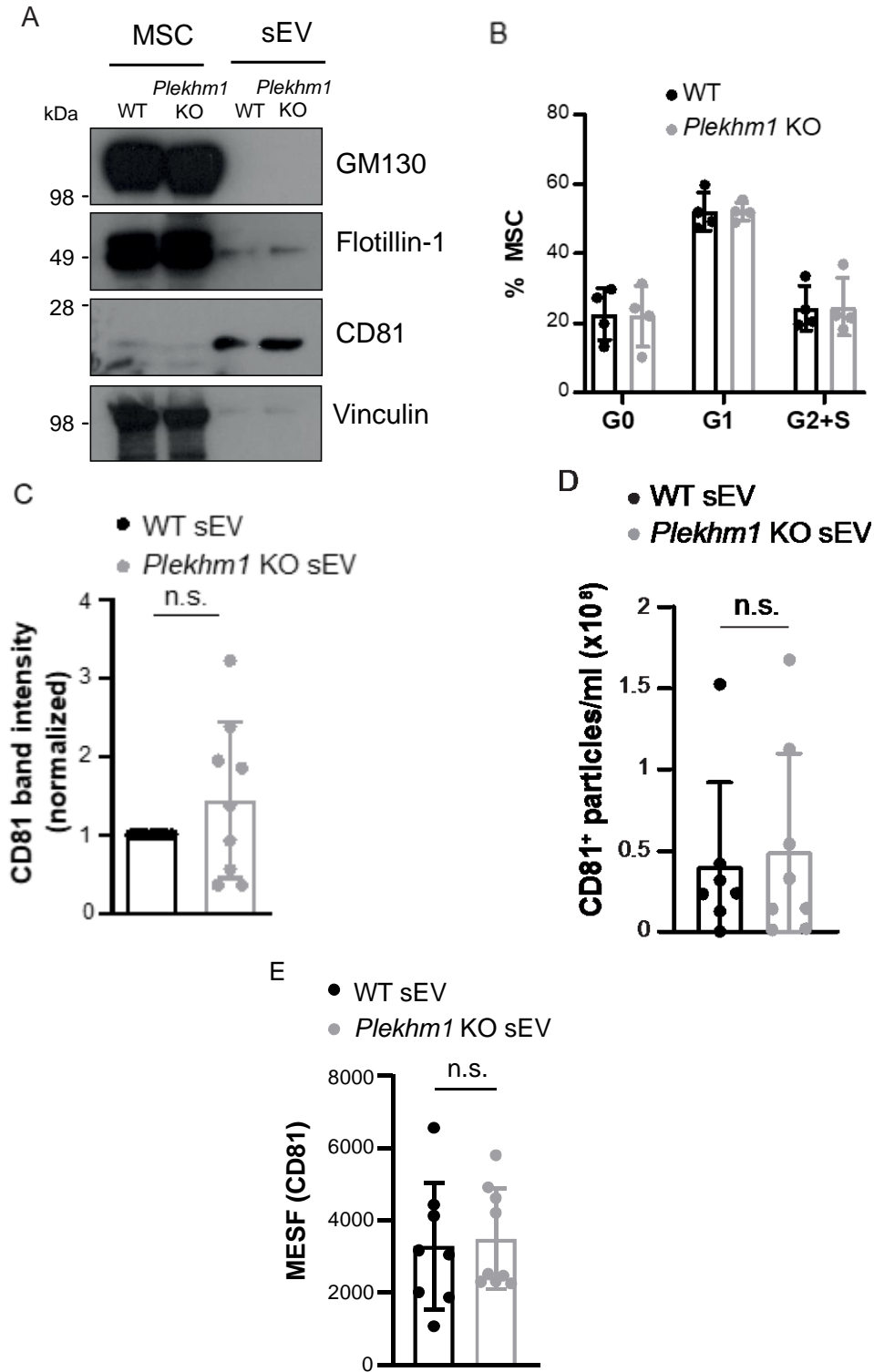
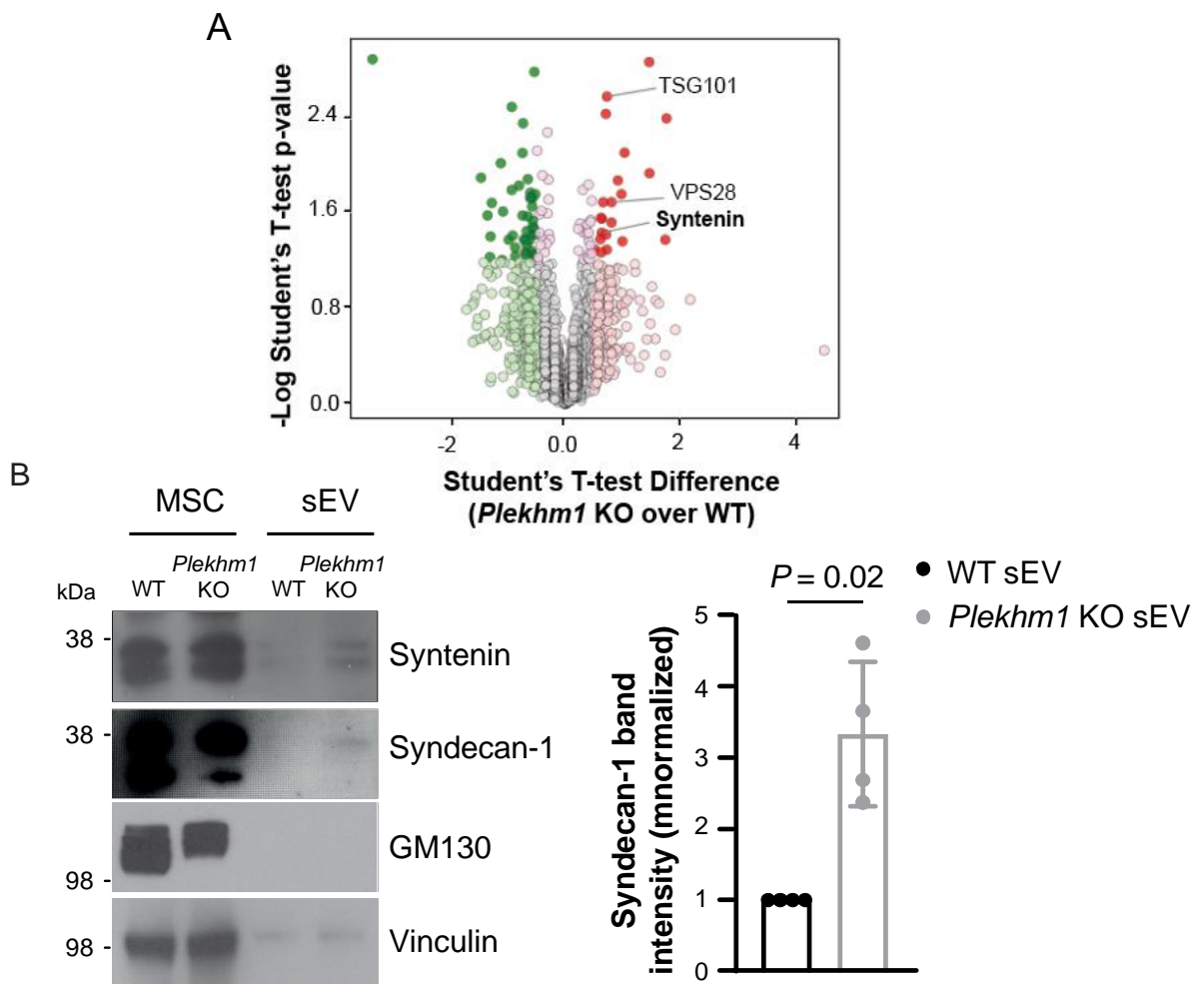


Figure 19: A) Representative immunoblot showing expression of GM130, CD81, and flotillin-1 in WT or *Plekhh1* KO MSC or sEV derived from WT or *Plekhh1* KO MSC. Vinculin was used as a loading control of MSC and negative marker for sEV. B) Percentage of WT (black) or *Plekhh1* KO (grey) MSC in the G0, G1, or G2 and S phases of the cell cycle. (WT n = 4; *Plekhh1* KO n = 4; t-test). The values are normalized to the WT for each individual experiment (n = 9; t-test). C) Quantification of CD81 band intensity in sEV isolated from WT (black) or *Plekhh1* KO (grey) MSC D) Quantification of CD81⁺ particles/ml (x10⁸) in the sEV preparations derived from WT (black bar) or *Plekhh1* KO (grey bar) MSC (WT n = 7; *Plekhh1* KO n = 8; t-test). E) Quantification of molecules of equivalent soluble fluorochrome (MESF) of CD81 in sEV isolated from WT (black) or *Plekhh1* KO (grey) MSC. The values are normalized to the WT for each individual experiment (n=8; t-test).

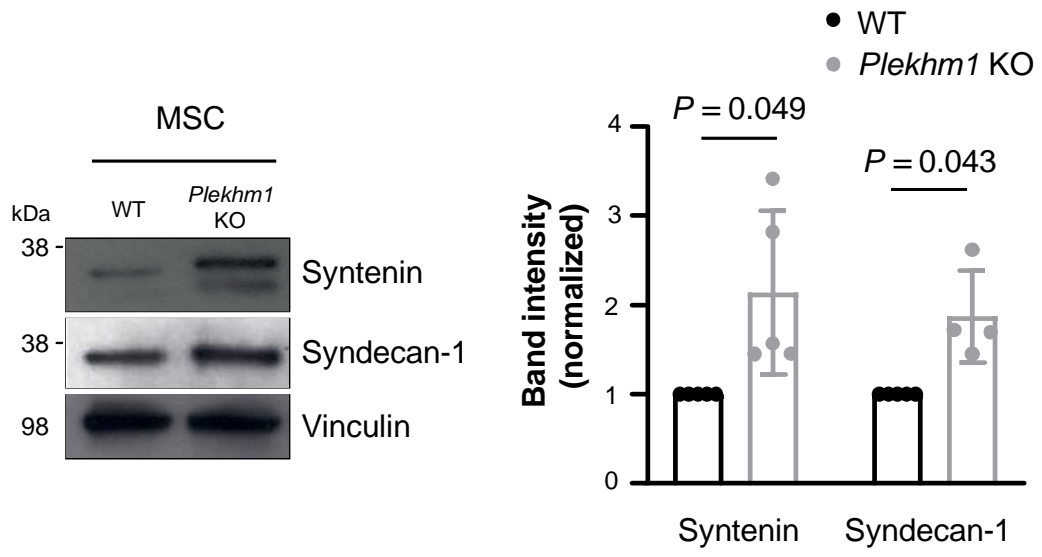
ii. PLEKHM1 regulates MSC-derived sEV cargo

Given that the increased CD63⁺ MVB in *Plekhh1* KO MSC did not result in differences in sEV number we investigated whether it affected sEV cargo. Proteomic analysis of MSC-derived sEV showed increased levels of vacuolar protein sorting (VPS)23 (TSG101) and VPS28 in the sEV preparations from *Plekhh1* KO compared to WT MSC (Figure 20A). These are proteins that belong to the ESCRT-I complex²⁵⁶ and are responsible for the formation and sorting of cargo into intraluminal vesicles supporting the hypothesis that there are differences in the cargo rather than the number of sEV derived from *Plekhh1* KO versus WT MSC. Similarly, syntenin, which is not a part of the ESCRT-I complex, but is involved in ESCRT-dependent exosomal biogenesis¹⁹⁶, was also found significantly increased in the *Plekhh1* KO sEV preparations (Figure 20A). Immunoblot analysis further confirmed the enriched presence of syntenin in the *Plekhh1* KO MSC-derived exosomes (Figure 20B). Syntenin directly interacts with syndecan-1, a heparan sulfate proteoglycan and integral membrane protein present in both healthy and tumor cells including leukemia cells²⁵⁷. In line with the enrichment of syntenin, we observed increased syndecan-1 protein levels in sEV from *Plekhh1*

KO MSC (Figure 20B). Immunoblot analysis of MSC, i.e. the donor cells of sEV, similarly, revealed enrichment of syntenin and syndecan-1 in *Plekhm1* KO compared to WT MSC (Figure 20C). Increased levels of syndecan-1 were also confirmed in *Plekhm1* KO MSC by immunofluorescence (Figure 20D). Our data suggest that deficiency of PLEKHM1 leads to increased levels of syntenin and syndecan-1 in MSC and MSC-derived sEV while leaving the number of released sEV unaffected. These findings are consistent with reports that support the notion that overexpression of the cytoplasmic adaptor molecule syntenin and syndecan-1 in donor cells may enhance their exosomal expression¹⁹⁶.



C



D

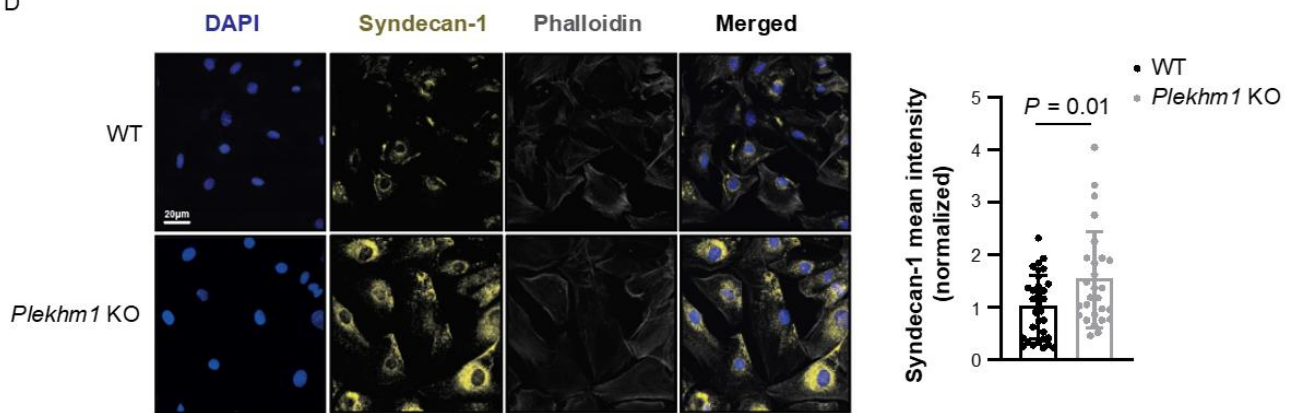


Figure 20: A) Volcano plot showing protein expression in sEV preparations isolated from WT versus *Plekhh1* KO MSC. Samples were normalized for protein content prior to mass spectrometry. The x-axis indicates the difference in protein abundance between sEV derived from *Plekhh1* KO and WT MSC, while the y-axis indicates the $-\log p$ value (Student's t-test). Proteins in dark red are expressed significantly higher and in dark green significantly lower in exosomes from *Plekhh1* KO MSC (WT n = 4; *Plekhh1* KO n=4). B) Representative immunoblot showing expression of syntenin and syndecan-1 in WT or *Plekhh1* KO MSC or sEV derived from WT or *Plekhh1* KO MSC (left). Quantification of syndecan-1 band intensity in sEV isolated from WT (black) or *Plekhh1* KO (grey) MSC (right). The values are normalized to the WT for each individual experiment (WT n = 7; *Plekhh1* KO n = 7; t-test). C) Representative immunoblot showing expression of syntenin and syndecan-1 in WT or *Plekhh1* KO MSC (left). Quantification of syntenin and syndecan-1 band intensity in WT versus *Plekhh1* KO MSC (right). The values are normalized to WT for each individual experiment and are results of 5 (syntenin) or 4 (syndecan-1) biological replicates (t-test). D) Representative immunofluorescence images of syndecan-1 staining on WT or *Plekhh1* KO MSC. The nuclei are counterstained with DAPI (blue) (left). The scale bar depicts 20 μ m. Quantification of syndecan-1 fluorescence intensity of WT (black) or *Plekhh1* KO (grey) MSC normalized to WT. The data are the result of 4 biological replicates (right) (t-test).

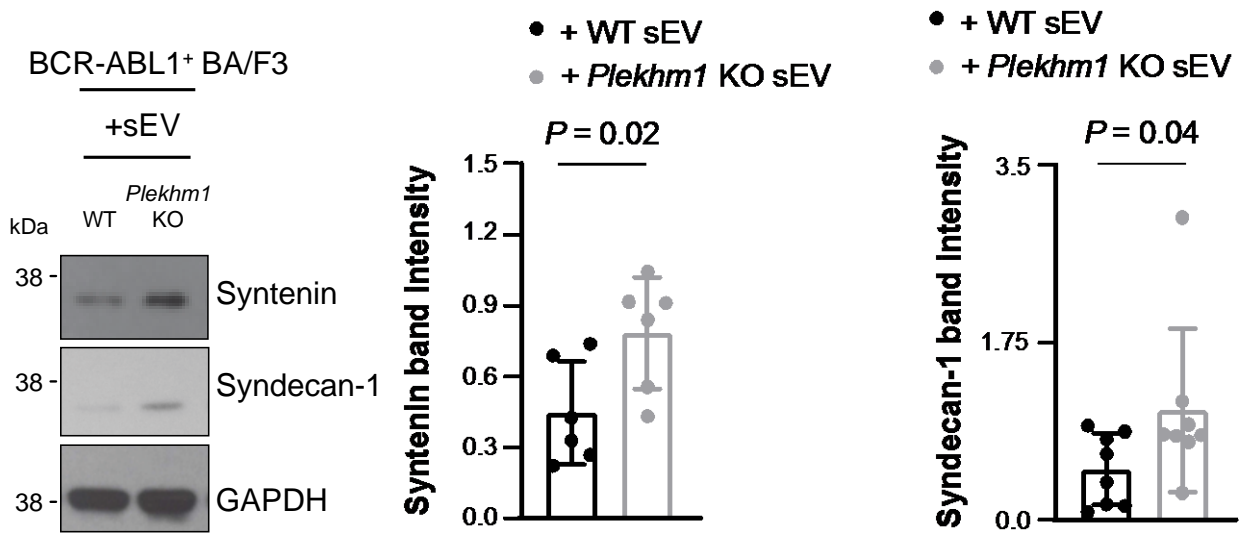
8. *Plekhm1* KO MSC-derived sEV alter B-ALL cells

i. *Plekhm1* KO MSC-derived sEV increase syntenin, syndecan-1, pAKT and pFAK in BCR-ABL1⁺ BA/F3 cells

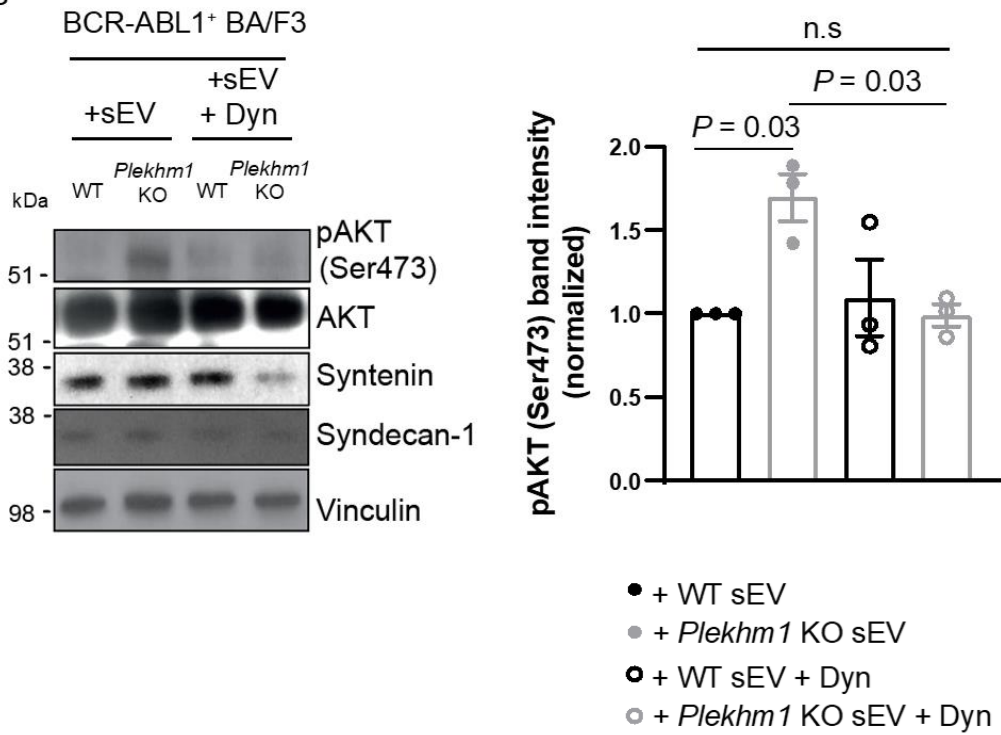
Next, we tested whether the differences in the cargo of sEV released by *Plekhm1* KO or WT MSC differentially affect B-ALL cells. BCR-ABL1⁺ BA/F3 cells were treated with WT or *Plekhm1* KO MSC-derived sEV in a ratio of 1:5 donor (MSC) to recipient (BCR-ABL1⁺ BA/F3) cells. Treatment of BCR-ABL1⁺ BA/F3 for 40 min with *Plekhm1* KO sEV led to a significant increase in the intracellular levels of syntenin and syndecan-1 compared to BCR-ABL1⁺ BA/F3 cells treated with WT sEV (Figure 21A). Additionally, exposure of BCR-ABL1⁺ BA/F3 cells to *Plekhm1* KO sEV for 6h significantly increased phosphorylation of AKT on the Ser473 residue compared to WT sEV (Figure 21B). AKT phosphorylation on Ser473 is required for maximal AKT activation which controls cell cycle, cell proliferation, and cell survival^{58,258}. To prove that the increase in pAKT is due to uptake of sEV by the BCR-ABL1⁺ BA/F3 cells rather than an extracellular effect of sEV, e.g. via interaction of proteins of sEV and cellular plasma membrane proteins, we treated BCR-ABL1⁺ BA/F3 cells with dynasore and exposed them to *Plekhm1* KO or WT MSC-derived sEV. Dynasore is a GTPase inhibitor that inhibits dynamin activity, which prevents clathrin-mediated endocytosis²⁵⁹. Exosomes have been reported to be taken up by dynamin-mediated endocytosis²⁶⁰, and dynasore has been used to block dynamin-mediated exosome endocytosis²⁶¹. Treatment with dynasore reversed the increase in the levels of pAKT after exposure of BCR-ABL1⁺ BA/F3 cells to *Plekhm1* KO sEV. This supported the hypothesis that an increase of pAKT levels in BCR-ABL1⁺ BA/F3 cells was due to uptake of *Plekhm1* KO sEV (Figure 21B). Additionally, we observed a small trend towards increased levels of pAKT in B-ALL cells derived from *Plekhm1* KO mice with B-ALL on day 20 after transplantation

compared to WT counterparts (Figure 21C). This supported the hypothesis that sEV derived from *Plekhh1* KO BMM might increase B-ALL cell aggressiveness via increase of pAKT. However, at 6h we did not observe differences in syntenin and syndecan-1 levels between cells exposed to WT and *Plekhh1* KO exosomes any more (Figure 21D). Syndecan-1 has been proposed to form complexes with growth factor receptors and/or integrins, and this results in integrin stabilization with subsequent enhancement of the downstream signaling pathway^{262,263}. In agreement with this, we observed a significant increase in the phosphorylation of focal adhesion kinase (FAK) on residue Tyr397. FAK is known to serve as a mediator of activated integrin signal transduction²⁶⁴ (Figure 21E). Taken together, these data suggest that *Plekhh1* KO MSC-derived exosomes increase the levels of syntenin and syndecan-1 in B-ALL cells, while, activating proliferative signaling pathways which involve AKT and FAK activation.

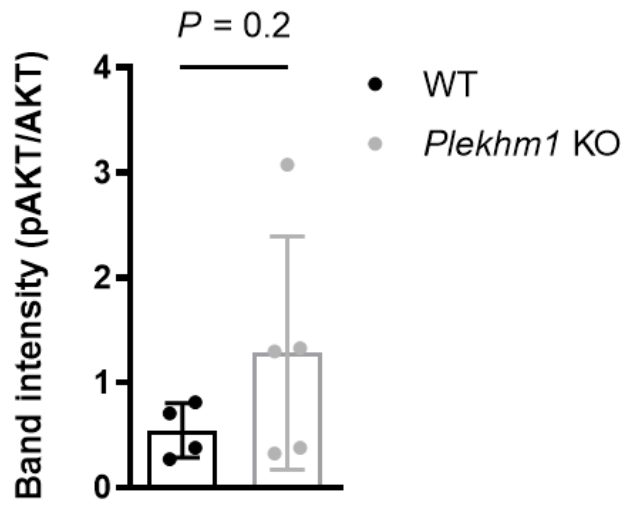
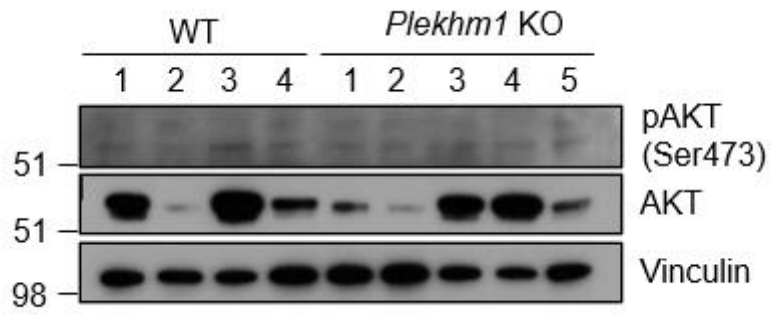
A



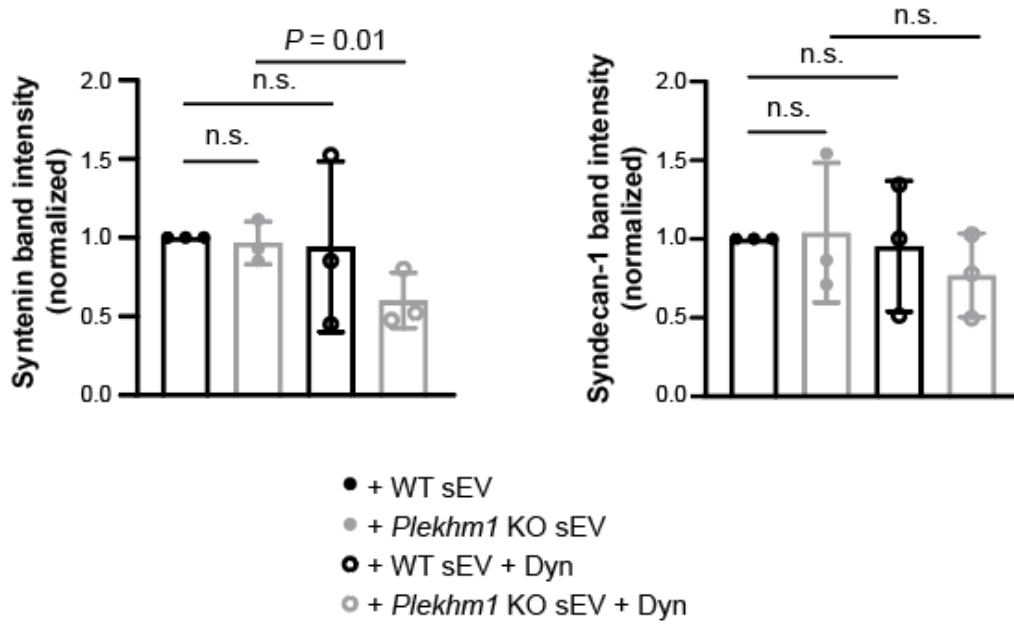
B



C



D



E

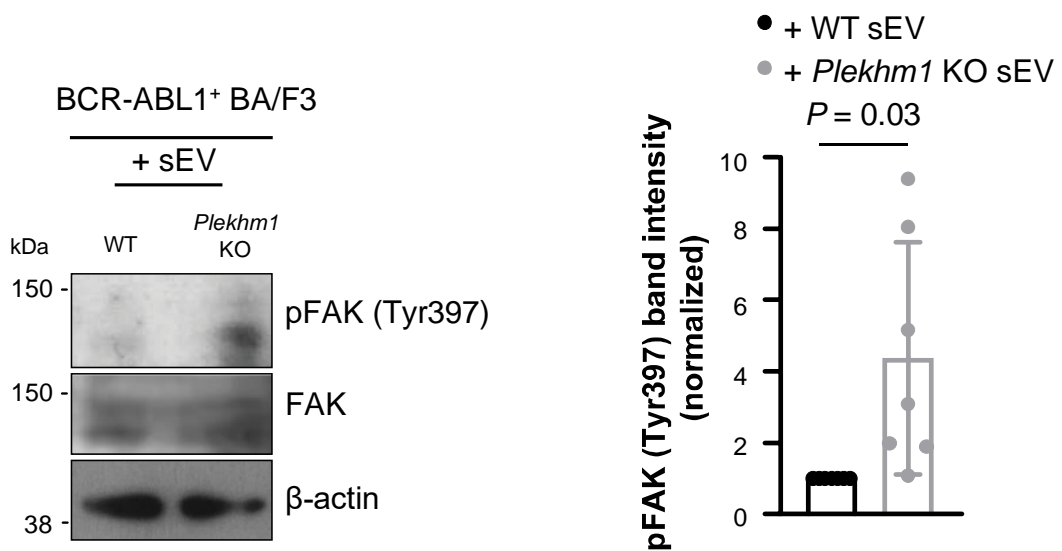
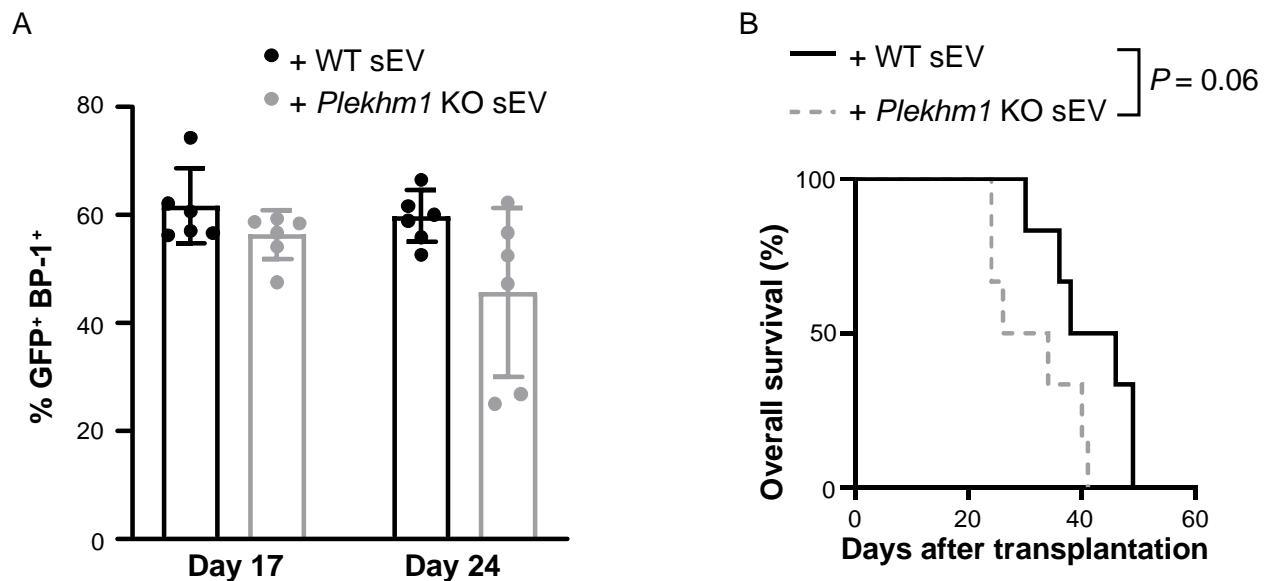


Figure 21: A) Representative immunoblot showing the expression of syntenin and syndecan-1 in BCR-ABL1⁺ BA/F3 cells after exposure to WT and *Plekhh1* KO sEV (left) for 40 min. Quantification of syntenin (middle) and syndecan-1 (right) protein expression normalized over the housekeeping protein. The data are the results of 6 (syntenin) or 7 (syndecan-1) independent experiments (*t*-test). B) Representative immunoblot showing the expression of pAKT (Ser473) and AKT in BCR-ABL1⁺ BA/F3 cells after treatment with WT sEV or *Plekhh1* KO sEV with or without dynasore for 6h (left) and quantification of pAKT expression in the different conditions. The data are the results of 3 independent experiments (right) (one-way ANOVA). C) Immunoblot showing pAKT (Ser473) and AKT expression in BM of WT or *Plekhh1* KO recipient mice transplanted with BCR-ABL1- transduced BM cells on day 20 after transplantation. Each lane represents a different mouse (left). Quantification of the pAKT (Ser473) band intensity in BM cells of WT or *Plekhh1* KO recipient mice transplanted with BCR-ABL1-transduced BM cells (WT n = 4; *Plekhh1* KO n = 5; *t*-test) (right). D) Quantification of syntenin and syndecan-1 protein expression in BCR-ABL1⁺ BA/F3 cells treated with WT (black) or *Plekhh1* KO sEV (grey) for 6h (one-way ANOVA). The data are the results of 3 independent experiments. E) Representative immunoblot showing the expression of pFAK (Tyr 397) and FAK in BCR-ABL1⁺ BA/F3 cells after exposure for 6h to WT or *Plekhh1* KO sEV (left). Quantification of pFAK (Tyr397) band intensity in BCR-ABL1⁺ BA/F3 cells treated with WT (black) or *Plekhh1* KO sEV for 6h. The data are the results of 5 independent experiments (*t*-test) (right).

ii. *Plekhm1* KO MSC-derived sEV may increase B-ALL aggressiveness

To test whether sEV from *Plekhm1* KO MSC might lead to an acceleration of B-ALL *in vivo*, we treated BCR-ABL1-transduced WT BM with WT or *Plekhm1* KO sEV in a ratio of 1:5 donor (MSC) to recipient (WT BM) cells and transplanted them into WT recipient mice. There were no differences in the GFP⁺ (BCR-ABL1⁺) cells in the PB of the mice on days 17 and 24 after transplantation between the two groups (Figure 22A). However, a strong trend towards a more aggressive disease in mice that received BCR-ABL1⁺ BM cells previously exposed to *Plekhm1* KO sEV was observed (Figure 22B). Furthermore, BALL-initiating cells previously exposed to *Plekhm1* KO sEV led to increased levels of pAKT at Ser473 in GFP⁺ (BCR-ABL1⁺) BP-1⁺ cells from the recipient mice (Figure 22C).



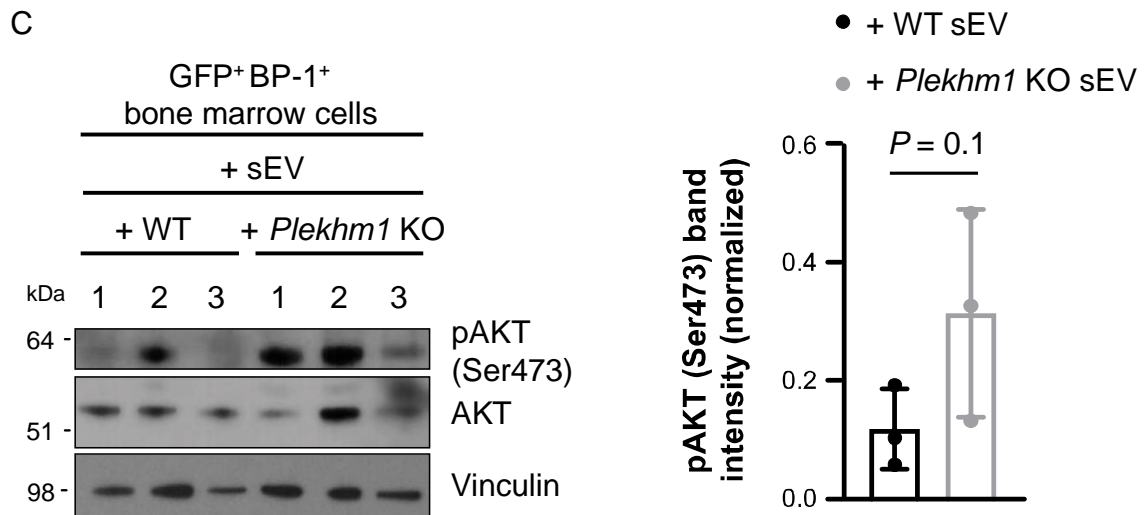
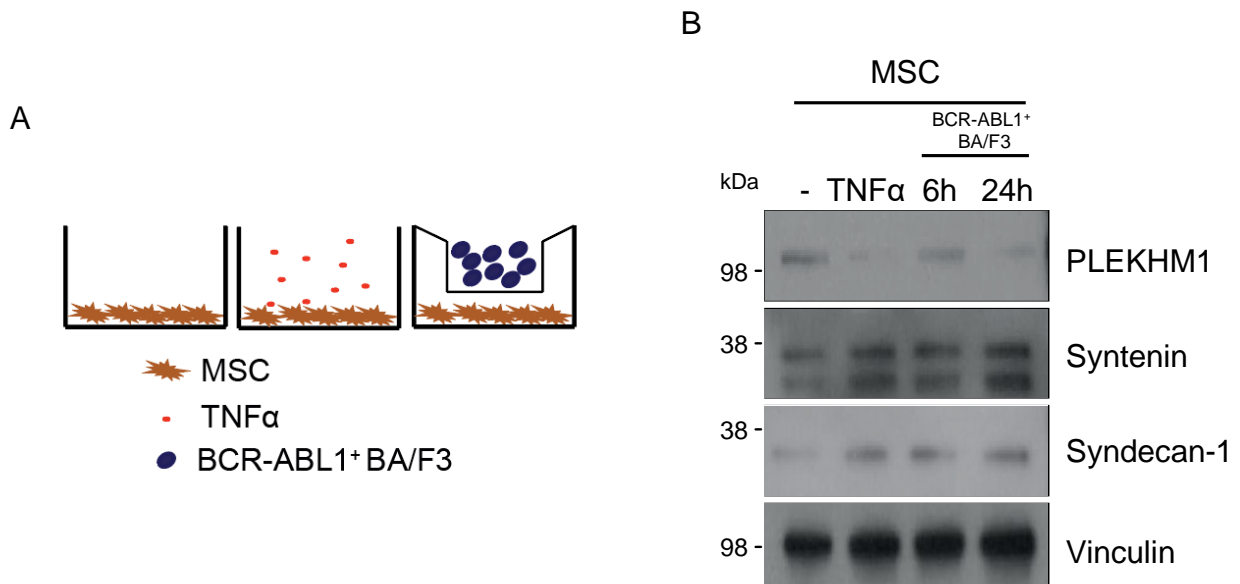


Figure 22: A) Percentage of GFP⁺ (BCR-ABL1⁺) BP-1⁺ cells in the PB of mice transplanted with BCR-ABL1-transduced BM previously treated with WT or *Plekhh1* KO sEV for 1h on days 17 and 24 after transplantation (+ WT sEV n = 6; + *Plekhh1* KO sEV n = 6; t-test). B) Kaplan-Meier-style survival curve of mice transplanted with BCR-ABL1-transduced BM previously treated with WT (black solid line) or *Plekhh1* KO (grey-dashed line) sEV for 1h (+ WT sEV n = 6; + *Plekhh1* KO sEV n = 6; Log-rank test). C) Immunoblot showing pAKT (Ser473) and AKT expression in sorted primary GFP⁺ (BCR-ABL1⁺) BP-1⁺ cells from the BM of WT recipient mice transplanted with BCR-ABL1-transduced BM cells previously exposed to WT or *Plekhh1* KO sEV. Each lane represents a different mouse (left). Quantification of the pAKT (Ser473) band intensity in sorted GFP⁺ (BCR-ABL1⁺) BP-1⁺ cells from the BM of WT recipient mice transplanted with BCR-ABL1-transduced BM previously exposed to WT or *Plekhh1* KO sEV for 1h (+ WT sEV n = 3; + *Plekhh1* KO sEV n = 3; t-test) (right).

9. Leukemia cells or TNF α reduce PLEKHM1 levels in BM MSC

Our group has previously shown that B-ALL cells release tumor necrosis factor (TNF) α that in turn modulates MSC function¹³⁷. In order to test whether treatment with TNF α recapitulates the increase of syntenin and syndecan-1 we observed in *Plekhm1* KO MSC we treated WT MSC with either TNF α or co-cultured them with BCR-ABL1⁺ BA/F3 cells. In the co-culture model, the two cell populations were separated by a membrane with 0.4 μ m pore, in a transwell system, that would not allow direct cell-cell interaction (Figure 23A). Interestingly, both TNF α - and BCR-ABL1⁺ BA/F3-treated MSC showed decreased expression of PLEKHM1 with concomitant upregulation of both syntenin and syndecan-1 (Figure 23B and Figure 23C). Taken together these results suggest that BCR-ABL1⁺ BA/F3, possibly via TNF α , reprogramme BMM MSC leading to reduced expression of PLEKHM1 and increased levels of syntenin and syndecan-1. These MSC possibly promote B-ALL aggressiveness via exosome release.



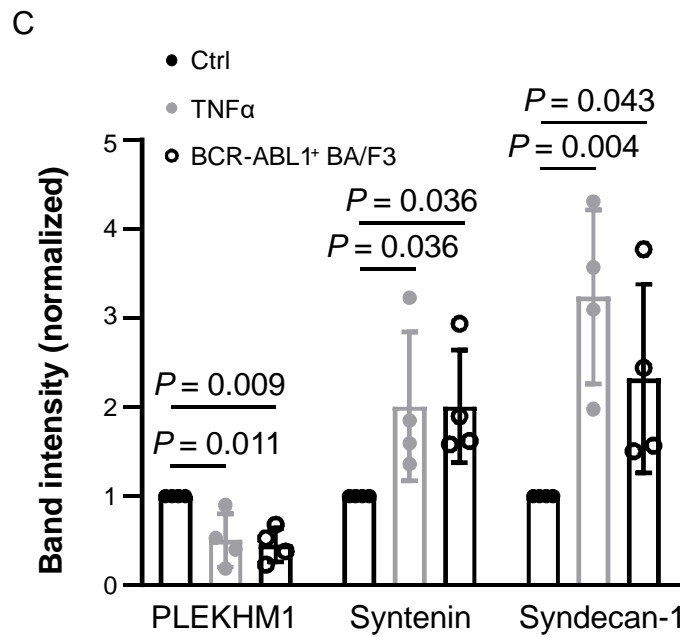


Figure 23: A) Schematic representation of the transwell system used for the experiment in figure 22B. The pore of the transwell is 0.4 μ m. B) Representative immunoblot showing expression of PLEKHM1, syntenin, and syndecan-1 in WT MSC treated with TNF α for 24h or BCR-ABL1+ BA/F3 cells for 6h or 24h. C) Quantification of PLEKHM1, syntenin, and syndecan-1 in untreated WT MSC, treated with TNF α or treated with BCR-ABL1+ BA/F3 cells for 24h. The values are normalized to the WT and represent the results of 4 independent experiments (one-way ANOVA for each protein).

Discussion

In this study we propose a circuit in which B-ALL cells, possibly via the release of TNF α , induce the development of a tumor-promoting BMM via the reduction of the autophagy adaptor protein PLEKHM1. PLEKHM1 absence leads to the release of sEV by BM MSC which carry qualitatively abnormal cargo. Specifically, the absence of PLEKHM1 in BM MSC leads to increased levels of syntenin and syndecan-1, proteins involved in exosome biogenesis¹⁹⁶ and correlated with cancer aggressiveness^{257,265}, in both MSC and MSC-derived sEV. Uptake of these sEV by the B-ALL cells leads to an increase in their proliferation via activation of pAKT and pFAK pathways (figure 24).

The BMM, possibly via education by leukemia cells, has been proposed to specifically support different leukemias. For example, it has been shown that manipulation of the BMM by parathyroid hormone (PTH) differentially affects two types of leukemia of the myeloid lineage, CML and AML²²¹. In our study, we observed opposite outcomes of two leukemias of different lineage B-ALL (lymphoid lineage) and CML (myeloid lineage) in mice when PLEKHM1 is absent from the BMM. In our models these two diseases are characterized by the presence of the same oncogene, *BCR-ABL1*, but the LIC belong to different cell lineages. In B-ALL the malignant cells are BCR-ABL1⁺ pre-B cells¹³⁷, while in the case of CML-like MPN the involved cells are BCR-ABL1⁺ myeloid cells²⁶⁶. Our observations suggest that absence of PLEKHM1 from the BMM might affect B-cell maturation since B-cells from a *Plekhm1* KO BMM have decreased levels of specific maturation markers like CD19 and B220, while they also show downregulation of Pax5 a transcription factor which regulates B-cell differentiation¹⁷. While a block in BCR-ABL1⁺ pre-B cells maturation might contribute

to the more aggressive phenotype we observed in B-ALL *Plekhm1* KO mice, in CML further studies need to be conducted to explain the prolonged survival in the *Plekhm1* KO mice. For example, it might worth conducting a more in-depth analysis of the common myeloid progenitors as well as their proliferation status in a WT versus *Plekhm1* KO BMM in both normal and CML mice. It is possible that the absence of PLEKHM1 in the BMM affects leukemia cells of different lineages differently. Additionally, B-ALL and CML cells might release different cytokines or growth factors that promote the loading of different proteins in the sEV that are released by the BM MSC. In turn, these sEV might either prolong, in the case of CML, or accelerate, in the case of B-ALL, the disease. To address these questions further studies, like coculture assays with MSC and CML or B-ALL cells, need to be conducted.

The effect of the BMM on the stemness and cell cycle status of leukemia cells has been studied. Specifically, CD44 mediates the interaction of CML cells with the BMM²⁶⁶. CD44 also mediates the interaction of AML cells with their niche leading to maintenance of the leukemic stem cell properties and, as a consequence, their ability to cause leukemia in serially transplanted mice²⁶⁷. The increased viability, the immature phenotype, indicated by decreased *Pax5* mRNA levels, and the significantly increased leukemia initiating potential of B-ALL cells exposed to a *Plekhm1* KO BMM advocate that these cells acquire “stem-like” features. However, in B-ALL, less is known about the population that acts as LIC and give rise to the disease. Further study is needed to explain how absence of PLEKHM1 from the BMM affect B-ALL cells stem-like phenotype. Given that the hematological profile did not reveal any differences in the LKS and LKS SLAM cells between WT and *Plekhm1* KO mice it might worth studying more in depth the differentiation of normal B-cells in healthy WT versus *Plekhm1* KO mice.

Deletion of Pax5 causes a pre-B-cell differentiation block. This prevents immunoglobulin heavy chain (*Igh*) gene rearrangements leading to clonal expansion of B-cells²⁶⁸. Suppression of Pax5 levels with concomitant activation of signal transducer and activator of transcription (STAT5) in a mouse model led to B-ALL induction and maintenance²⁶⁹. B-ALL cells show increased self-renewal capacity and impaired differentiation, while the restoration of Pax5 levels in B-ALL cells released the differentiation blockade, promoted Igk recombination, increased the levels of the Pax5 target gene *CD19*, disabled leukemia-initiating capacity and led to tumor regression²⁶⁹. Furthermore, it has been proposed that loss of *Pax5* transcriptional activation promotes leukemogenesis and alterations of Pax5 levels in B-ALL patients are often accompanied by secondary genetic mutations in genes that code for proteins and pathways affecting B-cell development. More specifically, these involve mutations in the gene that codes for the tumor suppressor Ras, in genes that code for cytokine receptors as well as mutations in pathways that control cell growth like the Janus kinase-signal transducer and activator of transcription signaling (JAK/STAT) pathway^{270,271}. It is possible that PLEKHM1 in the BMM impairs the survival of B-ALL cells probably by promoting a differentiated phenotype. This therefore may decrease the proliferation or survival of B-ALL cells and the leukemogenic potential of B-ALL LIC. Overall, our *in vivo* phenotype suggests a contribution of the *Plekhh1* KO niche for the regulation of B-ALL progression with respect to increased proliferation and aggressiveness of B-ALL cells, as well as, potentially the survival and protection of LIC.

PLEKHM1 loss inhibits autophagy flux in mouse embryonic fibroblasts (MEFs) and HeLa cells, suggesting it has a role as an autophagy adaptor protein¹⁶². In contrast, studies on the autophagy of osteoclasts and lung cells show that PLEKHM1

has modest or no impact on this process, supporting the concept that its autophagy-related role might be context-dependent^{218,272}. A common feature of PLEKHM1, as demonstrated by several studies, is its role in vesicular trafficking and the fusion of intracellular vesicles^{215,217,272}. In agreement with these observations, we showed that loss of PLEKHM1 from the BMM did not affect autophagy of BM MSC. However, PLEKHM1 deficiency leads to accumulation of MVB, a type of late endosomes, possibly due to impairment of their fusion with lysosomes.

The role of autophagy in cancer is context dependent¹⁷⁰. Inhibition of autophagy induces tumor initiation in the pancreas or liver, but, impairs cancer invasiveness^{273,274}, while, in CML it potentiates the efficacy of tyrosine kinase inhibitors (TKI)²⁷⁵. In the CML context autophagy inhibitors, like hydroxychloroquine, have been used in combination with targeted therapies in clinical trials¹⁶⁸. Fewer studies have focused on autophagy in the cancer microenvironment where it can metabolically support tumor growth^{171,172,175,276}. Our data suggest that manipulation of autophagy related proteins, like PLEKHM1, in the BMM can significantly increase B-ALL aggressiveness and leukemia-initiating capacity by alteration of EV protein cargo via affecting lysosomal degradation of MVB. Degradation of MVB after fusion with lysosomes or via autophagy leads to the removal of proteins including proteins related with exosomal biogenesis like TSG101²⁰⁶. In line with this, accumulation of MVB due to deficiency of PLEKHM1 leads to increased syntenin and syndecan-1 in the released sEV. As there are other proteins known to control MVB degradation, like the small GTPase Rab7¹⁷⁸, it is possible that MVB in *Plekhh1* KO MSC are still degraded to a significant extent. This may explain the similar number of sEV that are still released from these cells compared to WT. Given the above, targeting autophagy either intrinsically or in the BMM, as it was recently proposed²⁷⁷, should be further studied to exclude the promotion of cancer

cell aggressiveness and an increased risk of disease recurrence. For example, it might worth investigating how the usage of autophagy inhibitors in combination with chemotherapy affect sEV cargo of the BMM throughout the course of the disease. Specifically, it might worth assessing whether continuous autophagy inhibition leads to a BMM with impaired sEV cargo and subsequent increase of the number or function of leukemia initiating cells as we showed in this current study. In that case it might be important to consider the termination of the usage of the autophagy inhibitors at an earlier stage.

Exosomes which are a type of EV represent one of the means of communication between cancer cells and their microenvironment²⁷⁸. MSC have been introduced as a strategy to treat acute graft versus host disease²⁷⁹, and exosomes have been suggested as one of their therapeutically active components²⁸⁰. In the context of cancer, including leukemia, studies have mainly focused on cancer cell-derived exosomes that can re-program the microenvironment^{116,252}. In solid tumors cancer-cell derived exosomes travel through distant sites, including the bone, and transform the BM into a pre-metastatic niche²⁸¹. In breast cancer CAF release EV that affect the migration and invasion of the malignant cells²⁰⁰, while, BM-MSCs support gastric cancer growth by enhancing angiogenesis²⁰⁵. Lastly, in the head and neck squamous cell carcinoma (HNSCC) microenvironment tumor-associated endothelial cells were found to release EV carrying specific protein and RNA cargo that promotes immune suppression. This in turn enhances HNSCC cell proliferation, invasion and adhesion²⁸².

In non-solid malignancies the role of EV from BM MSC has been studied to a lesser extent. BM MSC from multiple myeloma (MM) patients transfer miR-15a-carrying exosomes to the MM cells promoting tumor growth, while exosomes released

by MSC from healthy individuals have the opposite result²⁰². Similarly, we showed that exosomes released by *Plekhh1* KO MSC might increase the aggressiveness of B-ALL compared to exosomes derived from WT MSC.

In line with other observations showing involvement of autophagy proteins (or proteins involved in vesicular trafficking) for the regulation of EV cargo²⁵³ we found that expression of PLEKHM1 affects the loading of syntenin and syndecan-1 into sEV. A recent study has identified syndecan-1 as an important promoter of CML cell proliferation, migration and travel to distant sites, and this study has linked syndecan-1 loss with impaired integrin β_7 activity²⁵⁷. Our observations suggest that this might also be the result of the transfer of syndecan-1, possibly in combination with syntenin, by BMM-derived sEV. Syntenin and syndecan-1 have been involved in exosome biogenesis¹⁹⁶. Syntenin is found to be elevated in many cancers, and it is known to promote tumor metastasis^{265,283,284}. The PDZ domain is a common structural domain of 80-90 amino-acids found in signaling proteins which play a key role in anchoring receptor proteins in the membrane to cytoskeletal components. PDZ is an initialism combining the first letters of the first three proteins discovered to share the domain — post synaptic density protein (PSD95), Drosophila disc large tumor suppressor (Dlg1), and zonula occludens-1 protein (zo-1). Furthermore, the PDZ domain is important in an important role in metastasis^{265,285} and is the domain by this domain syntenin interacts with syndecans²⁶⁰. Given that novel inhibitors which interfere with these interactions and specifically affect syntenin-exosome release are under investigation²⁸⁶, these may also be worth testing in our study. As *Plekhh1* KO MSC release increased levels of syntenin-sEV, inhibiting syntenin-exosome release with these compounds in BM-MSC may result in the reversal of the effect of PLEKHM1 absence and reduce B-ALL aggressiveness.

Syndecan-1 and syntenin have been suggested to stabilize growth factor receptors and/or integrins on the cell surface^{262,287,288}. Our results indicate that there might be an increased activation of downstream signaling of integrin⁵⁶ or growth factor receptors, as was suggested by an increase in pAKT and pFAK. However, further studies are needed to identify the specific integrins or growth factor receptors implicated in this process. Finally, the identification of the upstream molecular pathways mediating the phosphorylation of AKT and FAK remains a necessity.

Studies from our group and others have implicated inflammatory cytokines and specifically TNF α in the remodeling of the BMM which, in turn, promotes tumor growth¹³⁷. Interestingly, healthy B cells were identified as a source of TNF α ²⁸⁹. Our results show that B-ALL cells reduce the expression of PLEKHM1 and increase syntenin and syndecan-1 levels in WT BMM, possibly via the release of TNF α . Previous studies have shown that TNF α can promote EV release, as well as, modify their cargo^{290,291}. One possible mechanism could be via the regulation of PLEKHM1.

Given the above, inhibition of TNF α signaling may affect the EV-phenotype of BMM-associated MSC, possibly leading to an improved outcome in B-ALL progression. Treatment of patients with antibodies against TNF α or inhibitors has been employed for diseases like rheumatoid arthritis. However, their negative impact on the activation of the immune system have precluded their use in leukemia patients. Therefore, targeting the loading of exosomal cargo in MSC could be a less toxic alternative to TNF α treatment for the treatment of B-ALL. Finally, as an increase of TNF α is also tumor-promoting in other cancers²⁹² our findings could potentially be applicable to other non-leukemic cancer types as well. This needs to be studied in the future.

The role of PLEKHM1 in the BMM is not well defined, and our study proposes a novel role of this protein in the B-ALL BMM. So far, the role of PLEKHM1 has only been demonstrated for the fusion of autophagosomes or late endosomes and lysosomes, as well as for the trafficking of different vesicles. We identified its involvement in the loading of sEV with syntenin and syndecan-1 in BMM MSC. This is of interest since these two proteins are involved in exosome biogenesis and at the same time in adhesion, migration and invasion in different cancer types. The mechanisms by which protein cargo is loaded onto the ILV of the MVB is not fully elucidated, and a further analysis of the role of PLEKHM1 for the loading of protein cargo might shed some light onto this. A possible transfer of these proteins from sEV of the BMM to the cancer cells, in our case B-ALL, could serve as an alternative pathway promoting the malignant phenotype of cancer cells. PLEKHM1, thus, could be an important protein for quality control of the cells of the BMM in the context of B-ALL. Importantly, in the absence of PLEKHM1 from the BMM, partly due to the transfer of specific protein cargo via sEV, B-ALL cells acquire a more immature phenotype with increased viability in a secondary transplantation setting. It would be of great interest to identify whether exposure of B-ALL cells to a *Plekhh1* KO BMM enhances B-ALL cell resistance to chemotherapy in order to identify ways to target these pathways. Finally, further investigation of the levels of *PLEKHM1* in the BMM MSC of patients compared to healthy individuals, as well as patients with different stages of B-ALL, might also be worth addressing for its possible prognostic value.

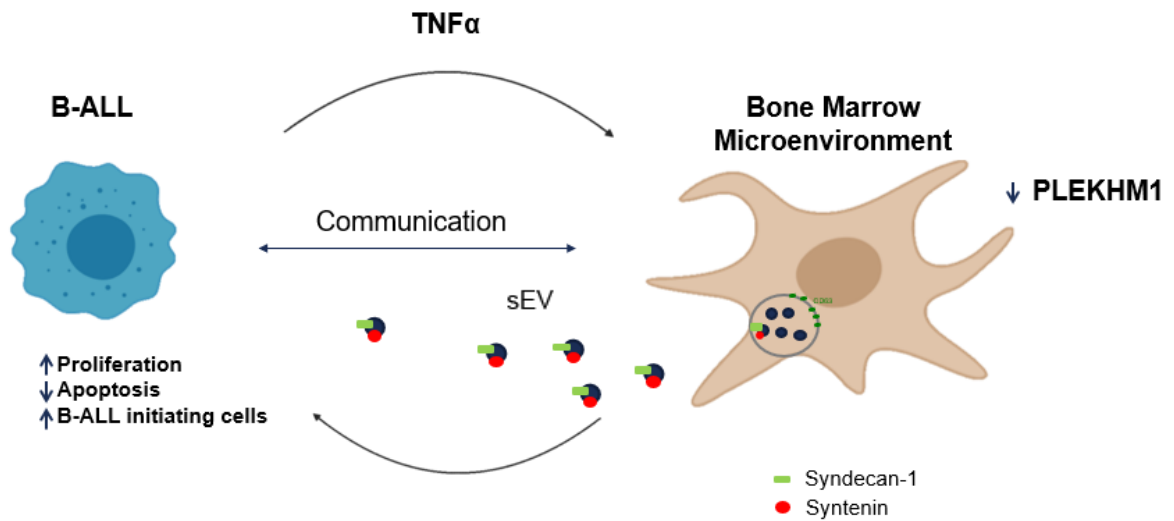


Figure 24: Proposed model of B-ALL progression in a *Plekhh1* KO BMM. B-ALL cells release $TNF\alpha$ which acts on BMM MSC reducing PLEKHM1 levels. Reduction of PLEKHM1 leads to impaired protein loading on ILV which are released as exosomes. sEV with impaired cargo carrying increased syntenin and syndecan-1 levels increase B-ALL aggressiveness by activating signaling pathways related to cell proliferation and survival.

References

- 1 Jagannathan-Bogdan, M. & Zon, L. I. Hematopoiesis. *Development* **140**, 2463-2467, doi:10.1242/dev.083147 (2013).
- 2 Palis, J. & Yoder, M. C. Yolk-sac hematopoiesis: the first blood cells of mouse and man. *Exp Hematol* **29**, 927-936, doi:10.1016/s0301-472x(01)00669-5 (2001).
- 3 Cumano, A. & Godin, I. Ontogeny of the hematopoietic system. *Annu Rev Immunol* **25**, 745-785, doi:10.1146/annurev.immunol.25.022106.141538 (2007).
- 4 Kaushansky, K. Lineage-specific hematopoietic growth factors. *N Engl J Med* **354**, 2034-2045, doi:10.1056/NEJMra052706 (2006).
- 5 Orkin, S. H. Diversification of haematopoietic stem cells to specific lineages. *Nat Rev Genet* **1**, 57-64, doi:10.1038/35049577 (2000).
- 6 Challen, G. A., Boles, N., Lin, K. K. & Goodell, M. A. Mouse hematopoietic stem cell identification and analysis. *Cytometry A* **75**, 14-24, doi:10.1002/cyto.a.20674 (2009).
- 7 Kondo, M., Weissman, I. L. & Akashi, K. Identification of clonogenic common lymphoid progenitors in mouse bone marrow. *Cell* **91**, 661-672, doi:10.1016/s0092-8674(00)80453-5 (1997).
- 8 Akashi, K., Traver, D., Miyamoto, T. & Weissman, I. L. A clonogenic common myeloid progenitor that gives rise to all myeloid lineages. *Nature* **404**, 193-197, doi:10.1038/35004599 (2000).
- 9 Seita, J. & Weissman, I. L. Hematopoietic stem cell: self-renewal versus differentiation. *Wiley Interdiscip Rev Syst Biol Med* **2**, 640-653, doi:10.1002/wsbm.86 (2010).
- 10 Pinho, S. & Frenette, P. S. Haematopoietic stem cell activity and interactions with the niche. *Nat Rev Mol Cell Biol* **20**, 303-320, doi:10.1038/s41580-019-0103-9 (2019).
- 11 Zhu, J. & Emerson, S. G. Hematopoietic cytokines, transcription factors and lineage commitment. *Oncogene* **21**, 3295-3313, doi:10.1038/sj.onc.1205318 (2002).
- 12 Cantor, A. B., Katz, S. G. & Orkin, S. H. Distinct domains of the GATA-1 cofactor FOG-1 differentially influence erythroid versus megakaryocytic maturation. *Mol Cell Biol* **22**, 4268-4279, doi:10.1128/mcb.22.12.4268-4279.2002 (2002).
- 13 Iwasaki, H. *et al.* Distinctive and indispensable roles of PU.1 in maintenance of hematopoietic stem cells and their differentiation. *Blood* **106**, 1590-1600, doi:10.1182/blood-2005-03-0860 (2005).
- 14 Sellars, M., Kastner, P. & Chan, S. Ikaros in B cell development and function. *World J Biol Chem* **2**, 132-139, doi:10.4331/wjbc.v2.i6.132 (2011).
- 15 Wang, J. H. *et al.* Selective defects in the development of the fetal and adult lymphoid system in mice with an Ikaros null mutation. *Immunity* **5**, 537-549, doi:10.1016/s1074-7613(00)80269-1 (1996).
- 16 Cobaleda, C., Schebesta, A., Delogu, A. & Busslinger, M. Pax5: the guardian of B cell identity and function. *Nat Immunol* **8**, 463-470, doi:10.1038/ni1454 (2007).
- 17 O'Brien, P., Morin, P., Jr., Ouellette, R. J. & Robichaud, G. A. The Pax-5 gene: a pluripotent regulator of B-cell differentiation and cancer disease. *Cancer Res* **71**, 7345-7350, doi:10.1158/0008-5472.CAN-11-1874 (2011).
- 18 Butler, J. M. *et al.* Endothelial cells are essential for the self-renewal and repopulation of Notch-dependent hematopoietic stem cells. *Cell Stem Cell* **6**, 251-264, doi:10.1016/j.stem.2010.02.001 (2010).
- 19 Krause, D. S. Regulation of hematopoietic stem cell fate. *Oncogene* **21**, 3262-3269, doi:10.1038/sj.onc.1205316 (2002).
- 20 Xu, C. *et al.* Stem cell factor is selectively secreted by arterial endothelial cells in bone marrow. *Nat Commun* **9**, 2449, doi:10.1038/s41467-018-04726-3 (2018).

- 21 Grover, A. *et al.* Erythropoietin guides multipotent hematopoietic progenitor cells toward an erythroid fate. *J Exp Med* **211**, 181-188, doi:10.1084/jem.20131189 (2014).
- 22 Broudy, V. C. Stem cell factor and hematopoiesis. *Blood* **90**, 1345-1364 (1997).
- 23 Eaves, C. J. *et al.* Mechanisms that regulate the cell cycle status of very primitive hematopoietic cells in long-term human marrow cultures. II. Analysis of positive and negative regulators produced by stromal cells within the adherent layer. *Blood* **78**, 110-117 (1991).
- 24 Robb, L. Cytokine receptors and hematopoietic differentiation. *Oncogene* **26**, 6715-6723, doi:10.1038/sj.onc.1210756 (2007).
- 25 Schofield, R. The relationship between the spleen colony-forming cell and the haemopoietic stem cell. *Blood Cells* **4**, 7-25 (1978).
- 26 Kumar, R., Godavarthy, P. S. & Krause, D. S. The bone marrow microenvironment in health and disease at a glance. *J Cell Sci* **131**, doi:10.1242/jcs.201707 (2018).
- 27 Knospe, W. H., Gregory, S. A., Husseini, S. G., Fried, W. & Trobaugh, F. E., Jr. Origin and recovery of colony-forming units in locally curetted bone marrow of mice. *Blood* **39**, 331-340 (1972).
- 28 Krause, D. S. & Scadden, D. T. A hostel for the hostile: the bone marrow niche in hematologic neoplasms. *Haematologica* **100**, 1376-1387, doi:10.3324/haematol.2014.113852 (2015).
- 29 Ramalingam, P., Poulos, M. G. & Butler, J. M. Regulation of the hematopoietic stem cell lifecycle by the endothelial niche. *Curr Opin Hematol* **24**, 289-299, doi:10.1097/MOH.0000000000000350 (2017).
- 30 Acar, M. *et al.* Deep imaging of bone marrow shows non-dividing stem cells are mainly perisinusoidal. *Nature* **526**, 126-130, doi:10.1038/nature15250 (2015).
- 31 Sugiyama, T., Kohara, H., Noda, M. & Nagasawa, T. Maintenance of the hematopoietic stem cell pool by CXCL12-CXCR4 chemokine signaling in bone marrow stromal cell niches. *Immunity* **25**, 977-988, doi:10.1016/j.immuni.2006.10.016 (2006).
- 32 Kobayashi, H. *et al.* Angiocrine factors from Akt-activated endothelial cells balance self-renewal and differentiation of haematopoietic stem cells. *Nat Cell Biol* **12**, 1046-1056, doi:10.1038/ncb2108 (2010).
- 33 Ding, L., Saunders, T. L., Enikolopov, G. & Morrison, S. J. Endothelial and perivascular cells maintain haematopoietic stem cells. *Nature* **481**, 457-462, doi:10.1038/nature10783 (2012).
- 34 Kunisaki, Y. *et al.* Arteriolar niches maintain haematopoietic stem cell quiescence. *Nature* **502**, 637-643, doi:10.1038/nature12612 (2013).
- 35 Gur-Cohen, S. *et al.* Corrigendum: PAR1 signaling regulates the retention and recruitment of EPCR-expressing bone marrow hematopoietic stem cells. *Nat Med* **22**, 446, doi:10.1038/nm0416-446b (2016).
- 36 Calvi, L. M. *et al.* Osteoblastic cells regulate the haematopoietic stem cell niche. *Nature* **425**, 841-846, doi:10.1038/nature02040 (2003).
- 37 Visnjic, D. *et al.* Hematopoiesis is severely altered in mice with an induced osteoblast deficiency. *Blood* **103**, 3258-3264, doi:10.1182/blood-2003-11-4011 (2004).
- 38 Zhu, J. *et al.* Osteoblasts support B-lymphocyte commitment and differentiation from hematopoietic stem cells. *Blood* **109**, 3706-3712, doi:10.1182/blood-2006-08-041384 (2007).
- 39 Adams, G. B. *et al.* Stem cell engraftment at the endosteal niche is specified by the calcium-sensing receptor. *Nature* **439**, 599-603, doi:10.1038/nature04247 (2006).
- 40 Boyle, W. J., Simonet, W. S. & Lacey, D. L. Osteoclast differentiation and activation. *Nature* **423**, 337-342, doi:10.1038/nature01658 (2003).
- 41 Kollet, O. *et al.* Osteoclasts degrade endosteal components and promote mobilization of hematopoietic progenitor cells. *Nat Med* **12**, 657-664, doi:10.1038/nm1417 (2006).
- 42 Mendez-Ferrer, S. *et al.* Mesenchymal and haematopoietic stem cells form a unique bone marrow niche. *Nature* **466**, 829-834, doi:10.1038/nature09262 (2010).

- 43 Ehninger, A. & Trumpp, A. The bone marrow stem cell niche grows up: mesenchymal stem cells and macrophages move in. *J Exp Med* **208**, 421-428, doi:10.1084/jem.20110132 (2011).
- 44 Omatsu, Y. *et al.* The essential functions of adipo-osteogenic progenitors as the hematopoietic stem and progenitor cell niche. *Immunity* **33**, 387-399, doi:10.1016/j.immuni.2010.08.017 (2010).
- 45 Mendez-Ferrer, S. *et al.* Bone marrow niches in haematological malignancies. *Nat Rev Cancer* **20**, 285-298, doi:10.1038/s41568-020-0245-2 (2020).
- 46 Kfoury, Y. & Scadden, D. T. Mesenchymal cell contributions to the stem cell niche. *Cell Stem Cell* **16**, 239-253, doi:10.1016/j.stem.2015.02.019 (2015).
- 47 Greenbaum, A. *et al.* CXCL12 in early mesenchymal progenitors is required for haematopoietic stem-cell maintenance. *Nature* **495**, 227-230, doi:10.1038/nature11926 (2013).
- 48 Zanetti, C. & Krause, D. S. "Caught in the net": the extracellular matrix of the bone marrow in normal hematopoiesis and leukemia. *Exp Hematol* **89**, 13-25, doi:10.1016/j.exphem.2020.07.010 (2020).
- 49 Humphries, J. D., Byron, A. & Humphries, M. J. Integrin ligands at a glance. *J Cell Sci* **119**, 3901-3903, doi:10.1242/jcs.03098 (2006).
- 50 Arroyo, A. G., Yang, J. T., Rayburn, H. & Hynes, R. O. Alpha4 integrins regulate the proliferation/differentiation balance of multilineage hematopoietic progenitors in vivo. *Immunity* **11**, 555-566, doi:10.1016/s1074-7613(00)80131-4 (1999).
- 51 Bouvard, D. *et al.* Functional consequences of integrin gene mutations in mice. *Circ Res* **89**, 211-223, doi:10.1161/hh1501.094874 (2001).
- 52 Bodo, M., Baroni, T. & Tabilio, A. Haematopoietic and stromal stem cell regulation by extracellular matrix components and growth factors. *J Stem Cells* **4**, 57-69, doi:jsc.2009.4.1.57 (2009).
- 53 Itkin, T. *et al.* FGF-2 expands murine hematopoietic stem and progenitor cells via proliferation of stromal cells, c-Kit activation, and CXCL12 down-regulation. *Blood* **120**, 1843-1855, doi:10.1182/blood-2011-11-394692 (2012).
- 54 Tzaphlidou, M. The role of collagen in bone structure: an image processing approach. *Micron* **36**, 593-601, doi:10.1016/j.micron.2005.05.009 (2005).
- 55 Probst, K. *et al.* Depletion of Collagen IX Alpha1 Impairs Myeloid Cell Function. *Stem Cells* **36**, 1752-1763, doi:10.1002/stem.2892 (2018).
- 56 Kumar, R. *et al.* Specific, targetable interactions with the microenvironment influence imatinib-resistant chronic myeloid leukemia. *Leukemia* **34**, 2087-2101, doi:10.1038/s41375-020-0866-1 (2020).
- 57 Khurana, S. *et al.* Outside-in integrin signalling regulates haematopoietic stem cell function via Periostin-Itgav axis. *Nat Commun* **7**, 13500, doi:10.1038/ncomms13500 (2016).
- 58 Verma, D. *et al.* Vitamin K antagonism impairs the bone marrow microenvironment and hematopoiesis. *Blood* **134**, 227-238, doi:10.1182/blood.2018874214 (2019).
- 59 Swerdlow, S. H. *et al.* The 2016 revision of the World Health Organization classification of lymphoid neoplasms. *Blood* **127**, 2375-2390, doi:10.1182/blood-2016-01-643569 (2016).
- 60 Arber, D. A. *et al.* The 2016 revision to the World Health Organization classification of myeloid neoplasms and acute leukemia. *Blood* **127**, 2391-2405, doi:10.1182/blood-2016-03-643544 (2016).
- 61 Rowley, J. D. Letter: A new consistent chromosomal abnormality in chronic myelogenous leukaemia identified by quinacrine fluorescence and Giemsa staining. *Nature* **243**, 290-293, doi:10.1038/243290a0 (1973).
- 62 Groffen, J. *et al.* Philadelphia chromosomal breakpoints are clustered within a limited region, bcr, on chromosome 22. *Cell* **36**, 93-99, doi:10.1016/0092-8674(84)90077-1 (1984).

- 63 Institute, N. C. *BCR-ABL fusion gene*,
<<https://www.cancer.gov/publications/dictionaries/cancer-terms/def/bcr-abl-fusion-gene>>
(n.d.).
- 64 <<https://www.cancer.gov/publications/dictionaries/cancer-terms/def/bcr-abl-fusion-gene>> (
- 65 Daley, G. Q., Van Etten, R. A. & Baltimore, D. Induction of chronic myelogenous leukemia in
mice by the P210bcr/abl gene of the Philadelphia chromosome. *Science* **247**, 824-830,
doi:10.1126/science.2406902 (1990).
- 66 Lugo, T. G., Pendergast, A. M., Muller, A. J. & Witte, O. N. Tyrosine kinase activity and
transformation potency of bcr-abl oncogene products. *Science* **247**, 1079-1082,
doi:10.1126/science.2408149 (1990).
- 67 Daley, G. Q. & Baltimore, D. Transformation of an interleukin 3-dependent hematopoietic
cell line by the chronic myelogenous leukemia-specific P210bcr/abl protein. *Proc Natl Acad
Sci U S A* **85**, 9312-9316, doi:10.1073/pnas.85.23.9312 (1988).
- 68 Minciocchi, V. R., Kumar, R. & Krause, D. S. Chronic Myeloid Leukemia: A Model Disease of
the Past, Present and Future. *Cells* **10**, doi:10.3390/cells10010117 (2021).
- 69 Jabbour, E. & Kantarjian, H. Chronic myeloid leukemia: 2020 update on diagnosis, therapy
and monitoring. *Am J Hematol* **95**, 691-709, doi:10.1002/ajh.25792 (2020).
- 70 Silver, R. T. *et al.* An evidence-based analysis of the effect of busulfan, hydroxyurea,
interferon, and allogeneic bone marrow transplantation in treating the chronic phase of
chronic myeloid leukemia: developed for the American Society of Hematology. *Blood* **94**,
1517-1536 (1999).
- 71 Jabbour, E., Kantarjian, H. & Cortes, J. Use of second- and third-generation tyrosine kinase
inhibitors in the treatment of chronic myeloid leukemia: an evolving treatment paradigm.
Clin Lymphoma Myeloma Leuk **15**, 323-334, doi:10.1016/j.clml.2015.03.006 (2015).
- 72 Bernt, K. M. & Hunger, S. P. Current concepts in pediatric Philadelphia chromosome-positive
acute lymphoblastic leukemia. *Front Oncol* **4**, 54, doi:10.3389/fonc.2014.00054 (2014).
- 73 Terwilliger, T. & Abdul-Hay, M. Acute lymphoblastic leukemia: a comprehensive review and
2017 update. *Blood Cancer J* **7**, e577, doi:10.1038/bcj.2017.53 (2017).
- 74 Yeoh, E. J. *et al.* Classification, subtype discovery, and prediction of outcome in pediatric
acute lymphoblastic leukemia by gene expression profiling. *Cancer Cell* **1**, 133-143,
doi:10.1016/s1535-6108(02)00032-6 (2002).
- 75 Greaves, M. F. & Wiemels, J. Origins of chromosome translocations in childhood leukaemia.
Nat Rev Cancer **3**, 639-649, doi:10.1038/nrc1164 (2003).
- 76 Look, A. T. Oncogenic transcription factors in the human acute leukemias. *Science* **278**, 1059-
1064, doi:10.1126/science.278.5340.1059 (1997).
- 77 Malouf, C. & Ottersbach, K. Molecular processes involved in B cell acute lymphoblastic
leukaemia. *Cell Mol Life Sci* **75**, 417-446, doi:10.1007/s00018-017-2620-z (2018).
- 78 Fielding, A. K. Treatment of Philadelphia chromosome-positive acute lymphoblastic leukemia
in adults: a broader range of options, improved outcomes, and more therapeutic dilemmas.
Am Soc Clin Oncol Educ Book, e352-359, doi:10.14694/EdBook_AM.2015.35.e352 (2015).
- 79 Li, W. J., Dreazen, O., Kloetzer, W., Gale, R. P. & Arlinghaus, R. B. Characterization of bcr
gene products in hematopoietic cells. *Oncogene* **4**, 127-138 (1989).
- 80 Maru, Y. & Witte, O. N. The BCR gene encodes a novel serine/threonine kinase activity
within a single exon. *Cell* **67**, 459-468, doi:10.1016/0092-8674(91)90521-y (1991).
- 81 Pane, F. *et al.* BCR/ABL genes and leukemic phenotype: from molecular mechanisms to
clinical correlations. *Oncogene* **21**, 8652-8667, doi:10.1038/sj.onc.1206094 (2002).
- 82 Perez-Losada, J., Gutierrez-Cianca, N. & Sanchez-Garcia, I. Philadelphia-positive B-cell acute
lymphoblastic leukemia is initiated in an uncommitted progenitor cell. *Leuk Lymphoma* **42**,
569-576, doi:10.3109/10428190109099316 (2001).
- 83 Li, S., Ilaria, R. L., Jr., Million, R. P., Daley, G. Q. & Van Etten, R. A. The P190, P210, and P230
forms of the BCR/ABL oncogene induce a similar chronic myeloid leukemia-like syndrome in

- mice but have different lymphoid leukemogenic activity. *J Exp Med* **189**, 1399-1412, doi:10.1084/jem.189.9.1399 (1999).
- 84 Zou, X. & Calame, K. Signaling pathways activated by oncogenic forms of Abl tyrosine kinase. *J Biol Chem* **274**, 18141-18144, doi:10.1074/jbc.274.26.18141 (1999).
- 85 Sanchez-Garcia, I. & Grutz, G. Tumorigenic activity of the BCR-ABL oncogenes is mediated by BCL2. *Proc Natl Acad Sci U S A* **92**, 5287-5291, doi:10.1073/pnas.92.12.5287 (1995).
- 86 Skorski, T. *et al.* Phosphatidylinositol-3 kinase activity is regulated by BCR/ABL and is required for the growth of Philadelphia chromosome-positive cells. *Blood* **86**, 726-736 (1995).
- 87 Skorski, T. *et al.* Transformation of hematopoietic cells by BCR/ABL requires activation of a PI-3k/Akt-dependent pathway. *EMBO J* **16**, 6151-6161, doi:10.1093/emboj/16.20.6151 (1997).
- 88 Burger, J. A. Treatment of Chronic Lymphocytic Leukemia. *N Engl J Med* **383**, 460-473, doi:10.1056/NEJMra1908213 (2020).
- 89 Hallek, M. *et al.* Addition of rituximab to fludarabine and cyclophosphamide in patients with chronic lymphocytic leukaemia: a randomised, open-label, phase 3 trial. *Lancet* **376**, 1164-1174, doi:10.1016/S0140-6736(10)61381-5 (2010).
- 90 Goede, V. *et al.* Obinutuzumab plus chlorambucil in patients with CLL and coexisting conditions. *N Engl J Med* **370**, 1101-1110, doi:10.1056/NEJMoa1313984 (2014).
- 91 Seymour, J. F. *et al.* Venetoclax-Rituximab in Relapsed or Refractory Chronic Lymphocytic Leukemia. *N Engl J Med* **378**, 1107-1120, doi:10.1056/NEJMoa1713976 (2018).
- 92 Woyach, J. A. *et al.* Ibrutinib Regimens versus Chemoimmunotherapy in Older Patients with Untreated CLL. *N Engl J Med* **379**, 2517-2528, doi:10.1056/NEJMoa1812836 (2018).
- 93 Jemal, A., Siegel, R., Xu, J. & Ward, E. Cancer statistics, 2010. *CA Cancer J Clin* **60**, 277-300, doi:10.3322/caac.20073 (2010).
- 94 Dohner, H., Weisdorf, D. J. & Bloomfield, C. D. Acute Myeloid Leukemia. *N Engl J Med* **373**, 1136-1152, doi:10.1056/NEJMra1406184 (2015).
- 95 Ley, T. J. *et al.* DNMT3A mutations in acute myeloid leukemia. *N Engl J Med* **363**, 2424-2433, doi:10.1056/NEJMoa1005143 (2010).
- 96 Chou, W. C. *et al.* TET2 mutation is an unfavorable prognostic factor in acute myeloid leukemia patients with intermediate-risk cytogenetics. *Blood* **118**, 3803-3810, doi:10.1182/blood-2011-02-339747 (2011).
- 97 Muntean, A. G. & Hess, J. L. The pathogenesis of mixed-lineage leukemia. *Annu Rev Pathol* **7**, 283-301, doi:10.1146/annurev-pathol-011811-132434 (2012).
- 98 Tamai, H. & Inokuchi, K. 11q23/MLL acute leukemia : update of clinical aspects. *J Clin Exp Hematop* **50**, 91-98, doi:10.3960/jslrt.50.91 (2010).
- 99 Walkley, C. R. *et al.* A microenvironment-induced myeloproliferative syndrome caused by retinoic acid receptor gamma deficiency. *Cell* **129**, 1097-1110, doi:10.1016/j.cell.2007.05.014 (2007).
- 100 Fulzele, K. *et al.* Myelopoiesis is regulated by osteocytes through Gsalpha-dependent signaling. *Blood* **121**, 930-939, doi:10.1182/blood-2012-06-437160 (2013).
- 101 Kode, A. *et al.* Leukaemogenesis induced by an activating beta-catenin mutation in osteoblasts. *Nature* **506**, 240-244, doi:10.1038/nature12883 (2014).
- 102 Rupec, R. A. *et al.* Stroma-mediated dysregulation of myelopoiesis in mice lacking I kappa B alpha. *Immunity* **22**, 479-491, doi:10.1016/j.immuni.2005.02.009 (2005).
- 103 Raaijmakers, M. H. *et al.* Bone progenitor dysfunction induces myelodysplasia and secondary leukaemia. *Nature* **464**, 852-857, doi:10.1038/nature08851 (2010).
- 104 Schepers, K. *et al.* Myeloproliferative neoplasia remodels the endosteal bone marrow niche into a self-reinforcing leukemic niche. *Cell Stem Cell* **13**, 285-299, doi:10.1016/j.stem.2013.06.009 (2013).

- 105 Frisch, B. J. *et al.* Functional inhibition of osteoblastic cells in an in vivo mouse model of
myeloid leukemia. *Blood* **119**, 540-550, doi:10.1182/blood-2011-04-348151 (2012).
- 106 Zhang, B. *et al.* Altered microenvironmental regulation of leukemic and normal stem cells in
chronic myelogenous leukemia. *Cancer Cell* **21**, 577-592, doi:10.1016/j.ccr.2012.02.018
(2012).
- 107 van den Berk, L. C. *et al.* Disturbed CXCR4/CXCL12 axis in paediatric precursor B-cell acute
lymphoblastic leukaemia. *Br J Haematol* **166**, 240-249, doi:10.1111/bjh.12883 (2014).
- 108 Arranz, L. *et al.* Neuropathy of haematopoietic stem cell niche is essential for
myeloproliferative neoplasms. *Nature* **512**, 78-81, doi:10.1038/nature13383 (2014).
- 109 Aguayo, A. *et al.* Angiogenesis in acute and chronic leukemias and myelodysplastic
syndromes. *Blood* **96**, 2240-2245 (2000).
- 110 Passaro, D. *et al.* Increased Vascular Permeability in the Bone Marrow Microenvironment
Contributes to Disease Progression and Drug Response in Acute Myeloid Leukemia. *Cancer
Cell* **32**, 324-341 e326, doi:10.1016/j.ccell.2017.08.001 (2017).
- 111 Veiga, J. P., Costa, L. F., Sallan, S. E., Nadler, L. M. & Cardoso, A. A. Leukemia-stimulated bone
marrow endothelium promotes leukemia cell survival. *Exp Hematol* **34**, 610-621,
doi:10.1016/j.exphem.2006.01.013 (2006).
- 112 Poulos, M. G. *et al.* Activation of the vascular niche supports leukemic progression and
resistance to chemotherapy. *Exp Hematol* **42**, 976-986 e973,
doi:10.1016/j.exphem.2014.08.003 (2014).
- 113 Duarte, D. *et al.* Inhibition of Endosteal Vascular Niche Remodeling Rescues Hematopoietic
Stem Cell Loss in AML. *Cell Stem Cell* **22**, 64-77 e66, doi:10.1016/j.stem.2017.11.006 (2018).
- 114 Schmidt, T. *et al.* Loss or inhibition of stromal-derived PIGF prolongs survival of mice with
imatinib-resistant Bcr-Abl1(+) leukemia. *Cancer Cell* **19**, 740-753,
doi:10.1016/j.ccr.2011.05.007 (2011).
- 115 Huan, J. *et al.* RNA trafficking by acute myelogenous leukemia exosomes. *Cancer Res* **73**,
918-929, doi:10.1158/0008-5472.CAN-12-2184 (2013).
- 116 Kumar, B. *et al.* Acute myeloid leukemia transforms the bone marrow niche into a leukemia-
permissive microenvironment through exosome secretion. *Leukemia* **32**, 575-587,
doi:10.1038/leu.2017.259 (2018).
- 117 Doron, B. *et al.* Transmissible ER stress reconfigures the AML bone marrow compartment.
Leukemia **33**, 918-930, doi:10.1038/s41375-018-0254-2 (2019).
- 118 Corrado, C. *et al.* Exosome-mediated crosstalk between chronic myelogenous leukemia cells
and human bone marrow stromal cells triggers an interleukin 8-dependent survival of
leukemia cells. *Cancer Lett* **348**, 71-76, doi:10.1016/j.canlet.2014.03.009 (2014).
- 119 Valadi, H. *et al.* Exosome-mediated transfer of mRNAs and microRNAs is a novel mechanism
of genetic exchange between cells. *Nat Cell Biol* **9**, 654-659, doi:10.1038/ncb1596 (2007).
- 120 Taverna, S. *et al.* Exosomal shuttling of miR-126 in endothelial cells modulates adhesive and
migratory abilities of chronic myelogenous leukemia cells. *Mol Cancer* **13**, 169,
doi:10.1186/1476-4598-13-169 (2014).
- 121 Huntly, B. J. & Gilliland, D. G. Leukaemia stem cells and the evolution of cancer-stem-cell
research. *Nat Rev Cancer* **5**, 311-321, doi:10.1038/nrc1592 (2005).
- 122 Bhatia, R. Targeting Leukemia Stem Cell Resistance in Chronic Myelogenous Leukemia. *Trans
Am Clin Climatol Assoc* **130**, 246-254 (2019).
- 123 Tavor, S. *et al.* CXCR4 regulates migration and development of human acute myelogenous
leukemia stem cells in transplanted NOD/SCID mice. *Cancer Res* **64**, 2817-2824,
doi:10.1158/0008-5472.can-03-3693 (2004).
- 124 Nervi, B. *et al.* Chemosensitization of acute myeloid leukemia (AML) following mobilization
by the CXCR4 antagonist AMD3100. *Blood* **113**, 6206-6214, doi:10.1182/blood-2008-06-
162123 (2009).

- 125 Uy, G. L. *et al.* A phase 1/2 study of chemosensitization with the CXCR4 antagonist plerixafor in relapsed or refractory acute myeloid leukemia. *Blood* **119**, 3917-3924, doi:10.1182/blood-2011-10-383406 (2012).
- 126 Tabe, Y. *et al.* Role of stromal microenvironment in nonpharmacological resistance of CML to imatinib through Lyn/CXCR4 interactions in lipid rafts. *Leukemia* **26**, 883-892, doi:10.1038/leu.2011.291 (2012).
- 127 Azab, A. K. *et al.* CXCR4 inhibitor AMD3100 disrupts the interaction of multiple myeloma cells with the bone marrow microenvironment and enhances their sensitivity to therapy. *Blood* **113**, 4341-4351, doi:10.1182/blood-2008-10-186668 (2009).
- 128 Lundell, B. I., McCarthy, J. B., Kovach, N. L. & Verfaillie, C. M. Activation of beta1 integrins on CML progenitors reveals cooperation between beta1 integrins and CD44 in the regulation of adhesion and proliferation. *Leukemia* **11**, 822-829, doi:10.1038/sj.leu.2400653 (1997).
- 129 Matsunaga, T. *et al.* Interaction between leukemic-cell VLA-4 and stromal fibronectin is a decisive factor for minimal residual disease of acute myelogenous leukemia. *Nat Med* **9**, 1158-1165, doi:10.1038/nm909 (2003).
- 130 Maffei, R. *et al.* Physical contact with endothelial cells through beta1- and beta2- integrins rescues chronic lymphocytic leukemia cells from spontaneous and drug-induced apoptosis and induces a peculiar gene expression profile in leukemic cells. *Haematologica* **97**, 952-960, doi:10.3324/haematol.2011.054924 (2012).
- 131 Jacamo, R. *et al.* Reciprocal leukemia-stroma VCAM-1/VLA-4-dependent activation of NF-kappaB mediates chemoresistance. *Blood* **123**, 2691-2702, doi:10.1182/blood-2013-06-511527 (2014).
- 132 Krause, D. S., Lazarides, K., Lewis, J. B., von Andrian, U. H. & Van Etten, R. A. Selectins and their ligands are required for homing and engraftment of BCR-ABL1+ leukemic stem cells in the bone marrow niche. *Blood* **123**, 1361-1371, doi:10.1182/blood-2013-11-538694 (2014).
- 133 Godavarthy, P. S. *et al.* The vascular bone marrow niche influences outcome in chronic myeloid leukemia via the E-selectin - SCL/TAL1 - CD44 axis. *Haematologica* **105**, 136-147, doi:10.3324/haematol.2018.212365 (2020).
- 134 Manabe, A., Coustan-Smith, E., Behm, F. G., Raimondi, S. C. & Campana, D. Bone marrow-derived stromal cells prevent apoptotic cell death in B-lineage acute lymphoblastic leukemia. *Blood* **79**, 2370-2377 (1992).
- 135 Shiozawa, Y., Pedersen, E. A. & Taichman, R. S. GAS6/Mer axis regulates the homing and survival of the E2A/PBX1-positive B-cell precursor acute lymphoblastic leukemia in the bone marrow niche. *Exp Hematol* **38**, 132-140, doi:10.1016/j.exphem.2009.11.002 (2010).
- 136 Boyerinas, B. *et al.* Adhesion to osteopontin in the bone marrow niche regulates lymphoblastic leukemia cell dormancy. *Blood* **121**, 4821-4831, doi:10.1182/blood-2012-12-475483 (2013).
- 137 Verma, D. *et al.* Bone marrow niche-derived extracellular matrix-degrading enzymes influence the progression of B-cell acute lymphoblastic leukemia. *Leukemia* **34**, 1540-1552, doi:10.1038/s41375-019-0674-7 (2020).
- 138 Hsieh, Y. T. *et al.* Integrin alpha4 blockade sensitizes drug resistant pre-B acute lymphoblastic leukemia to chemotherapy. *Blood* **121**, 1814-1818, doi:10.1182/blood-2012-01-406272 (2013).
- 139 Hu, Z. & Slayton, W. B. Integrin VLA-5 and FAK are Good Targets to Improve Treatment Response in the Philadelphia Chromosome Positive Acute Lymphoblastic Leukemia. *Front Oncol* **4**, 112, doi:10.3389/fonc.2014.00112 (2014).
- 140 Parameswaran, R., Yu, M., Lim, M., Groffen, J. & Heisterkamp, N. Combination of drug therapy in acute lymphoblastic leukemia with a CXCR4 antagonist. *Leukemia* **25**, 1314-1323, doi:10.1038/leu.2011.76 (2011).
- 141 Churchman, M. L. *et al.* Efficacy of Retinoids in IKZF1-Mutated BCR-ABL1 Acute Lymphoblastic Leukemia. *Cancer Cell* **28**, 343-356, doi:10.1016/j.ccell.2015.07.016 (2015).

- 142 de Vasconcellos, J. F. *et al.* Increased CCL2 and IL-8 in the bone marrow microenvironment in
acute lymphoblastic leukemia. *Pediatr Blood Cancer* **56**, 568-577, doi:10.1002/pbc.22941
(2011).
- 143 Vicente Lopez, A. *et al.* Mesenchymal stromal cells derived from the bone marrow of acute
lymphoblastic leukemia patients show altered BMP4 production: correlations with the
course of disease. *PLoS One* **9**, e84496, doi:10.1371/journal.pone.0084496 (2014).
- 144 Tiziani, S. *et al.* Metabolomics of the tumor microenvironment in pediatric acute
lymphoblastic leukemia. *PLoS One* **8**, e82859, doi:10.1371/journal.pone.0082859 (2013).
- 145 Boutter, J. *et al.* Image-based RNA interference screening reveals an individual dependence
of acute lymphoblastic leukemia on stromal cysteine support. *Oncotarget* **5**, 11501-11512,
doi:10.18632/oncotarget.2572 (2014).
- 146 Liu, J. *et al.* Stromal cell-mediated mitochondrial redox adaptation regulates drug resistance
in childhood acute lymphoblastic leukemia. *Oncotarget* **6**, 43048-43064,
doi:10.18632/oncotarget.5528 (2015).
- 147 Park, E. *et al.* Stromal cell protein kinase C-beta inhibition enhances chemosensitivity in B
cell malignancies and overcomes drug resistance. *Sci Transl Med* **12**,
doi:10.1126/scitranslmed.aax9340 (2020).
- 148 Gang, E. J. *et al.* Integrin alpha6 mediates the drug resistance of acute lymphoblastic B-cell
leukemia. *Blood* **136**, 210-223, doi:10.1182/blood.2019001417 (2020).
- 149 Dikic, I. & Elazar, Z. Mechanism and medical implications of mammalian autophagy. *Nat Rev
Mol Cell Biol* **19**, 349-364, doi:10.1038/s41580-018-0003-4 (2018).
- 150 De Duve, C., Pressman, B. C., Gianetto, R., Wattiaux, R. & Appelmans, F. Tissue fractionation
studies. 6. Intracellular distribution patterns of enzymes in rat-liver tissue. *Biochem J* **60**,
604-617, doi:10.1042/bj0600604 (1955).
- 151 Deter, R. L., Baudhuin, P. & De Duve, C. Participation of lysosomes in cellular autophagy
induced in rat liver by glucagon. *J Cell Biol* **35**, C11-16, doi:10.1083/jcb.35.2.c11 (1967).
- 152 Tsukada, M. & Ohsumi, Y. Isolation and characterization of autophagy-defective mutants of
Saccharomyces cerevisiae. *FEBS Lett* **333**, 169-174, doi:10.1016/0014-5793(93)80398-e
(1993).
- 153 Mizushima, N. & Komatsu, M. Autophagy: renovation of cells and tissues. *Cell* **147**, 728-741,
doi:10.1016/j.cell.2011.10.026 (2011).
- 154 Zhao, Y. G. & Zhang, H. Autophagosome maturation: An epic journey from the ER to
lysosomes. *J Cell Biol* **218**, 757-770, doi:10.1083/jcb.201810099 (2019).
- 155 Gubas, A. & Dikic, I. A guide to the regulation of selective autophagy receptors. *FEBS J*,
doi:10.1111/febs.15824 (2021).
- 156 Wirth, M. *et al.* Molecular determinants regulating selective binding of autophagy adapters
and receptors to ATG8 proteins. *Nat Commun* **10**, 2055, doi:10.1038/s41467-019-10059-6
(2019).
- 157 Pankiv, S. *et al.* p62/SQSTM1 binds directly to Atg8/LC3 to facilitate degradation of
ubiquitinated protein aggregates by autophagy. *J Biol Chem* **282**, 24131-24145,
doi:10.1074/jbc.M702824200 (2007).
- 158 von Muhlinen, N. *et al.* LC3C, bound selectively by a noncanonical LIR motif in NDP52, is
required for antibacterial autophagy. *Mol Cell* **48**, 329-342,
doi:10.1016/j.molcel.2012.08.024 (2012).
- 159 Kirkin, V. *et al.* A role for NBR1 in autophagosomal degradation of ubiquitinated substrates.
Mol Cell **33**, 505-516, doi:10.1016/j.molcel.2009.01.020 (2009).
- 160 Zaffagnini, G. & Martens, S. Mechanisms of Selective Autophagy. *J Mol Biol* **428**, 1714-1724,
doi:10.1016/j.jmb.2016.02.004 (2016).
- 161 Alemu, E. A. *et al.* ATG8 family proteins act as scaffolds for assembly of the ULK complex:
sequence requirements for LC3-interacting region (LIR) motifs. *J Biol Chem* **287**, 39275-
39290, doi:10.1074/jbc.M112.378109 (2012).

- 162 McEwan, D. G. *et al.* PLEKHM1 regulates autophagosome-lysosome fusion through HOPS complex and LC3/GABARAP proteins. *Mol Cell* **57**, 39-54, doi:10.1016/j.molcel.2014.11.006 (2015).
- 163 Pankiv, S. *et al.* FYCO1 is a Rab7 effector that binds to LC3 and PI3P to mediate microtubule plus end-directed vesicle transport. *J Cell Biol* **188**, 253-269, doi:10.1083/jcb.200907015 (2010).
- 164 Rabinowitz, J. D. & White, E. Autophagy and metabolism. *Science* **330**, 1344-1348, doi:10.1126/science.1193497 (2010).
- 165 Liang, X. H. *et al.* Induction of autophagy and inhibition of tumorigenesis by beclin 1. *Nature* **402**, 672-676, doi:10.1038/45257 (1999).
- 166 Liu, D., Yang, Y., Liu, Q. & Wang, J. Inhibition of autophagy by 3-MA potentiates cisplatin-induced apoptosis in esophageal squamous cell carcinoma cells. *Med Oncol* **28**, 105-111, doi:10.1007/s12032-009-9397-3 (2011).
- 167 Apel, A., Herr, I., Schwarz, H., Rodemann, H. P. & Mayer, A. Blocked autophagy sensitizes resistant carcinoma cells to radiation therapy. *Cancer Res* **68**, 1485-1494, doi:10.1158/0008-5472.CAN-07-0562 (2008).
- 168 Horne, G. A. *et al.* A randomised phase II trial of hydroxychloroquine and imatinib versus imatinib alone for patients with chronic myeloid leukaemia in major cytogenetic response with residual disease. *Leukemia* **34**, 1775-1786, doi:10.1038/s41375-019-0700-9 (2020).
- 169 Rao, S. *et al.* A dual role for autophagy in a murine model of lung cancer. *Nat Commun* **5**, 3056, doi:10.1038/ncomms4056 (2014).
- 170 White, E. Deconvoluting the context-dependent role for autophagy in cancer. *Nat Rev Cancer* **12**, 401-410, doi:10.1038/nrc3262 (2012).
- 171 Poillet-Perez, L. & White, E. Role of tumor and host autophagy in cancer metabolism. *Genes Dev* **33**, 610-619, doi:10.1101/gad.325514.119 (2019).
- 172 Karsli-Uzunbas, G. *et al.* Autophagy is required for glucose homeostasis and lung tumor maintenance. *Cancer Discov* **4**, 914-927, doi:10.1158/2159-8290.CD-14-0363 (2014).
- 173 Yang, A. *et al.* Autophagy Sustains Pancreatic Cancer Growth through Both Cell-Autonomous and Nonautonomous Mechanisms. *Cancer Discov* **8**, 276-287, doi:10.1158/2159-8290.CD-17-0952 (2018).
- 174 Sousa, C. M. *et al.* Pancreatic stellate cells support tumour metabolism through autophagic alanine secretion. *Nature* **536**, 479-483, doi:10.1038/nature19084 (2016).
- 175 Poillet-Perez, L. *et al.* Autophagy maintains tumour growth through circulating arginine. *Nature* **563**, 569-573, doi:10.1038/s41586-018-0697-7 (2018).
- 176 Wendland, B. Everything you ever wanted to know about endocytosis. *Nature Cell Biology* **3**, E254-E254, doi:10.1038/ncb1101-e254 (2001).
- 177 Traub, L. M. & Bonifacino, J. S. Cargo recognition in clathrin-mediated endocytosis. *Cold Spring Harb Perspect Biol* **5**, a016790, doi:10.1101/cshperspect.a016790 (2013).
- 178 Fader, C. M. & Colombo, M. I. Autophagy and multivesicular bodies: two closely related partners. *Cell Death Differ* **16**, 70-78, doi:10.1038/cdd.2008.168 (2009).
- 179 Babst, M. MVB vesicle formation: ESCRT-dependent, ESCRT-independent and everything in between. *Curr Opin Cell Biol* **23**, 452-457, doi:10.1016/j.ceb.2011.04.008 (2011).
- 180 Sanchez-Wandelmer, J. & Reggiori, F. Amphisomes: out of the autophagosome shadow? *EMBO J* **32**, 3116-3118, doi:10.1038/emboj.2013.246 (2013).
- 181 Klumperman, J. & Raposo, G. The complex ultrastructure of the endolysosomal system. *Cold Spring Harb Perspect Biol* **6**, a016857, doi:10.1101/cshperspect.a016857 (2014).
- 182 Colombo, M. *et al.* Analysis of ESCRT functions in exosome biogenesis, composition and secretion highlights the heterogeneity of extracellular vesicles. *J Cell Sci* **126**, 5553-5565, doi:10.1242/jcs.128868 (2013).
- 183 Raposo, G. & Stoorvogel, W. Extracellular vesicles: exosomes, microvesicles, and friends. *J Cell Biol* **200**, 373-383, doi:10.1083/jcb.201211138 (2013).

- 184 Pan, B. T., Teng, K., Wu, C., Adam, M. & Johnstone, R. M. Electron microscopic evidence for
externalization of the transferrin receptor in vesicular form in sheep reticulocytes. *J Cell Biol*
101, 942-948, doi:10.1083/jcb.101.3.942 (1985).
- 185 Gould, S. J. & Raposo, G. As we wait: coping with an imperfect nomenclature for
extracellular vesicles. *J Extracell Vesicles* **2**, doi:10.3402/jev.v2i0.20389 (2013).
- 186 Minciacchi, V. R., Freeman, M. R. & Di Vizio, D. Extracellular vesicles in cancer: exosomes,
microvesicles and the emerging role of large oncosomes. *Semin Cell Dev Biol* **40**, 41-51,
doi:10.1016/j.semcdb.2015.02.010 (2015).
- 187 Minciacchi, V. R. *et al.* Large oncosomes contain distinct protein cargo and represent a
separate functional class of tumor-derived extracellular vesicles. *Oncotarget* **6**, 11327-
11341, doi:10.18632/oncotarget.3598 (2015).
- 188 Matarredona, E. R. & Pastor, A. M. Extracellular Vesicle-Mediated Communication between
the Glioblastoma and Its Microenvironment. *Cells* **9**, doi:10.3390/cells9010096 (2019).
- 189 Gyorgy, B. *et al.* Membrane vesicles, current state-of-the-art: emerging role of extracellular
vesicles. *Cell Mol Life Sci* **68**, 2667-2688, doi:10.1007/s00018-011-0689-3 (2011).
- 190 Ambattu, L. A. *et al.* High frequency acoustic cell stimulation promotes exosome generation
regulated by a calcium-dependent mechanism. *Commun Biol* **3**, 553, doi:10.1038/s42003-
020-01277-6 (2020).
- 191 Hedlund, M., Nagaeva, O., Kargl, D., Baranov, V. & Mincheva-Nilsson, L. Thermal- and
oxidative stress causes enhanced release of NKG2D ligand-bearing immunosuppressive
exosomes in leukemia/lymphoma T and B cells. *PLoS One* **6**, e16899,
doi:10.1371/journal.pone.0016899 (2011).
- 192 de Jong, O. G. *et al.* Cellular stress conditions are reflected in the protein and RNA content of
endothelial cell-derived exosomes. *J Extracell Vesicles* **1**, doi:10.3402/jev.v1i0.18396 (2012).
- 193 Mathieu, M., Martin-Jaular, L., Lavieu, G. & Thery, C. Specificities of secretion and uptake of
exosomes and other extracellular vesicles for cell-to-cell communication. *Nat Cell Biol* **21**, 9-
17, doi:10.1038/s41556-018-0250-9 (2019).
- 194 Aheget, H. *et al.* Exosome: A New Player in Translational Nanomedicine. *J Clin Med* **9**,
doi:10.3390/jcm9082380 (2020).
- 195 Raiborg, C. *et al.* Hrs sorts ubiquitinated proteins into clathrin-coated microdomains of early
endosomes. *Nat Cell Biol* **4**, 394-398, doi:10.1038/ncb791 (2002).
- 196 Baietti, M. F. *et al.* Syndecan-syntenin-ALIX regulates the biogenesis of exosomes. *Nat Cell*
Biol **14**, 677-685, doi:10.1038/ncb2502 (2012).
- 197 Roucourt, B., Meeussen, S., Bao, J., Zimmermann, P. & David, G. Heparanase activates the
syndecan-syntenin-ALIX exosome pathway. *Cell Res* **25**, 412-428, doi:10.1038/cr.2015.29
(2015).
- 198 Zhang, Y., Liu, Y., Liu, H. & Tang, W. H. Exosomes: biogenesis, biologic function and clinical
potential. *Cell Biosci* **9**, 19, doi:10.1186/s13578-019-0282-2 (2019).
- 199 Webber, J. P. *et al.* Differentiation of tumour-promoting stromal myofibroblasts by cancer
exosomes. *Oncogene* **34**, 290-302, doi:10.1038/onc.2013.560 (2015).
- 200 Luga, V. *et al.* Exosomes mediate stromal mobilization of autocrine Wnt-PCP signaling in
breast cancer cell migration. *Cell* **151**, 1542-1556, doi:10.1016/j.cell.2012.11.024 (2012).
- 201 Shimoda, M. *et al.* Loss of the Timp gene family is sufficient for the acquisition of the CAF-
like cell state. *Nat Cell Biol* **16**, 889-901, doi:10.1038/ncb3021 (2014).
- 202 Roccaro, A. M. *et al.* BM mesenchymal stromal cell-derived exosomes facilitate multiple
myeloma progression. *J Clin Invest* **123**, 1542-1555, doi:10.1172/JCI66517 (2013).
- 203 Steinbichler, T. B. *et al.* Therapy resistance mediated by exosomes. *Mol Cancer* **18**, 58,
doi:10.1186/s12943-019-0970-x (2019).
- 204 Shedden, K., Xie, X. T., Chandaroy, P., Chang, Y. T. & Rosania, G. R. Expulsion of small
molecules in vesicles shed by cancer cells: association with gene expression and
chemosensitivity profiles. *Cancer Res* **63**, 4331-4337 (2003).

- 205 Zhu, W. *et al.* Exosomes derived from human bone marrow mesenchymal stem cells promote tumor growth in vivo. *Cancer Lett* **315**, 28-37, doi:10.1016/j.canlet.2011.10.002 (2012).
- 206 Villarroya-Beltri, C. *et al.* ISGylation controls exosome secretion by promoting lysosomal degradation of MVB proteins. *Nat Commun* **7**, 13588, doi:10.1038/ncomms13588 (2016).
- 207 Xu, J., Camfield, R. & Gorski, S. M. The interplay between exosomes and autophagy - partners in crime. *J Cell Sci* **131**, doi:10.1242/jcs.215210 (2018).
- 208 Mazure, N. M. & Pouyssegur, J. Hypoxia-induced autophagy: cell death or cell survival? *Curr Opin Cell Biol* **22**, 177-180, doi:10.1016/j.ceb.2009.11.015 (2010).
- 209 Kumar, A. & Deep, G. Hypoxia in tumor microenvironment regulates exosome biogenesis: Molecular mechanisms and translational opportunities. *Cancer Lett* **479**, 23-30, doi:10.1016/j.canlet.2020.03.017 (2020).
- 210 Corazzari, M., Gagliardi, M., Fimia, G. M. & Piacentini, M. Endoplasmic Reticulum Stress, Unfolded Protein Response, and Cancer Cell Fate. *Front Oncol* **7**, 78, doi:10.3389/fonc.2017.00078 (2017).
- 211 Kanemoto, S. *et al.* Multivesicular body formation enhancement and exosome release during endoplasmic reticulum stress. *Biochem Biophys Res Commun* **480**, 166-172, doi:10.1016/j.bbrc.2016.10.019 (2016).
- 212 Ender, F., N. V. O. N. B. & Gieseler, F. Extracellular Vesicles: Subcellular Organelles With the Potential to Spread Cancer Resistance. *Anticancer Res* **39**, 3395-3404, doi:10.21873/anticancer.13483 (2019).
- 213 Yun, C. W. & Lee, S. H. The Roles of Autophagy in Cancer. *Int J Mol Sci* **19**, doi:10.3390/ijms19113466 (2018).
- 214 Wang, B. *et al.* Exosomal miR-1910-3p promotes proliferation, metastasis, and autophagy of breast cancer cells by targeting MTMR3 and activating the NF-kappaB signaling pathway. *Cancer Lett* **489**, 87-99, doi:10.1016/j.canlet.2020.05.038 (2020).
- 215 Van Wesenbeeck, L. *et al.* Involvement of PLEKHM1 in osteoclastic vesicular transport and osteopetrosis in incisors absent rats and humans. *J Clin Invest* **117**, 919-930, doi:10.1172/JCI30328 (2007).
- 216 Gubas, A. *et al.* The endolysosomal adaptor PLEKHM1 is a direct target for both mTOR and MAPK pathways. *FEBS Lett* **595**, 864-880, doi:10.1002/1873-3468.14041 (2021).
- 217 Marwaha, R. *et al.* The Rab7 effector PLEKHM1 binds Arl8b to promote cargo traffic to lysosomes. *J Cell Biol* **216**, 1051-1070, doi:10.1083/jcb.201607085 (2017).
- 218 Tabata, K. *et al.* Rubicon and PLEKHM1 negatively regulate the endocytic/autophagic pathway via a novel Rab7-binding domain. *Mol Biol Cell* **21**, 4162-4172, doi:10.1091/mbc.E10-06-0495 (2010).
- 219 Van Etten, R. A. Retroviral transduction models of Ph⁺ leukemia: advantages and limitations for modeling human hematological malignancies in mice. *Blood Cells Mol Dis* **27**, 201-205, doi:10.1006/bcmd.2000.0370 (2001).
- 220 Wolff, N. C. & Ilaria, R. L., Jr. Establishment of a murine model for therapy-treated chronic myelogenous leukemia using the tyrosine kinase inhibitor STI571. *Blood* **98**, 2808-2816, doi:10.1182/blood.v98.9.2808 (2001).
- 221 Krause, D. S. *et al.* Differential regulation of myeloid leukemias by the bone marrow microenvironment. *Nat Med* **19**, 1513-1517, doi:10.1038/nm.3364 (2013).
- 222 Wheat, J. C. *et al.* The corepressor Tle4 is a novel regulator of murine hematopoiesis and bone development. *PLoS One* **9**, e105557, doi:10.1371/journal.pone.0105557 (2014).
- 223 Fulzele, K. *et al.* Loss of Gsalpha in osteocytes leads to osteopenia due to sclerostin induced suppression of osteoblast activity. *Bone* **117**, 138-148, doi:10.1016/j.bone.2018.09.021 (2018).
- 224 Merrild, D. M. *et al.* Pit- and trench-forming osteoclasts: a distinction that matters. *Bone Res* **3**, 15032, doi:10.1038/boneres.2015.32 (2015).

- 225 Houlihan, D. D. *et al.* Isolation of mouse mesenchymal stem cells on the basis of expression of Sca-1 and PDGFR-alpha. *Nat Protoc* **7**, 2103-2111, doi:10.1038/nprot.2012.125 (2012).
- 226 Kulak, N. A., Pichler, G., Paron, I., Nagaraj, N. & Mann, M. Minimal, encapsulated proteomic-sample processing applied to copy-number estimation in eukaryotic cells. *Nat Methods* **11**, 319-324, doi:10.1038/nmeth.2834 (2014).
- 227 Tyanova, S., Temu, T. & Cox, J. The MaxQuant computational platform for mass spectrometry-based shotgun proteomics. *Nat Protoc* **11**, 2301-2319, doi:10.1038/nprot.2016.136 (2016).
- 228 Cox, J. & Mann, M. MaxQuant enables high peptide identification rates, individualized p.p.b.-range mass accuracies and proteome-wide protein quantification. *Nat Biotechnol* **26**, 1367-1372 (2008).
- 229 Cox, J. *et al.* Andromeda: a peptide search engine integrated into the MaxQuant environment. *J Proteome Res* **10**, 1794-1805 (2011).
- 230 Elias, J. E. & Gygi, S. P. Target-decoy search strategy for increased confidence in large-scale protein identifications by mass spectrometry. *Nat Methods* **4**, 207-214, doi:10.1038/nmeth1019 (2007).
- 231 Deutsch, E. W. *et al.* The ProteomeXchange consortium in 2017: supporting the cultural change in proteomics public data deposition. *Nucleic acids research* **45**, D1100-d1106, doi:10.1093/nar/gkw936 (2017).
- 232 Perez-Riverol, Y. *et al.* The PRIDE database and related tools and resources in 2019: improving support for quantification data. *Nucleic acids research* **47**, D442-d450, doi:10.1093/nar/gky1106 (2019).
- 233 Tertel, T., Gorgens, A. & Giebel, B. Analysis of individual extracellular vesicles by imaging flow cytometry. *Methods Enzymol* **645**, 55-78, doi:10.1016/bs.mie.2020.05.013 (2020).
- 234 Gorgens, A. *et al.* Optimisation of imaging flow cytometry for the analysis of single extracellular vesicles by using fluorescence-tagged vesicles as biological reference material. *J Extracell Vesicles* **8**, 1587567, doi:10.1080/20013078.2019.1587567 (2019).
- 235 Welsh, J. A. *et al.* MIFlowCyt-EV: a framework for standardized reporting of extracellular vesicle flow cytometry experiments. *J Extracell Vesicles* **9**, 1713526, doi:10.1080/20013078.2020.1713526 (2020).
- 236 Tertel, T. *et al.* High-Resolution Imaging Flow Cytometry Reveals Impact of Incubation Temperature on Labeling of Extracellular Vesicles with Antibodies. *Cytometry A* **97**, 602-609, doi:10.1002/cyto.a.24034 (2020).
- 237 Mayle, A., Luo, M., Jeong, M. & Goodell, M. A. Flow cytometry analysis of murine hematopoietic stem cells. *Cytometry A* **83**, 27-37, doi:10.1002/cyto.a.22093 (2013).
- 238 Bruno, S. & Darzynkiewicz, Z. Cell cycle dependent expression and stability of the nuclear protein detected by Ki-67 antibody in HL-60 cells. *Cell Prolif* **25**, 31-40, doi:10.1111/j.1365-2184.1992.tb01435.x (1992).
- 239 Kennedy, D. E. & Knight, K. L. Inhibition of B Lymphopoiesis by Adipocytes and IL-1-Producing Myeloid-Derived Suppressor Cells. *J Immunol* **195**, 2666-2674, doi:10.4049/jimmunol.1500957 (2015).
- 240 Nutt, S. L. & Kee, B. L. The transcriptional regulation of B cell lineage commitment. *Immunity* **26**, 715-725, doi:10.1016/j.immuni.2007.05.010 (2007).
- 241 Wang, K., Wei, G. & Liu, D. CD19: a biomarker for B cell development, lymphoma diagnosis and therapy. *Exp Hematol Oncol* **1**, 36, doi:10.1186/2162-3619-1-36 (2012).
- 242 Coffman, R. L. & Weissman, I. L. B220: a B cell-specific member of the T200 glycoprotein family. *Nature* **289**, 681-683, doi:10.1038/289681a0 (1981).
- 243 Kozmik, Z., Wang, S., Dorfler, P., Adams, B. & Busslinger, M. The promoter of the CD19 gene is a target for the B-cell-specific transcription factor BSAP. *Mol Cell Biol* **12**, 2662-2672, doi:10.1128/mcb.12.6.2662 (1992).

- 244 Mullighan, C. G. *et al.* Genome-wide analysis of genetic alterations in acute lymphoblastic leukaemia. *Nature* **446**, 758-764, doi:10.1038/nature05690 (2007).
- 245 Singh, H., Pongubala, J. M. & Medina, K. L. Gene regulatory networks that orchestrate the development of B lymphocyte precursors. *Adv Exp Med Biol* **596**, 57-62, doi:10.1007/0-387-46530-8_5 (2007).
- 246 Alt, F. W., Zhang, Y., Meng, F. L., Guo, C. & Schwer, B. Mechanisms of programmed DNA lesions and genomic instability in the immune system. *Cell* **152**, 417-429, doi:10.1016/j.cell.2013.01.007 (2013).
- 247 Bonnet, D. & Dick, J. E. Human acute myeloid leukemia is organized as a hierarchy that originates from a primitive hematopoietic cell. *Nat Med* **3**, 730-737, doi:10.1038/nm0797-730 (1997).
- 248 Cappellen, D. *et al.* Transcriptional program of mouse osteoclast differentiation governed by the macrophage colony-stimulating factor and the ligand for the receptor activator of NFkappa B. *J Biol Chem* **277**, 21971-21982, doi:10.1074/jbc.M200434200 (2002).
- 249 Tikhonova, A. N. *et al.* The bone marrow microenvironment at single-cell resolution. *Nature* **569**, 222-228, doi:10.1038/s41586-019-1104-8 (2019).
- 250 Polak, R., de Rooij, B., Pieters, R. & den Boer, M. L. B-cell precursor acute lymphoblastic leukemia cells use tunneling nanotubes to orchestrate their microenvironment. *Blood* **126**, 2404-2414, doi:10.1182/blood-2015-03-634238 (2015).
- 251 Kobayashi, T. *et al.* The tetraspanin CD63/lamp3 cycles between endocytic and secretory compartments in human endothelial cells. *Mol Biol Cell* **11**, 1829-1843, doi:10.1091/mbc.11.5.1829 (2000).
- 252 Johnson, S. M. *et al.* Metabolic reprogramming of bone marrow stromal cells by leukemic extracellular vesicles in acute lymphoblastic leukemia. *Blood* **128**, 453-456, doi:10.1182/blood-2015-12-688051 (2016).
- 253 Gudbergsson, J. M. & Johnsen, K. B. Exosomes and autophagy: rekindling the vesicular waste hypothesis. *J Cell Commun Signal* **13**, 443-450, doi:10.1007/s12079-019-00524-8 (2019).
- 254 Shabbir, A., Cox, A., Rodriguez-Menocal, L., Salgado, M. & Van Badiavas, E. Mesenchymal Stem Cell Exosomes Induce Proliferation and Migration of Normal and Chronic Wound Fibroblasts, and Enhance Angiogenesis In Vitro. *Stem Cells Dev* **24**, 1635-1647, doi:10.1089/scd.2014.0316 (2015).
- 255 Lehmann, B. D. *et al.* Senescence-associated exosome release from human prostate cancer cells. *Cancer Res* **68**, 7864-7871, doi:10.1158/0008-5472.CAN-07-6538 (2008).
- 256 Kostelansky, M. S. *et al.* Structural and functional organization of the ESCRT-I trafficking complex. *Cell* **125**, 113-126, doi:10.1016/j.cell.2006.01.049 (2006).
- 257 Spinler, K. *et al.* A stem cell reporter based platform to identify and target drug resistant stem cells in myeloid leukemia. *Nat Commun* **11**, 5998, doi:10.1038/s41467-020-19782-x (2020).
- 258 Liu, P. *et al.* Cell-cycle-regulated activation of Akt kinase by phosphorylation at its carboxyl terminus. *Nature* **508**, 541-545, doi:10.1038/nature13079 (2014).
- 259 Macia, E. *et al.* Dynasore, a cell-permeable inhibitor of dynamin. *Dev Cell* **10**, 839-850, doi:10.1016/j.devcel.2006.04.002 (2006).
- 260 Kawamoto, T. *et al.* Tumor-derived microvesicles induce proangiogenic phenotype in endothelial cells via endocytosis. *PLoS One* **7**, e34045, doi:10.1371/journal.pone.0034045 (2012).
- 261 Chiba, M., Kubota, S., Sato, K. & Monzen, S. Exosomes released from pancreatic cancer cells enhance angiogenic activities via dynamin-dependent endocytosis in endothelial cells in vitro. *Sci Rep* **8**, 11972, doi:10.1038/s41598-018-30446-1 (2018).
- 262 Beauvais, D. M. & Rapraeger, A. C. Syndecan-1 couples the insulin-like growth factor-1 receptor to inside-out integrin activation. *J Cell Sci* **123**, 3796-3807, doi:10.1242/jcs.067645 (2010).

- 263 Wang, H., Jin, H. & Rapraeger, A. C. Syndecan-1 and Syndecan-4 Capture Epidermal Growth Factor Receptor Family Members and the alpha3beta1 Integrin Via Binding Sites in Their Ectodomains: NOVEL SYNSTATINS PREVENT KINASE CAPTURE AND INHIBIT alpha6beta4-INTEGRIN-DEPENDENT EPITHELIAL CELL MOTILITY. *J Biol Chem* **290**, 26103-26113, doi:10.1074/jbc.M115.679084 (2015).
- 264 Parsons, J. T. Focal adhesion kinase: the first ten years. *J Cell Sci* **116**, 1409-1416, doi:10.1242/jcs.00373 (2003).
- 265 Koo, T. H. *et al.* Syntenin is overexpressed and promotes cell migration in metastatic human breast and gastric cancer cell lines. *Oncogene* **21**, 4080-4088, doi:10.1038/sj.onc.1205514 (2002).
- 266 Krause, D. S., Lazarides, K., von Andrian, U. H. & Van Etten, R. A. Requirement for CD44 in homing and engraftment of BCR-ABL-expressing leukemic stem cells. *Nat Med* **12**, 1175-1180, doi:10.1038/nm1489 (2006).
- 267 Jin, L., Hope, K. J., Zhai, Q., Smadja-Joffe, F. & Dick, J. E. Targeting of CD44 eradicates human acute myeloid leukemic stem cells. *Nat Med* **12**, 1167-1174, doi:10.1038/nm1483 (2006).
- 268 Rolink, A. G., Winkler, T., Melchers, F. & Andersson, J. Precursor B cell receptor-dependent B cell proliferation and differentiation does not require the bone marrow or fetal liver environment. *J Exp Med* **191**, 23-32, doi:10.1084/jem.191.1.23 (2000).
- 269 Liu, G. J. *et al.* Pax5 loss imposes a reversible differentiation block in B-progenitor acute lymphoblastic leukemia. *Genes Dev* **28**, 1337-1350, doi:10.1101/gad.240416.114 (2014).
- 270 Gu, Z. *et al.* PAX5-driven subtypes of B-progenitor acute lymphoblastic leukemia. *Nat Genet* **51**, 296-307, doi:10.1038/s41588-018-0315-5 (2019).
- 271 Dang, J. *et al.* PAX5 is a tumor suppressor in mouse mutagenesis models of acute lymphoblastic leukemia. *Blood* **125**, 3609-3617, doi:10.1182/blood-2015-02-626127 (2015).
- 272 Fujiwara, T. *et al.* PLEKHM1/DEF8/RAB7 complex regulates lysosome positioning and bone homeostasis. *JCI Insight* **1**, e86330, doi:10.1172/jci.insight.86330 (2016).
- 273 Takamura, A. *et al.* Autophagy-deficient mice develop multiple liver tumors. *Genes Dev* **25**, 795-800, doi:10.1101/gad.2016211 (2011).
- 274 Yang, A. *et al.* Autophagy is critical for pancreatic tumor growth and progression in tumors with p53 alterations. *Cancer Discov* **4**, 905-913, doi:10.1158/2159-8290.CD-14-0362 (2014).
- 275 Bellodi, C. *et al.* Targeting autophagy potentiates tyrosine kinase inhibitor-induced cell death in Philadelphia chromosome-positive cells, including primary CML stem cells. *J Clin Invest* **119**, 1109-1123, doi:10.1172/JCI35660 (2009).
- 276 Capparelli, C. *et al.* Autophagy and senescence in cancer-associated fibroblasts metabolically supports tumor growth and metastasis via glycolysis and ketone production. *Cell Cycle* **11**, 2285-2302, doi:10.4161/cc.20718 (2012).
- 277 Ding, L. *et al.* Targeting the autophagy in bone marrow stromal cells overcomes resistance to vorinostat in chronic lymphocytic leukemia. *Onco Targets Ther* **11**, 5151-5170, doi:10.2147/OTT.S170392 (2018).
- 278 Muralidharan-Chari, V., Clancy, J. W., Sedgwick, A. & D'Souza-Schorey, C. Microvesicles: mediators of extracellular communication during cancer progression. *J Cell Sci* **123**, 1603-1611, doi:10.1242/jcs.064386 (2010).
- 279 Hashmi, S. *et al.* Survival after mesenchymal stromal cell therapy in steroid-refractory acute graft-versus-host disease: systematic review and meta-analysis. *Lancet Haematol* **3**, e45-52, doi:10.1016/S2352-3026(15)00224-0 (2016).
- 280 Kordelas, L. *et al.* MSC-derived exosomes: a novel tool to treat therapy-refractory graft-versus-host disease. *Leukemia* **28**, 970-973, doi:10.1038/leu.2014.41 (2014).
- 281 Peinado, H. *et al.* Melanoma exosomes educate bone marrow progenitor cells toward a pro-metastatic phenotype through MET. *Nat Med* **18**, 883-891, doi:10.1038/nm.2753 (2012).

- 282 Lopatina, T. *et al.* Extracellular Vesicles Released by Tumor Endothelial Cells Spread
Immunosuppressive and Transforming Signals Through Various Recipient Cells. *Front Cell
Dev Biol* **8**, 698, doi:10.3389/fcell.2020.00698 (2020).
- 283 Yang, Y. *et al.* Elevated expression of syntenin in breast cancer is correlated with lymph node
metastasis and poor patient survival. *Breast Cancer Res* **15**, R50, doi:10.1186/bcr3442
(2013).
- 284 Boukerche, H. *et al.* mda-9/Syntenin: a positive regulator of melanoma metastasis. *Cancer
Res* **65**, 10901-10911, doi:10.1158/0008-5472.CAN-05-1614 (2005).
- 285 Grootjans, J. J. *et al.* Syntenin, a PDZ protein that binds syndecan cytoplasmic domains. *Proc
Natl Acad Sci U S A* **94**, 13683-13688, doi:10.1073/pnas.94.25.13683 (1997).
- 286 Garcia, M. *et al.* Fragment-based drug design targeting syntenin PDZ2 domain involved in
exosomal release and tumour spread. *Eur J Med Chem* **223**, 113601,
doi:10.1016/j.ejmech.2021.113601 (2021).
- 287 Beauvais, D. M., Ell, B. J., McWhorter, A. R. & Rapraeger, A. C. Syndecan-1 regulates
alpha5beta3 and alpha5beta5 integrin activation during angiogenesis and is blocked by
synstatin, a novel peptide inhibitor. *J Exp Med* **206**, 691-705, doi:10.1084/jem.20081278
(2009).
- 288 Dasgupta, S. *et al.* Novel role of MDA-9/syntenin in regulating urothelial cell proliferation by
modulating EGFR signaling. *Clin Cancer Res* **19**, 4621-4633, doi:10.1158/1078-0432.CCR-13-
0585 (2013).
- 289 Schioppa, T. *et al.* B regulatory cells and the tumor-promoting actions of TNF-alpha during
squamous carcinogenesis. *Proc Natl Acad Sci U S A* **108**, 10662-10667,
doi:10.1073/pnas.1100994108 (2011).
- 290 Wang, K. *et al.* TNF-alpha promotes extracellular vesicle release in mouse astrocytes through
glutaminase. *J Neuroinflammation* **14**, 87, doi:10.1186/s12974-017-0853-2 (2017).
- 291 Chaudhuri, A. D. *et al.* TNFalpha and IL-1beta modify the miRNA cargo of astrocyte shed
extracellular vesicles to regulate neurotrophic signaling in neurons. *Cell Death Dis* **9**, 363,
doi:10.1038/s41419-018-0369-4 (2018).
- 292 Charles, K. A. *et al.* The tumor-promoting actions of TNF-alpha involve TNFR1 and IL-17 in
ovarian cancer in mice and humans. *J Clin Invest* **119**, 3011-3023, doi:10.1172/JCI39065
(2009).

Acknowledgments

First, I would like to acknowledge my supervisor Prof. Dr. Daniela S. Krause for being a continuously present and inspiring mentor and for her constant supervision, encouragement, and advice throughout my PhD. She has given me the chance to gain great experience in the field of laboratory-based leukemia research and knowledge on designing bench-to-bedside ideas and concepts. At the same time, I have been trained to work at a fast pace and in a productive and fun environment. I sincerely thank her for giving me this opportunity.

I would also like to sincerely thank Prof. Dr. Rolf Marschalek for his supervision, input and guidance during my PhD, as well as, his valuable mentorship during our one-to-one yearly meetings.

I would also like to express my gratitude to my colleague Valentina for her support and guidance during all these years, as well as her scientific input to this particular work. I thank Dr. Georg Tascher and Dr. Christian Münch for the production and analysis of the proteomic data, Tobias Tertel and Prof. Dr. Bernd Giebel for the production and analysis of the EV data and finally my colleagues Rahul and Costy for their contribution to the experiments and conceptual discussions. Finally, I thank especially Valentina, Rahul, Pablo, Robel and Theresa for their individual contributions to the writing of my PhD thesis.

I would also like to acknowledge my colleagues and friends Valentina, Rahul, Costy, Sonica, Raquel, Pablo and Divij who made my PhD a never-ending learning and fun process. I am delighted I met and worked with them.

Finally, I would like to thank my family and especially, my partner Fotis, my brother Theodore, my parents, and my friends Giota, Alexandra, Elina and Iris for their patience, support and encouragement in every step of my PhD career.

Curriculum Vitae

M.Sc. Christina Karantanou

Date of birth: 27.02.1991

Place of birth: Athens, Greece



Contact details:

Georg-Speyer-Haus

Institute for Tumor Biology and

Experimental Therapy

Paul Ehrlich Strasse 42-44

60596 Frankfurt am Main, Germany

email: Karantanou@gsh.uni-frankfurt.de, xristina.karantanou@gmail.com

CURRENT POSITION

PhD student in Leukaemia Research

Georg-Speyer-Haus, Institute for Tumor Biology and Experimental Therapy, Frankfurt am Main, Germany

EDUCATION

2017 – Present

PhD in Leukaemia Research

Department of Pharmaceutical Biology, Goethe University, Germany

Thesis: “Role of the autophagy adaptor protein PLEKHM1 in the leukemic niche”

Supervisor: Prof. Dr. Rolf Marschalek (Institute of Pharmaceutical Biology, Goethe University, Frankfurt am Main, Germany)

External Supervisors:

Prof. Dr. Daniela Krause (Georg -Speyer-Haus, Institute of Tumor Biology and Experimental Therapy, Frankfurt, Germany), (Goethe University, Frankfurt am Main, Germany)

2015 – 2016

Master of Sciences (M.Sc.) in Cancer Sciences

Institute of Cancer Sciences, University of Glasgow, UK

Thesis: “Role of autophagy in pancreatic cancer”

Supervisor: Dr. Vignir Helgason (Wolfson Wohl Cancer Research Centre, Institute of Cancer Sciences, University of Glasgow, UK)

2008 –2014

Bachelor Degree (B.Sc) in Biology

Faculty of Biology, National & Kapodistrian University of Athens, Greece

Thesis: “Role of clock genes in colorectal cancer”

Supervisors: Dr. Maria Gazouli (Medical School, University of Athens, Greece), Dr. Dimitrios Stravopodis (Faculty of Biology, National & Kapodistrian University of Athens, Greece)

HONORS AND AWARDS

- Oral Award Winner ISEV 2021
- Scholarship to study M.Sc. in Cancer Sciences, University of Glasgow, 2014
- 20th among 150 students introducing to Faculty of Biology on September 2008

ORIGINAL ARTICLES

1. Kumar R, Pereira R, Niemann J, Azimpour AI, Zanetti C, **Karantanou C**, Meister M, Godavarthy PS, Kowarz E, Marschalek R, Krause DS. The differential role of the lipid raft-associated protein flotillin 2 for progression of myeloid leukemia. *Manuscript under revision (Blood advances August 2021)*
2. **Karantanou C**, Minciocchi VR, Kumar R, Tascher G, Münch C, McEwan DG, Dikic I, Krause DS. Impact of mesenchymal stromal cell-derived exosomal cargo on B-cell acute lymphoblastic leukemia progression. *Manuscript under review (JEV August 2021)*
3. Minciocchi VR, **Karantanou C**, Zanetti C, Kumar R, Thomasberger N, Meister M, Hartmann S, Maguer-Satta V, Lefort S, Putyrski M, Ernst A, Krause DS. A differential role of annexins in the bone marrow

microenvironment for the progression of lymphoid versus myeloid leukemias. *Manuscript under revision (Blood 2021)*

- Zanetti C, Kumar R, Ender J, Godavarthy PS, Hartmann M, Hey J, Breuer K, Weissenberger ES, Minciacchi VR, **Karantanou C**, Gu Z, Roberts KG, Metzler M, Stock W, Mullighan CG, Bloomfield CD, Filmann N, Cousins A, Halsey C, Plass C, Lipka DB, Krause DS. The age of the bone marrow microenvironment influences B-cell acute lymphoblastic leukemia progression via CXCR5-CXCL13. *Blood 2021*
- Gubas A*, **Karantanou C***, Popovic D, Tascher G, Hoffmann ME, Dawe N, Dikic I, Krause DS, McEwan DG. PLEKHM1 is a direct target for both mTOR and MAPK pathways. *FEBS Letters 2021* *equally contributing authors
- Verma D, Fulzele K, Kumar R, **Karantanou C**, Pereira R, Kunz K, Hoelper S, Weissenberger E, Ziegler PK, Zia-Chahabi S, Fontenay M, Divieti Pajevic P, Krause DS. Warfarin Impairs the Bone Marrow Microenvironment and Hematopoiesis via the Periostin/Integrin b3 Pathway. *Blood 2019*
- Karantanos T, Theodoropoulos G, Gazouli M, Vaiopoulou A, **Karantanou C**, Stravopodis DJ, Bramis K, Lymperi M, Pektasidis D. Association of the clock genes polymorphisms with colorectal cancer susceptibility. *Journal of Surgical Oncology 2013*
- Karantanos T, Theodoropoulos G, Gazouli M, Vaiopoulou A, **Karantanou C**, Lymberi M, Pektasides D. Expression of clock genes in patients with colorectal cancer. *The International Journal of Biological Markers 2013*

REVIEW ARTICLES

- Karantanou C**, Godavarthy PS, Krause DS. Targeting the bone marrow microenvironment in acute leukemia. *Leuk Lymphoma 2018*

ABSTRACTS IN INTERNATIONAL CONFERENCES

- Karantanou C**, Minciacchi VR, Kumar R., Zanetti C, Tascher G, Münch C, Tertel T, Bernd G, McEwan DG, Dikic I, Krause DS. The role of the autophagy adaptor protein PLEKHM1 and exosome release in the leukaemic bone marrow microenvironment. *10th Annual Meeting International Society of Extracellular Vesicles 2021*
- Karantanou C**, Minciacchi VR, Kumar R, Tascher G, Münch C, McEwan DG, Dikic I, Krause DS. The role of the autophagy adaptor protein PLEKHM1 in the leukaemic bone marrow microenvironment. *22nd John Goldman E-conference on Chronic Myeloid Leukemia: Biology and Therapy 2020*

3. Minciacchi VR, Kumar R, Godavarthy PS, **Karantanou C**, Krause DS. The role of large oncosomes in leukaemia. *International Society for Extracellular Vesicles 2018*
4. Verma D, Fulzele K, Kumar R, **Karantanou C**, Pereira R, Kunz K, Hoelper S, Weissenberger E, Ziegler PK, Zia-Chahabi S, Fontenay M, Divieti Pajevic P, Krause DS. Warfarin Impairs the Bone Marrow Microenvironment and Hematopoiesis Via the Periostin/Integrin b3 Pathway. *60th American Society of Hematology Meeting 2017*

CERTIFICATES

- IELTS
- FELASA-B certificate- Animal handling experience